KINETICS AND SPECIFICITY OF NICOTINAMIDE NUCLEOTIDE BINDING TO THE dIII COMPONENT OF TRANSHYDROGENASE FROM *RHODOSPIRILLUM RUBRUM*.

by
LUCINDA HUXLEY

A thesis submitted to
The University of Birmingham
for the degree of
Doctor of Philosophy

UNIVERSITY OF BIRMINGHAM

School of Biosciences
The University of Birmingham
September 2010

Abstract

Transhydrogenase is an enzyme located in the cytoplasmic membrane of bacteria or the inner membrane of animal mitochondria. Using the energy of the proton electrochemical gradient (Δp), transhydrogenase translocates protons across the membrane whilst undergoing its redox reaction, in which hydride ion equivalents are transferred from NADH to $NADP^+$ producing NAD^+ and NADPH. Transhydrogenase comprises three components; dI binds NAD(H), dIII binds NADP(H) and dII spans the membrane. Transhydrogenase is thought to function by way of a binding-change mechanism, which involves "open" and "occluded" conformations of the enzyme. In the open conformation, nucleotides can readily bind and dissociate from the enzyme but the hydride transfer reaction is blocked. In the occluded conformation, hydride transfer is permitted but the binding and release of nucleotides is blocked. Hydride transfer and proton translocation are coupled. The coupling is not well understood due to the lack of structural information about the membrane-spanning dII component. However, it is believed to involve conformational changes of the enzyme, particularly the dII and dIII components, resulting in the switch between the open and occluded conformations.

Enzyme assays and tryptophan fluorescence experiments using apo-dIII in complex with dI revealed two features:

Firstly, the binding of NADP(H) to dIII is very slow and is probably limited by the conversion from the occluded to the open conformation. Since the switch between the occluded and open conformations is thought to be central in the coupling

of hydride transfer and proton translocation, the results presented here give an insight into the binding-change mechanism of transhydrogenase.

Secondly, NAD(H) is able to slowly bind into the NADP(H)-binding site of dIII (the "wrong" site). This brought into question the specificity of the dIII component of transhydrogenase for NADP(H). The significance and likelihood of NAD(H) binding to dIII in the intact enzyme in the living cell are discussed.

Publications

Lucinda Huxley, Philip G. Quirk, Nick P. J. Cotton, Scott A. White and J. Baz Jackson (2011). "The specificity of proton-translocating transhydrogenase for nicotinamide nucleotides." *Biochim Biophys Acta - Bioenergetics* **1807**: 85-94.

Dedicated to my wonderful parents.

Acknowledgments

There are so many people to say thank you to that I'm not quite sure where to start, but here goes...

First of all, a huge thank you goes to my PhD supervisors, Baz Jackson and Scott White. Scott for his crystallographic expertise and ideas, and for showing enthusiasm even when I hadn't crystallised the right protein!! Baz for his never ending brilliance and for the support and guidance that has been invaluable to me over the last 4 years. The next name that instantly springs to mind is Nick Cotton. My time in the lab would have been a lot more difficult if it weren't for his selfless and often volunteered help. Phil Quirk also deserves a thank you, who returned to our lab in August last year (we made a good team in those few weeks), and Andy Lovering who saved me when I was trying to teach myself Pymol. During my 4 years on the 3rd floor, there have been lots of people coming and going. All of them, in some way have made my time there a more enjoyable and successful one. So thank you to Pei, Simon (we had an awsome time in Dublin), Karina, Al, Mirian, Paul, Frank, Jaap, Bayo, Matt, Violet...I hope I haven't missed anyone!!

Of course, I am hugely grateful to my parents! Throughout my PhD, and indeed the whole of my life, they have been pillars of support not only financially but also emotionally. Their wisdom, kindness and excellent advice has made me who I am today and I hope that I have made them proud. Thanks Dad for enabling me to live in my lovely flat during my time in Birmingham, and thanks Mom and J for welcoming me back home 7 years after I'd apparently flown the nest. Their encouragement and support has enabled me to fulfill my dreams, and without their generosity I wouldn't have the opportunity to go travelling once I have finished my PhD. Words can't describe how grateful I am to them and I will never forget all that they have done for me!! As well as my parents, I want to thank my whole family for just being great; that includes my sister Jo for great advice, chats, laughs and nights out, Nan and Grandad for their support and care and for stashing all my stuff in their garage, and Billy the cat who actually made several contributions to this thesis when walking over the keyboard.

I would like to thank my friends who have been great fun and support for the last God knows how many years and Mike who has always shown such kindness and given me a place to stay in Birmingham whenever I returned.

Finally I would like to thank the Biotechnology and Biological Sciences Research Council (BBSRC), who funded my research and development for the 4 years of my PhD.

List of contents

Results and discussion: Part I

CHAPTER 3: The preparation of apo-dIII. Cyclic and aberrant cyclic reactions catalysed by dI_2dIII complexes made with apo-dIII from *R. rubrum* transhydrogenase. 68

List of figures

List of tables

List of abbreviations

$AcPdAD^+$	3-acetylpyridine adenine dinucleotide (oxidised)
AcPdADH	3-acetylpyridine adenine dinucleotide (reduced)
AcPdAD(H)	3-acetylpyridine adenine dinucleotide (oxidised or reduced)
ADH	Alcohol dehydrogenase
B. taurus	*Bos taurus*
Bis-tris	Bis(2-hydroxyethyl)aminotris(hydroxymethyl)methane
BSA	Bovine serum albumin
CHES	*N*-Cyclohexyl-2-aminoethanesulfonic acid
DMSO	Dimethyl sulfoxide
dNTP	deoxyribonucleotide
DTT	Dithiothreitol
E. coli	*Escherichia coli*
En. histolytica	*Entamoeba histolytica*
EDTA	Ethylene-diamine-tetra-acetic acid
GR	Glutathione reductase
GSH	Reduced glutathione
GSSG	Oxidised glutathione
GuHCl	Guanidine hydrochloride
H. sapiens	*Homo sapiens*
H_2NADH	1, 4, 5, 6-tetrahydronicotinamide adenine dinucleotide
H_2NADPH	1, 4, 5, 6-tetrahydronicotinamide adenine dinucleotide phosphate
HEPES	4-(2-hydroxyethyl)-1-piperazineethanesulphonic acid
ICDH	Isocitrate dehydrogenase
LB	Luria-Bertani
MOPS	3-(N-morpholino)propanesulphonic acid
NAD(H)	Nicotinamide adenine dinucleotide (oxidised or reduced)
$NAD(P)^+$	Nicotinamide adenine dinucleotide (oxidised) or Nicotinamide adenine dinucleotide phosphate (oxidised)
NADP(H)	Nicotinamide adenine dinucleotide phosphate (oxidised or reduced)
NAD(P)H	Nicotinamide adenine dinucleotide (reduced) or Nicotinamide adenine dinucleotide phosphate (reduced)
PCR	Polymerase chain reaction
PEG	Polyethylene glycol
Pi	Inorganic phosphate
PMSF	Phenylmethanesulfonyl fluoride
R. rubrum	*Rhodospirillum rubrum*
SDS	Sodium dodecyl sulphate
SDS PAGE	Sodium dodecyl sulphate polyacrylamide gel electrophoresis
tris	Tris(hydroxymethyl)aminomethane
v/v	volume/volume
w/v	weight/volume

CHAPTER 1

Introduction

1.1 Preliminary comments.

Transhydrogenase is a protein located in energy-transducing membranes; these include the cytoplasmic membrane of bacteria and the inner membrane of mitochondria. It is driven by the energy of the proton electrochemical gradient, Δp, which is generated by the action of the respiratory chain. Transhydrogenase catalyses the reduction of $NADP^+$ by NADH to produce NAD^+ and NADPH (equation 1). During this hydride transfer reaction protons are translocated inwards across the membrane from the *p*-phase to the *n*-phase. One proton is translocated across the membrane per hydride transferred, *i.e.* the H^+/H^- ratio is 1 (Bizouarn *et al.* 1996b). The reaction is reversible, although under most physiological conditions it is thought to operate in the forward direction (left to right).

$$NADH + NADP^+ + H^+_p \leftrightarrow NAD^+ + NADPH + H^+_n \qquad \text{equation 1}$$

H^+_n and H^+_p denote protons present in the *n* and *p* aqueous phases respectively. The *n*-phase represents the inside of the cell in bacteria or the matrix of mitochondria. The *p*-phase represents the outside of the cell in bacteria or the cytoplasmic side of the membrane in mitochondria.

In the presence of Δp the rate of the forward reaction is increased approximately 10 fold. The equilibrium is also shifted towards the formation of NADPH such that the mass action ratio in the presence of Δp is 500 and in the absence of Δp is 1 (Rydstrom *et al.* 1970).

1.2 An overview of respiratory and photosynthetic electron transfer.

During metabolism, glucose is converted to pyruvate by glycolysis. The pyruvate then enters the tricarboxylic acid cycle producing NADH, which can donate reducing equivalents to the electron transport chain. The electron transport chain is located in an "energy-transducing membrane" (Figure 1.1).

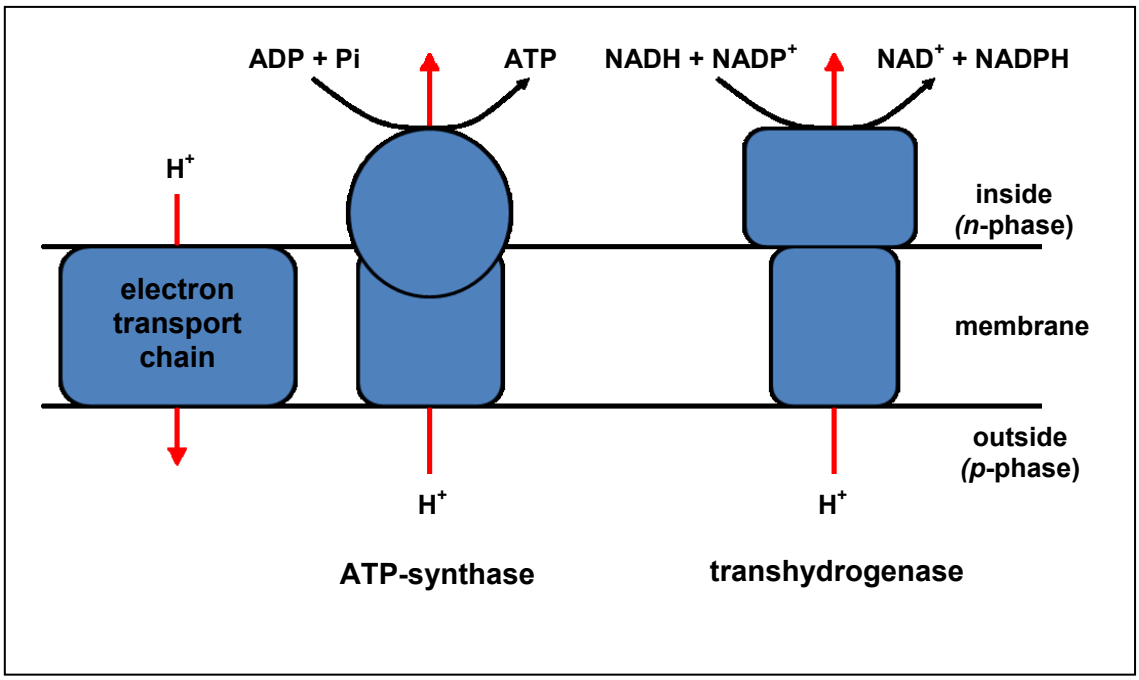

Figure 1.1 The chemiosmotic proton circuit.

The electron transport chain pumps protons across the membrane building up a proton electrochemical gradient, Δp. ATP-synthase and transhydrogenase use the energy of Δp to drive their reactions. Whilst translocating protons across the membrane, ATP-synthase produces ATP from ADP and Pi, and transhydrogenase transfers a hydride ion from NADH to $NADP^+$ producing NAD^+ and NADPH.

The electron transport chain comprises a set of proton pumping complexes such as the NADH dehydrogenase complex (complex I), the cytochrome bc_1 complex (complex III) and the cytochrome oxidase complex (complex IV). Typically, the reduction of

complex I by NADH initiates electron transfer through the complexes to oxygen. During electron flow, protons are pumped across the membrane into the *p*-phase by complexes I and III creating a proton electrochemical gradient, Δp. In photosynthetic bacteria, such as *Rhodospirillum rubrum*, a reaction centre uses light energy to drive cyclic electron transfer through a cytochrome bc_1 complex and hence to pump protons across the membrane.

ATP-synthase uses the energy of Δp, to translocate protons back across the membrane to the *n*-phase and synthesise ATP from ADP and inorganic phosphate (Mitchell 1966). Transhydrogenase also translocates protons back across the membrane to the *n*-phase using the energy of Δp to drive $NADP^+$ reduction by NADH.

1.3 The function of transhydrogenase.

Transhydrogenase catalyses the hydride transfer reaction (shown by equation 1) involving the nicotinamide nucleotides NAD(H) and NADP(H). These two nucleotides play very different roles in metabolism; NAD(H) being mostly involved in catabolism and NADP(H) being mostly involved in anabolism. Since transhydrogenase involves both nucleotides, it is clear that the enzyme has a role in regulating the relative cellular concentrations of NAD(H) and NADP(H) (Kaplan 1985). The crucial function of transhydrogenase may be to produce NADPH. NADPH is required by the cell for various processes and is an important molecule in anabolism. It is required for biosynthetic reactions in the cell (Hanson *et al.* 1980); examples of metabolic processes requiring NADPH are fatty acid and amino acid biosynthesis (Ambartsoumian *et al.* 1994). NADPH also plays an important role in protecting the cell against oxidative stress via the reduction of glutathione (Oshino *et*

al. 1977; Hoek *et al.* 1988; Arkblad 2005). The enzyme glutathione reductase uses the reducing power of NADPH to break a disulphide bond in oxidised glutathione (GSSG). The resulting reduced form of glutathione (GSH) is a cellular antioxidant and acts as a scavenger for reactive oxygen species (Hickman *et al.* 2002). Transhydrogenase is also believed to have a role in the regulation of the tricarboxylic acid cycle (Sazanov *et al.* 1994).

Other enzymes, including those involved in the pentose phosphate pathway, are also involved in the production of NADPH, and can contribute to NADPH production for biosynthesis (Hanson *et al.* 1980). In *Escherichia coli*, transhydrogenase produces ~40% of the NADPH needed for biosynthesis (Sauer *et al.* 2004). Deletion of the transhydrogenase gene from *Caenorhabditis elegans* did not lead to any effect on the life span of the organism (Pestov 2009). However, an increased sensitivity to oxidative stress was reported (Arkblad 2005).

Experiments using mice lacking a functional transhydrogenase (Toye *et al.* 2005; Freeman *et al.* 2006a; Freeman *et al.* 2006b) have showed increased glucose intolerance, and had impaired insulin secretion from their pancreatic β-cells in a glucose tolerance test compared to wild-type mice. Other evidence has shown that oxidative stress is a key factor in the progression of type-II diabetes (Kaneto *et al.* 2005; Lowell *et al.* 2005).

1.4 The polypeptide arrangement and architecture of transhydrogenase from different species.

Although the distribution of transhydrogenase is patchy among species (Jackson *et al.* 2009), the size and architecture of the enzyme is species independent. However, the polypeptide arrangements differ between species (Figure 1.2).

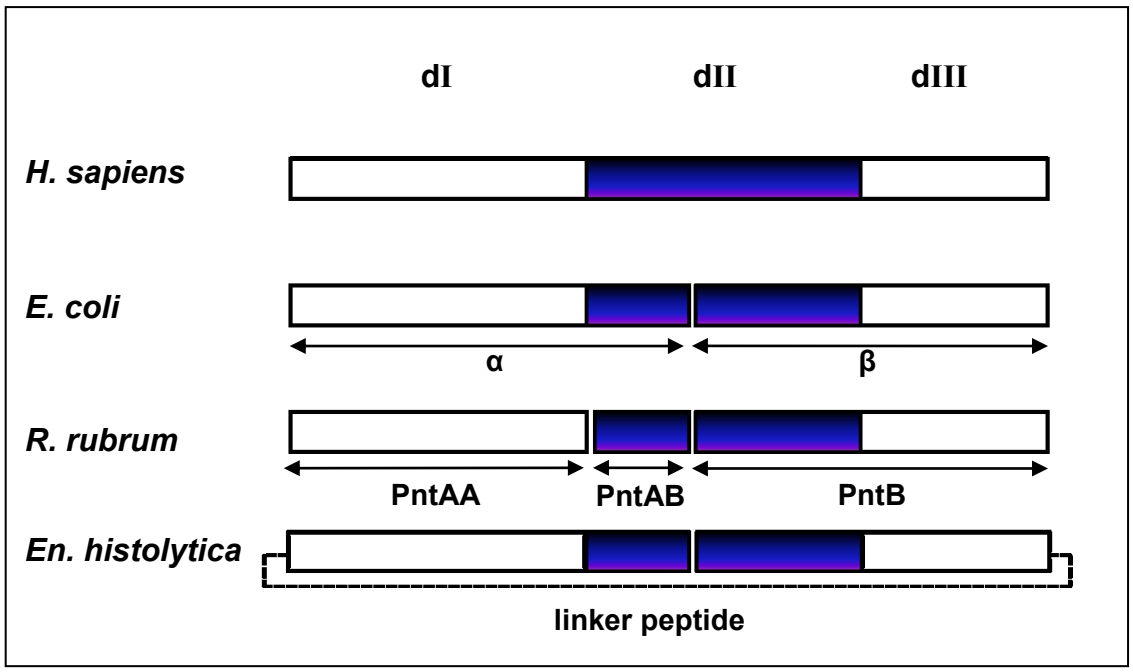

Figure 1.2 The polypeptide arrangement of transhydrogenase from different species.

The number of polypeptides that comprise transhydrogenase varies between species. However, in each species there is a region that comprises the hydrophilic dI and dIII components (white) and the membrane-spanning dII component (blue).

In mitochondria, transhydrogenase consists of a single polypeptide that is ~1000 amino acid residues in length (Hojeberg *et al.* 1977; Anderson *et al.* 1978). Two of these polypeptides form the dimeric intact enzyme. There are two types of polypeptide arrangement in bacterial species. Transhydrogenase from *E. coli* consists

of two polypeptides, α (502 residues) and β (462 residues) (Clarke *et al.* 1986). The intact enzyme consists of two α and two β polypeptides ($\alpha_2\beta_2$). Transhydrogenase from *Rhodospirillum rubrum* consists of three polypeptides, PntAA (384 residues), PntAB (139 residues) and PntB (464 residues) (Williams *et al.* 1994; Yamaguchi *et al.* 1994). The PntB polypeptide is similar to the β polypeptide of *E. coli*. Again, the intact enzyme consists of 2 of each polypeptide ($(PntAA)_2(PntAB)_2(PntB)_2$). Transhydrogenase, in some protozoan parasites, for example *Entamoeba histolytica*, exists as a single polypeptide with a different topology to that found in mammalian mitochondria. The N-terminus of the polypeptide corresponds to the N-terminus of PntB from bacteria. This is joined at the C-terminus to the equivalent of the PntA polypeptide by a 40-residue linker (Weston *et al.* 2001; Weston *et al.* 2002).

Transhydrogenase has three structural components: dI, dII and dIII (Figure 1.3). The dI component binds NADH, the dIII component binds $NADP^+$ and the dII component spans the membrane and translocates protons across the membrane.

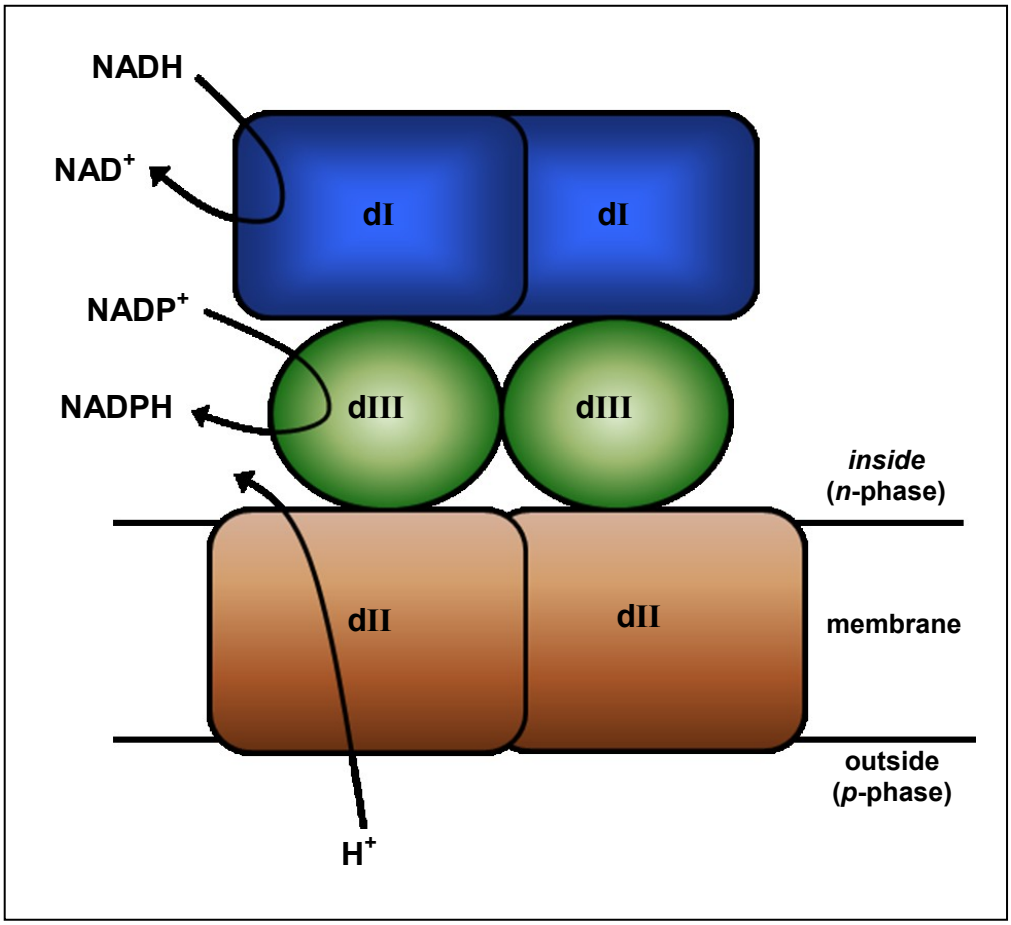

Figure 1.3 Cartoon of the architecture of the components of transhydrogenase.

Despite different polypeptide arrangements, the architecture of transhydrogenase is similar for all species. The dII component (brown) spans the membrane and is involved in proton translocation, the dI component (blue) binds NAD(H) and the dIII component (green) binds NADP(H). The redox reactions associated with the dI and dIII components are shown.

1.5 The chemical structure of the nicotinamide nucleotide substrates.

The physiological substrates for transhydrogenase are NAD(H) and NADP(H). These nicotinamide nucleotides have five functional chemical groups; a nicotinamide ring, two ribose groups, an adenine ring and a pyrophosphate group (Figure 1.4). Although the groups themselves are essentially rigid, rotation of the bonds between the groups

allows the nucleotides to adopt different conformations. When bound to proteins, the nucleotides adopt a conformation specified by the binding-site.

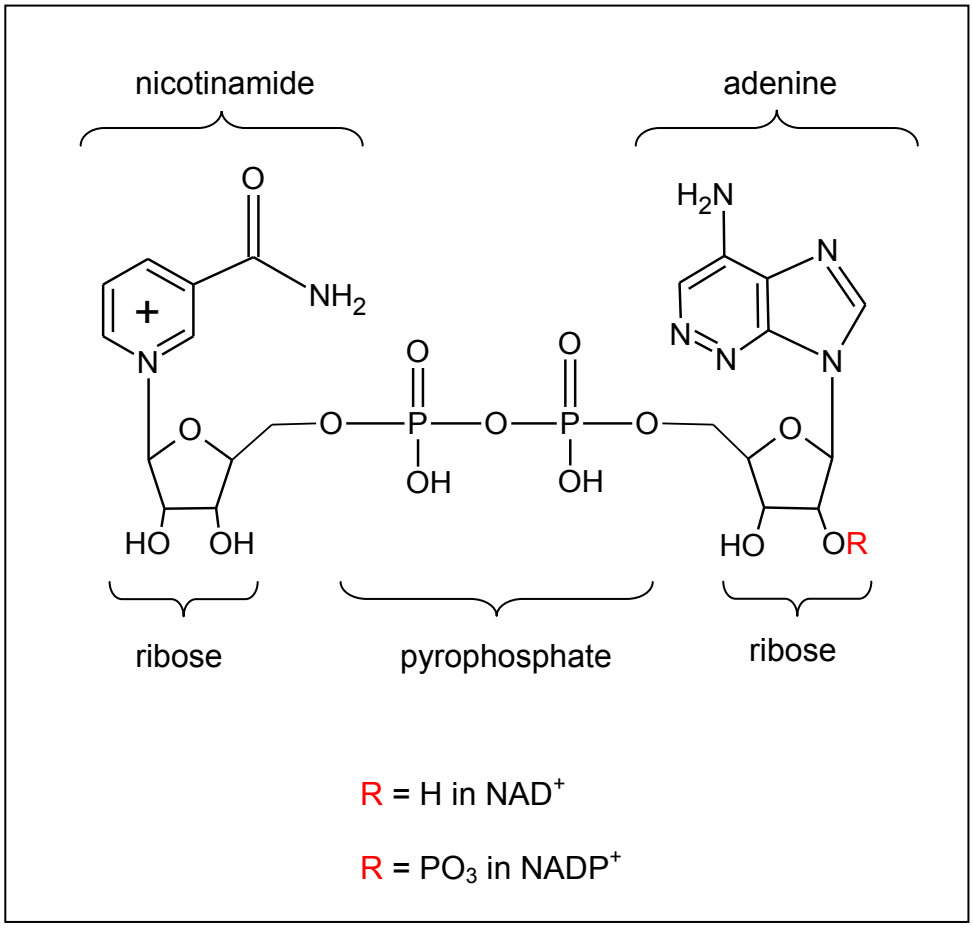

Figure 1.4 The chemical structure of nicotinamide nucleotides.

NAD(H) and NADP(H) are the physiological nucleotides for the dI and dIII components of transhydrogenase, respectively. They comprise 5 different moieties, the nicotinamide ring, the adenine ring, two ribose groups and a pyrophosphate group. NAD(H) and NADP(H) differ by a group at the C2 position of the adenine ribose (R). This group is a hydroxyl for NAD(H) and a phosphate for NADP(H). This figure was produced using ACD/ChemSketch freeware.

1.6 The stereospecificity of the hydride transfer reaction of transhydrogenase.

Hydride transfer between NADH and $NADP^+$ occurs between the C4 carbon atoms of the respective dihydronicotinamide and nicotinamide rings (Figure 1.5). The nicotinamide group of the oxidised form of the nucleotides holds a positive charge, whereas the reduced form does not. The reduced form has two pro-chiral hydrogen atoms at position C4. The positions of these hydrogen atoms are termed *pro-R* or *pro-S* depending on whether they are on the *re* face or the *si* face of the nicotinamide ring, respectively. During the hydride transfer reaction, a hydride ion can be transferred from either the *pro-R* or *pro-S* position. The hydride ion transferred is dictated by the binding-site of the enzyme. Usually, an enzyme binds the nucleotide in a particular orientation, either a *syn* or an *anti* conformation. These nucleotide conformations differ by a 180° rotation around the glycosidic bond between the nicotinamide ring and the adjacent ribose. Most enzymes that bind the nucleotide in the *anti* conformation will transfer the hydride ion in the *pro-R* position; these are grouped as A-specific enzymes. Similarly, most enzymes that bind the nucleotide in the *syn* conformation will transfer the hydride ion in the *pro-S* position; these are B-specific enzymes (Nambiar *et al.* 1983; Garcia *et al.* 1995).

The hydride transfer reaction of transhydrogenase is stereospecific, such that the hydride ion is transferred from the C4 *pro-R* position of the NADH dihydronicotinamide ring to the C4 *pro-S* position of the $NADP^+$ nicotinamide ring (Lee *et al.* 1965).

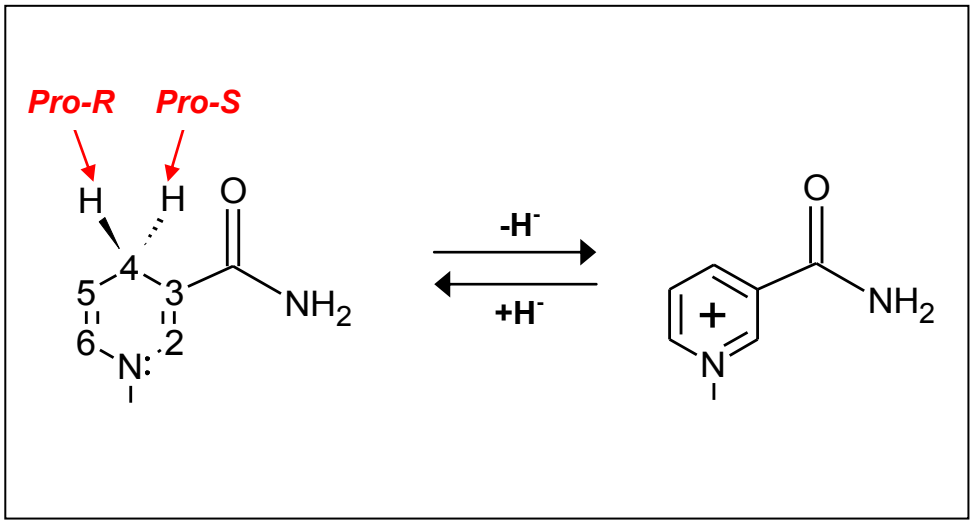

Figure 1.5 The stereospecificity of the hydride transfer reaction.

The forward hydride transfer reaction of transhydrogenase is stereospecific such that the *pro-R* hydride ion at position C4 of NADH is transferred to the C4 *pro-S* position of $NADP^+$. Shown, is the nicotinamide group of NADH and its conversion to NAD^+ during hydride transfer. The dihydronicotinamide ring of NADH is uncharged, whereas the nicotinamide ring of NAD^+ carries a net positive charge. This figure was produced using ACD/ChemSketch freeware.

1.7 Isolated recombinant forms of the dI and dIII components.

Recombinant dI and dIII from various species have been isolated and purified as soluble proteins (Diggle *et al.* 1995b; Diggle *et al.* 1996; Fjellstrom *et al.* 1997; Yamaguchi *et al.* 1997). The dI component of transhydrogenase contains the NAD^+/NADH binding site and, when isolated, exists as a dimer (Diggle *et al.* 1995b; Venning *et al.* 2001). The molecular weight of a dI monomer from *R. rubrum* is ~40 KDa (Venning *et al.* 1997). In transhydrogenase from *R. rubrum*, the dI component is a separate polypeptide. In chromatophores, dI can be washed away fully inactivating the enzyme (Cunningham *et al.* 1992; Williams *et al.* 1994). When

recombinant isolated dI is added to the chromatophores (now dI depleted), full activity is restored (Diggle *et al.* 1995b). This shows that recombinant dI retains full activity. The binding affinity of dI (from both *R. rubrum* and *E. coli*) for NAD(H) is similar in the isolated form of the protein and in the intact enzyme (K_d for NADH ≈ 20 μM; K_d for NAD^+ ≈ 300 μM) (Diggle *et al.* 1995a; Diggle *et al.* 1995b; Bizouarn *et al.* 1996a; Venning *et al.* 2001; Bizouarn *et al.* 2005).

In all species, the dIII component is present on the same polypeptide as at least part of dII. Therefore, to isolate dIII from *R. rubrum,* a plasmid was engineered where a start codon was inserted at the beginning of the dIII gene (Williams *et al.* 1994; Diggle *et al.* 1996). The molecular weight of a dIII monomer is ~21 KDa (Venning *et al.* 1997). Isolated dIII binds NADP(H) extremely tightly compared to the intact enzyme, and is believed to be locked predominantly in an occluded conformation, from which nucleotides dissociate extremely slowly. Throughout purification in the absence of added NADP(H), dIII remains almost fully occupied (Diggle *et al.* 1996). However, the protocol for the purification of isolated dIII used in this work included 4 μM $NADP^+$ in all buffers to ensure full occupancy of the protein. Since nucleotide binding to isolated dIII is so tight, measuring binding affinities for NADP(H) has been extremely difficult. However, first-order rate constants for $NADP^+$ and NADPH release were measured using two independent methods. Values were 0.018 s^{-1} and 0.03 s^{-1} for $NADP^+$ release and 0.00045 s^{-1} and 0.0006 s^{-1} for NADPH release (Diggle *et al.* 1996; Rodrigues *et al.* 2001). Within error, these results are in agreement and show that isolated dIII binds NADPH with a higher affinity than $NADP^+$.

When isolated dI and dIII are mixed they spontaneously form a complex comprising a dI dimer and a dIII monomer (dI_2dIII). The dI dimer and the dIII component are tightly bound with a K_d of ≤60 nM (Venning *et al.* 2001). This dI_2dIII

complex is catalytically active; it can catalyse hydride transfer without proton translocation (Yamaguchi *et al.* 1995; Diggle *et al.* 1996). This proves that hydride transfer involves only the dI and dIII components and not the membrane-spanning dII component. The dIII component, in dI_2dIII complexes, is predominantly locked in its occluded conformation and binds NADP(H) with an even higher affinity (~5 fold) than isolated dIII (Venning *et al.* 2001). In the complexes, the two dI components have different binding affinities for NAD(H). The first dI component binds NADH with a similar affinity as isolated dI and the other binds NADH much more weakly with a K_d of ~300 μM (Venning *et al.* 2001). The dI component with the weaker affinity for NADH is associated with the single dIII component.

There is more information on the structure of transhydrogenase from *R. rubrum* than on the enzyme from other species. Due to its polypeptide arrangement (see Figure 1.2), *R. rubrum* transhydrogenase can be separated into a soluble fraction and an insoluble fraction (Fisher *et al.* 1971); this makes it a useful experimental system. The dI_2dIII complex formed from reconstituted isolated *R. rubrum* dI_2 and dIII, is tightly bound with a K_d of ≤60 nM (Venning *et al.* 2001). The reconstitution of isolated *E. coli* dI_2 and dIII also form a dI_2dIII complex. However, the binding is much weaker (Fjellstrom *et al.* 1999b). Experiments showed that hybrid complexes of *E. coli* dIII and *R. rubrum* dI associate more tightly than do complexes of *E. coli* dIII and *E. coli* dI, and that their catalytic properties are similar to those of the *R. rubrum* heterotrimer. Thus, *E. coli* dIII is often used in complex with *R. rubrum* dI experimentally (for examples see Fjellstrom *et al.* 1999a; Bergkvist *et al.* 2000; Pedersen *et al.* 2003). The dI component from *R. rubrum* also makes catalytically active, stable complexes with dIII from *Homo sapiens* (Peake *et al.* 1999b), *Bos*

taurus (Yamaguchi *et al.* 1995), *En. histolytica* (Weston *et al.* 2002) and *Mycobacterium tuberculosis* (Wilson *et al.* 2006).

1.8 *In vitro* reactions catalysed by the *R. rubrum* dI_2dIII complex of transhydrogenase.

In the living cell, transhydrogenase catalyses a forward reaction (equation 1 from left to right) and a reverse reaction (equation 1 from right to left); these are the reduction of $NADP^+$ by NADH and the reduction of NAD^+ by NADPH, respectively. These two reactions are coupled to proton translocation across the membrane through dII. *In vitro*, dI_2dIII complexes, formed when isolated dI and dIII are reconstituted, catalyse the forward and reverse reactions without proton translocation. These reactions do not result in a net absorbance change because the maximum absorption wavelength is similar for both NADPH and NADH (340 nm). Thus, the forward and reverse reactions catalysed by dI_2dIII complexes are routinely measured using nucleotide analogues with distinct maximum absorption wavelengths. A commonly used $NADP^+$ analogue is thio-nicotinamide dinucleotide phosphate (thio-$NADP^+$), which in its reduced form has a maximum absorption wavelength of 395 nm. A useful analogue of NAD^+ or NADH is 3-acetylpyridine adenine dinucleotide ($AcPdAD^+$ in its oxidised form and AcPdADH in its reduced form), which in its reduced form has a maximum absorption wavelength of 375 nm. *In vitro,* dI_2dIII complexes also catalyse an unphysiological "cyclic" reaction; in which nucleotide analogues are also used.

1.8.1 The forward reaction catalysed by *R. rubrum* dI_2dIII complexes.

The forward transhydrogenation reaction is routinely measured as either the reduction of thio-$NADP^+$ by NADH or the reduction of $NADP^+$ by AcPdADH. In the latter reaction, the on-enzyme rate of AcPdADH oxidation was identical to the rate of $NADP^+$ reduction, showing that the reaction is direct and does not involve reduced-enzyme intermediates (Venning *et al.* 1999). In the experiments of Venning *et al.*, upon rapid mixing under stopped-flow conditions, dI and dIII quickly bound to form dI_2dIII complexes. $NADP^+$ was already bound to dIII, and AcPdADH bound rapidly to dI after mixing. An initial rapid single turnover burst was observed, which was due to hydride transfer producing NADPH bound to dIII and $AcPdAD^+$ bound to dI. After this initial single turnover burst, the reaction proceeded at an extremely slow steady-state rate. This is because the product NADPH dissociates very slowly from dIII in dI_2dIII complexes before fresh $NADP^+$ can bind. Thus NADPH release from dIII is the rate limiting step of the steady-state reaction.

1.8.2 The reverse reaction catalysed by *R. rubrum* dI_2dIII complexes.

The reverse reaction is routinely measured as the reduction of $AcPdAD^+$ by NADPH. The on-enzyme rate of $AcPdAD^+$ reduction was shown to be identical to the rate of NADPH oxidation in this reaction. Again, this shows that the reaction is direct and involves no reduced-enzyme intermediates (Venning *et al.* 1997). In the experiments of Venning *et al.*, under stopped-flow conditions dI and dIII were mixed and quickly bound to form dI_2dIII complexes. The isolated dIII was pre-treated such that it was fully occupied by NADPH, and after mixing, $AcPdAD^+$ rapidly bound to dI. This

resulted in a rapid single turnover burst of hydride transfer between the bound nucleotides producing $NADP^+$ bound to dIII and AcPdADH bound to dI. Following the initial burst, the reaction proceeded at an extremely slow steady-state rate. This is because after the first round of hydride transfer, $NADP^+$ slowly dissociates from dIII in dI_2dIII complexes before fresh NADPH can bind. Thus, $NADP^+$ release is the rate limiting step of the steady-state reaction.

1.8.3 The cyclic reaction catalysed by *R. rubrum* dI_2dIII complexes.

Although the cyclic reaction is a wholly unphysiological reaction, it is a useful system for studies on the transhydrogenase mechanism. The reaction is defined as the combined reduction of $NADP^+$ by NADH and oxidation of NADPH by $AcPdAD^+$, when both take place without either the $NADP^+$ or the NADPH dissociating from the enzyme (Whitehead *et al.* 2009) (Figure 1.6). The net reaction is the reduction of $AcPdAD^+$ by NADH, and is not accompanied by proton translocation through dII (Hutton *et al.* 1994; Bizouarn *et al.* 1997). The rate of the cyclic reaction in dI_2dIII complexes proceeds at least 1000 fold faster than the steady-state rates of the forward and reverse reactions (the rate of the cyclic reaction is typically ~2710 mol $AcPdAD^+$ reduced mol^{-1} dIII min^{-1}). This is because the very slow dissociation of $NADP^+$ and NADPH from the protein is not necessary for cyclic reaction turnover; NADP(H) remains tightly bound to dIII throughout. In dI_2dIII complexes, hydride transfer between bound nucleotides (Venning *et al.* 1997; Pinheiro *et al.* 2001), $AcPdAD^+$ binding and AcPdADH release, and NADH binding and NAD^+ release to/from dI (Venning *et al.* 1999; Venning *et al.* 2000) are all fast processes. However, NADP(H) dissociation from dIII is very slow (Diggle *et al.* 1996; Fjellstrom *et al.* 1999b). This

results in very slow steady-state rates of the forward and reverse reactions and a rapid cyclic reaction in dI_2dIII complexes.

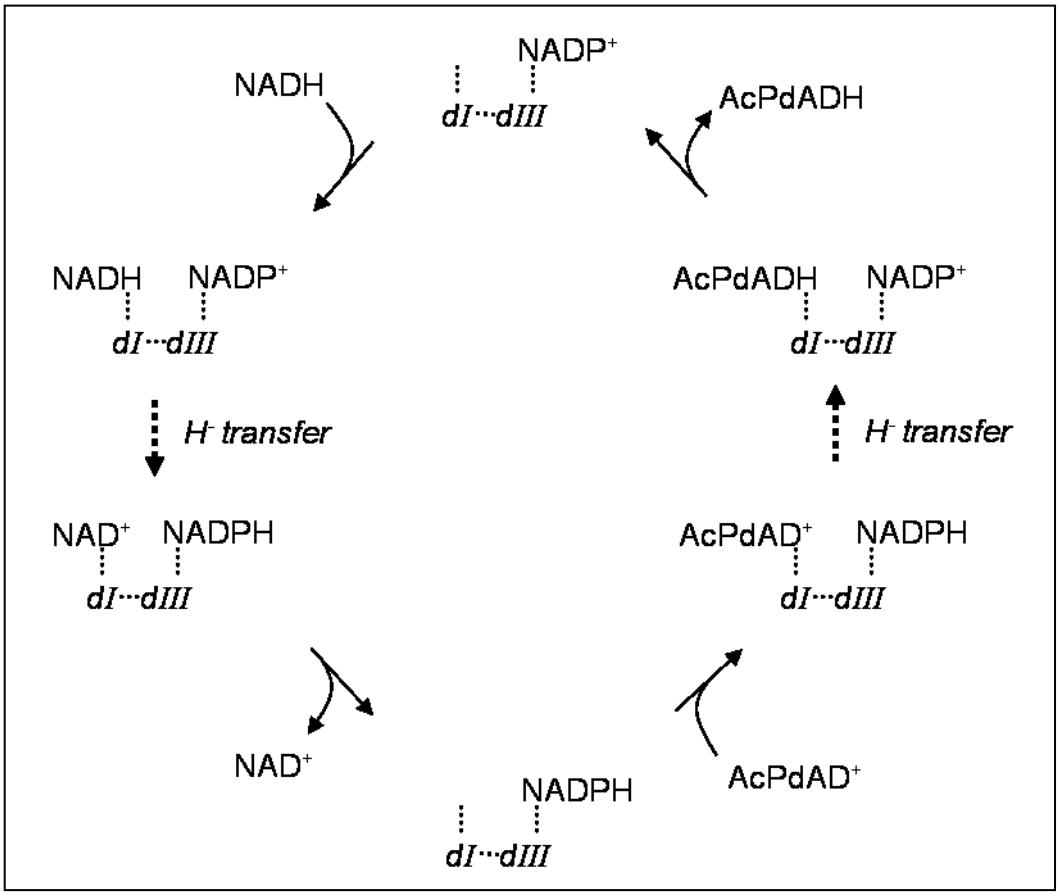

Figure 1.6 Scheme of the cyclic reaction.

In this scheme, the dotted lines indicate interactions between dI and dIII, and between the protein components and bound nucleotides. The dashed arrows show the two hydride transfer steps in the cyclic reaction. Only one of the two dI subunits is depicted.

Overall, the cyclic reaction is defined as the combined reduction of $NADP^+$ by NADH and oxidation of NADPH by $AcPdAD^+$, without $NADP^+$ or NADPH dissociating from the enzyme (Whitehead *et al.* 2009). When dI and dIII are mixed they spontaneously form a dI_2dIII complex. Purified under conditions described in Section 2.2.2, dIII contains tightly bound $NADP^+$. Once added, NADH rapidly binds to dI and reduces the $NADP^+$ bound to dIII. The resulting NAD^+ dissociates from dI whilst the NADPH remains tightly bound to dIII. $AcPdAD^+$ then binds to dI and is reduced by the NADPH on dIII. The resulting AcPdADH dissociates from dI whilst $NADP^+$ remains tightly bound to dIII. Another molecule of NADH binds to dI and the cycle is repeated.

In the intact enzyme, NADP(H) binding to, and release from, dIII are coupled to proton translocation through dII via long-distance conformational changes (see Jackson 2003) and are much faster (~1000 fold) than in dI_2dIII complexes. This results in much faster rates of the forward and reverse reactions in the intact enzyme. In the presence of the membrane-spanning dII component, NADP(H) dissociation is much faster and is driven by Δp. Depending on pH, the rates of the forward, reverse and cyclic reactions in the intact enzyme are similar (Bizouarn *et al.* 1997).

During the cyclic reaction, hydride ion equivalents are transferred first from the C4 *pro-R* position of the dihydronicotinamide ring of NADH to the C4 *pro-S* position of the nicotinamide ring of $NADP^+$, and then from the C4 *pro-S* position of the NADPH to the C4 *pro-R* position of $AcPdAD^+$. Overall this leads to the experimentally observed hydride transfer from the C4 *pro-R* position of NADH to the C4 *pro-R* position of $AcPdAD^+$ (Stilwell *et al.* 1997).

1.9 The structure of the membrane-spanning dII component of transhydrogenase.

Unfortunately, as yet no crystal structures of transhydrogenase have been solved that include the dII components. A high-resolution structure of the intact enzyme is extremely sought after; it will offer a better understanding of the role of dII in the coupling between proton translocation and hydride transfer. The dII component is central in the coupling mechanism. Other methods of structure determination, for example sequence analysis and cysteine labelling, have given some indication of the membrane topology of the dII component (Meuller *et al.* 1999; Studley *et al.* 1999). The dII component comprises 14 transmembrane helices in mammalian

transhydrogenase (Yamaguchi *et al.* 1988; Yamaguchi *et al.* 1991), 13 in *E. coli* transhydrogenase (Meuller *et al.* 1999) and 12 in *R. Rubrum* transhydrogenase (Yamaguchi *et al.* 1993; Jackson *et al.* 2002) (Figure 1.7). Transmembrane helices 1-4 are associated with the α-subunit in *E. coli* dII, and the remaining nine are associated with the β-subunit. It is supposed that located within these helices is a channel, through which the proton is translocated.

Mutagenesis experiments have identified residues in the dII component thought to be important for proton translocation (Hu *et al.* 1999; Bragg 2001; Yamaguchi *et al.* 2003; Whitehead *et al.* 2009). When the highly conserved residues βHis91, βSer139, βAsn222 and βGly252 (*E. coli* numbering) in dII were mutated in intact transhydrogenase from *E. coli,* the resulting mutant transhydrogenases behaved very similarly to dI_2dIII complexes lacking the dII component (Bragg 2001; Yamaguchi *et al.* 2003). There was a loss of proton pumping ability, and the rate of the reverse reaction was significantly inhibited. Furthermore, the release of NADP(H) from the dIII component of the mutant protein was extremely slow. Thus, the mutations were concluded to lock dIII in its occluded conformation by blocking proton translocation. The residues βHis91, βSer139, βAsn222 and βGly252 are present on helices 9, 10, 13 and 14, respectively. Therefore, a model was proposed in which a helix bundle involving these four helices form the proton channel. The residues identified in these mutagenesis experiments are thought to form a hydrogen bonding network to enable the conductance of a proton through the channel.

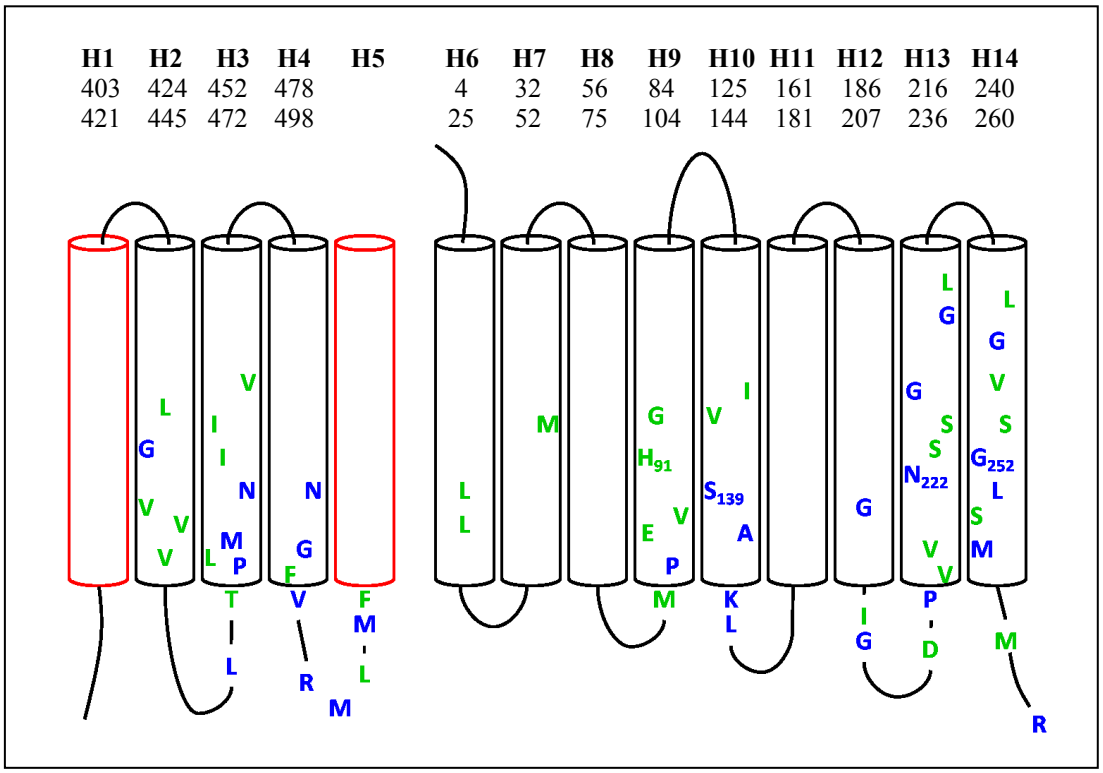

Figure 1.7 Model for the transmembrane dII component of transhydrogenase.

Taken from (Jackson *et al.* 2005). Transmembrane helices are numbered (H1-H14) according to mammalian transhydrogenase (Yamaguchi *et al.* 1988). The numbers on the rows underneath are of the N- and C-terminal residues of the transmembrane helices of *E. coli* transhydrogenase (Meuller *et al.* 1999); helices H1-H4 are present in the α subunit and helices H6-H14 are present in the β subunit. Helices in black appear to be transmembrane in all species and helices in red do not. Residues in blue are invariant and residues in green are highly conserved.

1.10 High-resolution structures of the hydrophilic components of transhydrogenase.

The crystal structure of the intact enzyme has not yet been solved. However, the hydrophilic components of transhydrogenase, dI and dIII, can be isolated and high resolution structures are available of dI from *E. coli* (Johansson *et al.* 2005) and *R.*

rubrum (Buckley *et al.* 2000; Prasad *et al.* 2002) and of dIII from *R. rubrum* (Jeeves *et al.* 2000; Sundaresan *et al.* 2003), *B. taurus* (Prasad *et al.* 1999) and *H. sapiens* (White *et al.* 2000). When isolated dI and dIII are reconstituted, they form a dI_2dIII complex. The crystal structure of this complex has been solved (Cotton *et al.* 2001; Mather *et al.* 2004; Bhakta *et al.* 2007) and its asymmetry described. For a more complete list of published crystal structures available for transhydrogenase, see Table 6.1.

1.10.1 The structure of the dI component of transhydrogenase.

The crystal structure of dI has been solved bound to NADH, NAD^+ or in its apo-protein form (Buckley *et al.* 2000; Prasad *et al.* 2002; Johansson *et al.* 2005) (Figure 1.8). As in solution, crystallised dI is dimeric. Each dI monomer comprises two domains, dI.1 and dI.2. Both domains comprise a Rossmann fold; that is a parallel, twisted six-stranded β-sheet flanked by α-helices and loops. This fold is typical for nicotinamide nucleotide-binding proteins (Rossmann *et al.* 1974; Eventoff *et al.* 1975). The domains dI.1 and dI.2 are separated by a deep cleft containing the NAD(H)-binding site, and are connected by two long α-helices. There is also a β-hairpin that protrudes from the dI.2 part of one monomer to the other.

Crystal structures (Buckley *et al.* 2000; Prasad *et al.* 2002) and NMR experiments (Diggle *et al.* 1995a; Quirk *et al.* 1999) have shown the so-called mobile loop of dI that is thought to close over NAD(H) when bound. The mobile loop has been compared to loop E of dIII (see Section 1.10.2.2). It contains a tyrosine residue, Tyr235, in a G-Y-A motif that forms hydrogen bonds with an arginine residue, Arg127. This arginine residue interacts with the nicotinamide ring and the

pyrophosphate of NAD(H). This set of interactions is very similar to those in loop E of dIII involving the nucleotide NADP(H) and the residues Tyr171 and Arg90.

The nicotinamide group of NAD(H) bound to dI can adopt either a "distal" or "proximal" position relative to the nicotinamide group of NADP(H) in dIII. There is a loop in dI called the "RQD-loop"; site-directed mutagenesis experiments have identified residues within this loop in *R. rubrum* dI that are thought to be important for stabilising the (dihydro)nicotinamide ring of NAD(H) in the proximal position for hydride transfer (van Boxel *et al.* 2003; Brondijk *et al.* 2006). The residue Gln132 forms hydrogen bonds with the carboxamide group of the NAD(H) (dihydro)nicotinamide as well as the hydroxyl group of the NADP(H) ribose. This residue is thought to maintain the proximal position of NADH by acting as a molecular tether, holding the two nucleotides in a position that allows hydride transfer (van Boxel *et al.* 2003). Crystal structures show hydrogen bonding between the side chain of Arg127 and the residues Asp135 and Ser138. It is proposed that these hydrogen bonds and the movement of the Arg127 side chain stabilise the (dihydro)nicotinamide ring of the bound NAD(H) in a proximal position (Brondijk *et al.* 2006). The mutation of all four of these residues (Gln132, Arg127, Asp135 and Ser138) results in pronounced inhibition of hydride transfer.

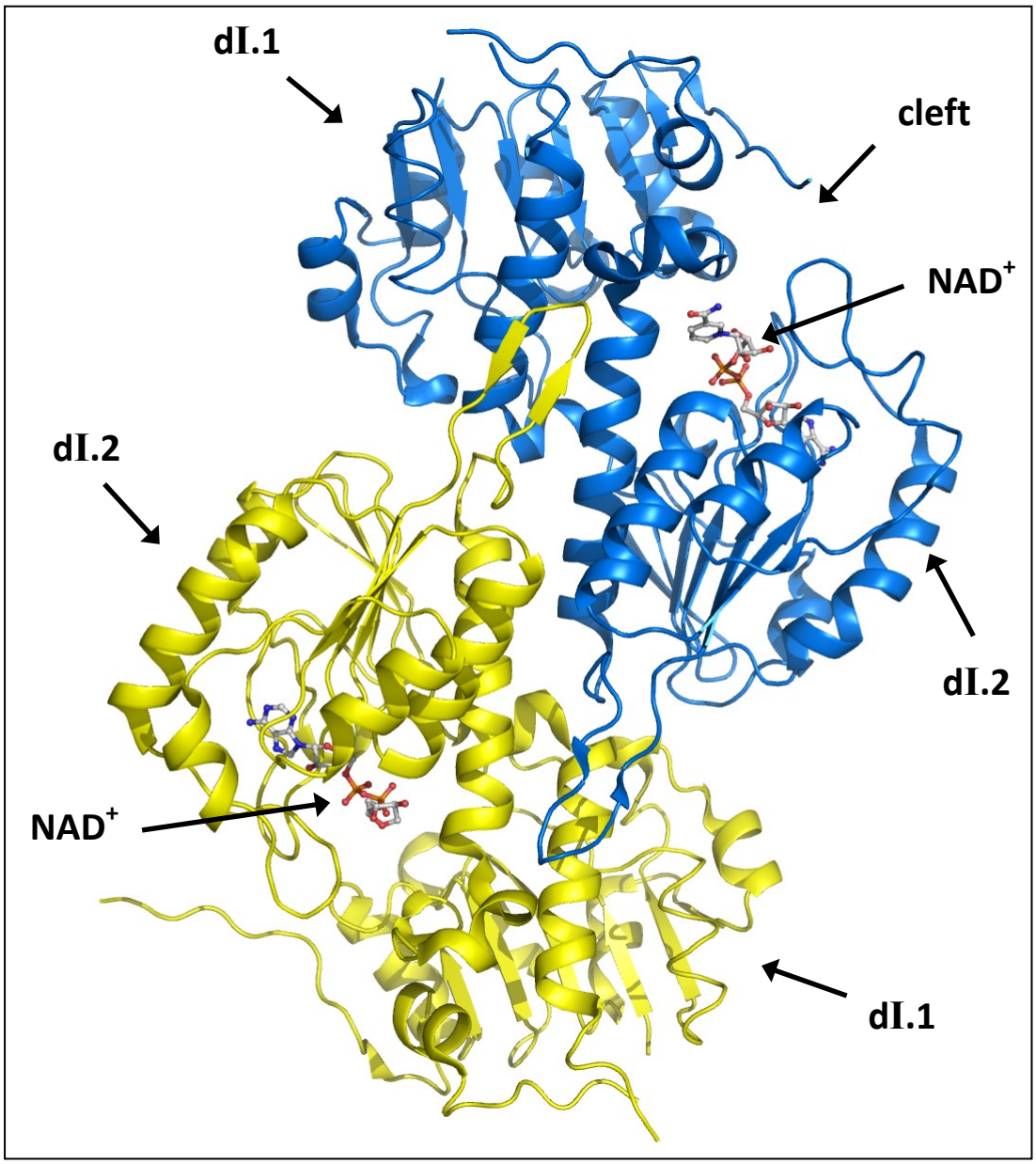

Figure 1.8 Crystal structure of the dI component from *R. rubrum* transhydrogenase.

When isolated in solution or crystallised, dI exists as a dimer. One monomer is shown in yellow and the other in blue. Each monomer comprises two domains, dI.1 and dI.2, which are separated by a cleft that houses the NAD^+-binding site. This figure was produced in Pymol using PDB ID 1F8G.

1.10.2 The structure of the dIII component of transhydrogenase.

Crystal structures (Prasad *et al.* 1999; White *et al.* 2000; Sundaresan *et al.* 2003; Mather *et al.* 2004) show that dIII comprises two βαβαβ motifs with the form and connectivity of a Rossmann fold. However, in transhydrogenase dIII the NADP(H) is bound in a "flipped" orientation compared to other NADP(H)-binding proteins, such that the adenosine group is positioned over the second βαβαβ motif and the nicotinamide group is positioned over the first. The dinucleotide binding site is located in a crevice formed by the βαβαβ motifs and is surrounded by loops including helix D/loop D and loop E (Figure 1.9).

The loop between the first β-sheet and helix contains a GXGXXA fingerprint motif (where X is any amino acid) that interacts with the pyrophosphate group of $NADP^+$. This feature is common to nicotinamide-binding proteins having a Rossmann fold (Bellamacina 1996) (see Section 1.12). NMR experiments, in which $NADP^+$ was replaced by NADPH, showed chemical shift changes in the NADP(H)-binding site, helix D/loop D and loop E (Quirk *et al.* 1999). Helix D/loop D and loop E appear to be important structural elements of dIII, and probably contribute significantly to the mechanism of coupling to proton translocation in the intact enzyme.

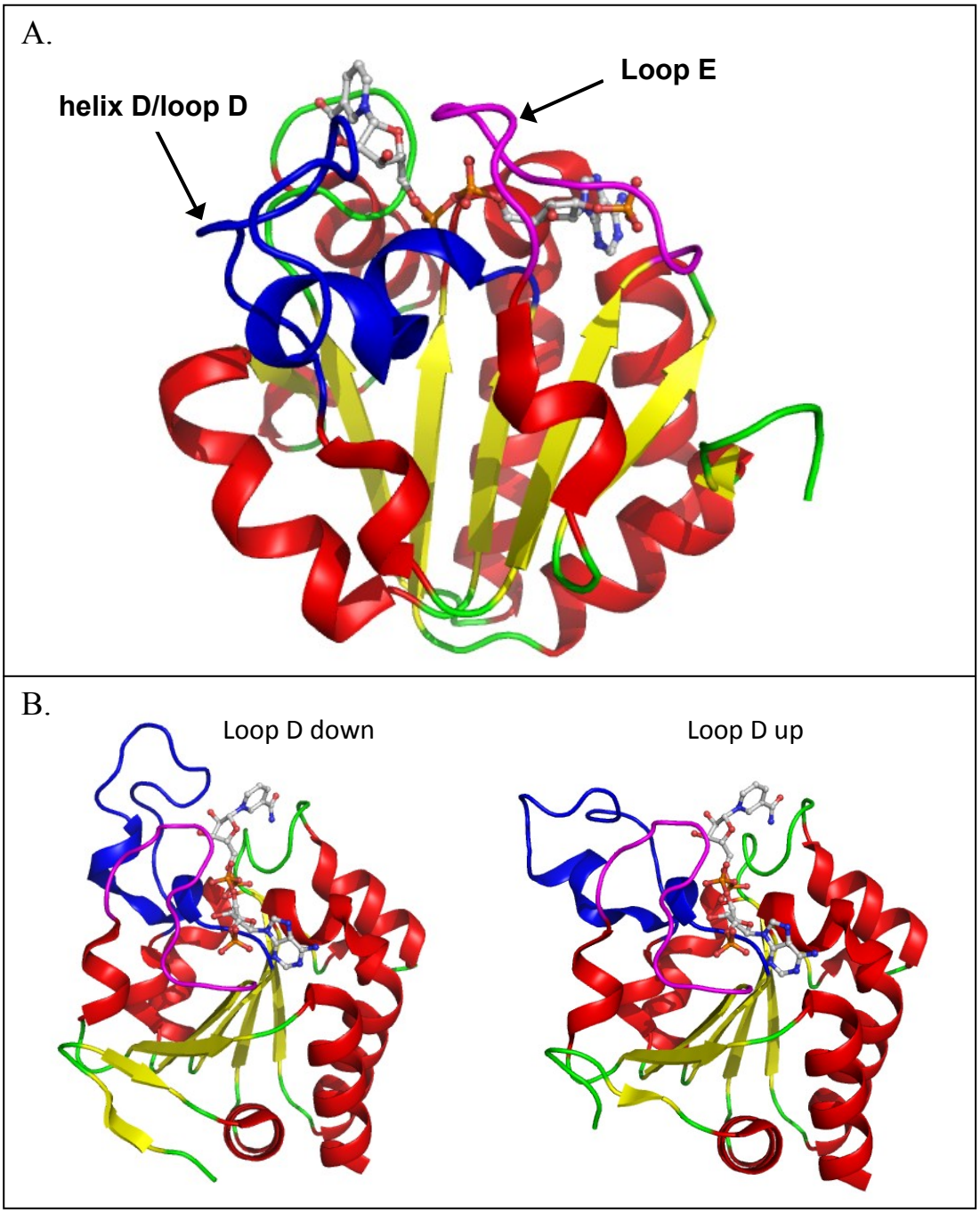

Figure 1.9 Crystal structure of the dIII component from *R. rubrum* transhydrogenase.

When isolated, dIII exists as a monomer (panel A). It is comprised of a parallel β-sheet (yellow) flanked by α-helices (red) and loops (green). The $NADP^+$-binding site is located in a crevice formed by loops, including helix D/loop D (blue) and loop E (magenta). In crystal structures of *R. rubrum* dIII (Sundaresan *et al.* 2003) Loop D can be seen in either an "up" or a "down" position (panel B). This figure was produced in Pymol using PDB ID 1PNO.

1.10.2.1 Helix D/loop D of dIII.

Helix D/loop D interacts with the pyrophosphate group and the ribose rings of NADP(H) as well as loop E of dIII. In crystal structures of dIII from *B. taurus* and *H. sapiens* with bound $NADP^+$, helix D/loop D is in an "up" position and the *si* face of the nicotinamide ring is exposed to solvent. In the crystal structure of isolated dIII from *R. rubrum*, helix D/loop D is shown to undergo a conformational change (Sundaresan *et al.* 2003). This conformational change was independent of the redox state of the bound nucleotide. In both the $NADP^+$-bound form and the NADPH-bound form helix D/loop D can be seen in either an "up" position or a "down" position (Figure 1.9B), suggesting that the mechanism of transhydrogenase involves four states with respect to helix D/loop D; $NADP^+$-loop D up, $NADP^+$-loop D down, NADPH-loop D up, NADPH-loop D down. When helix D/loop D adopted the up position, the *si* face of the nicotinamide ring was exposed to the solvent. When down, helix D/loop D shielded the *si* face of the nicotinamide ring from the solvent and NADP(H) formed close interactions with conserved residues Ser144, Pro145 and Ile146. It should be noted that in all four states there was no conformational change of loop E and it remained in an occluded conformation. From these structures of *R. rubrum* dIII (Sundaresan *et al.* 2003), the authors concluded that helix D/loop D would block hydride transfer when in the "down" position. However, previous experiments and analysis of crystal structures suggest that helix D/loop D has a role involved with information transmission between dIII and dI by regulating the opening and closing of the dI cleft (Cotton *et al.* 2001; Jackson *et al.* 2002; Mather *et al.* 2004).

The highly conserved residue, Asp132 of helix D/loop D interacts with both loop E of dIII and the RQD-loop of dI. Mutagenesis experiments of this residue

showed a significant decrease in affinity for NADP(H) as well as dI, and a loss of proton pumping ability (Meuller *et al.* 1996; Fjellstrom *et al.* 1999a). It was concluded that Asp132 was essential for catalytic and proton pumping activity, and is likely to contribute to the coupling of hydride transfer to proton translocation.

1.10.2.2 Loop E of dIII.

In all structures of isolated dIII (Prasad *et al.* 1999; White *et al.* 2000; Sundaresan *et al.* 2003; Mather *et al.* 2004), loop E is in an occluded conformation. When occluded, loop E acts as a "lid" and is closed over the bound nucleotide. Fluorescence resonance energy transfer experiments show that the loop E lid prevents the release of the nucleotide when occluded, and retracts to form the open conformation of the protein and allow nucleotide dissociation (Rodrigues *et al.* 2002). A structure showing the open conformation of loop E would be highly desirable to further understand the role of loop E in the coupling between hydride transfer and proton translocation.

Loop E contains residues that are present in the NADP(H) binding site and interact with NADP(H) when bound. Among these residues is a conserved G-Y-A motif, where Tyr171 interacts with the nicotinamide ring of NADP(H) and with the invariant residue Arg90. The mutagenesis of the equivalent of Tyr171 in *E. coli* dIII caused a significant decrease in the affinity for NADP(H) (Olausson *et al.* 1993; Johansson *et al.* 2002). Arg90 interacts with the nicotinamide ring and forms hydrogen bonds with the pyrophosphate of NADP(H). There is a similar set of interactions involving the mobile loop of dI and NAD(H) (see Section 1.10.1).

Loop E of dIII also contains a highly conserved K-R-S motif. In *R. rubrum* transhydrogenase this motif consists of the residues Lys164, Arg165 and Ser166,

(Figure 1.10). Of this K-R-S motif, the peptide backbone and the three side-chains form seven hydrogen bonds with the 2'-phosphate group of NADP(H); the side-chain guanidinium of Arg165 also stacks with the adenosine ring of NADP(H) (Figure 1.11).

```
R. rubrum        153-DVEKAGTVLFIKRSMA-SGYAGVENE-177
E. coli          413-EVWKAQNVIVFKRSMN-TGYAGVQNP-437
H. sapiens           EVWKSKQVIVMKRSLG-VGYAAVDNP
B. taurus            EVWKSKQVIVMKRSLG-VGYAAVDNP
```

Figure 1.10 Sequence of fragments from different species showing of the highly conserved K-R-S motif of loop E.

The K-R-S motif is highlighted in grey. Transhydrogenase from *R. rubrum* and *E. coli* are numbered by different conventions; residue numbers are indicated.

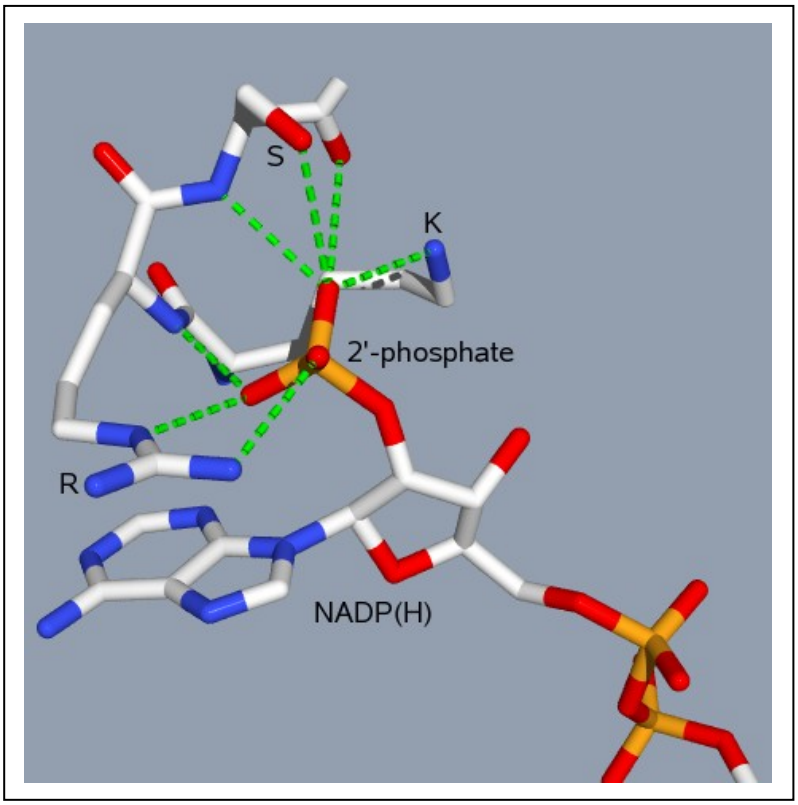

Figure legend over page

Figure 1.11 Hydrogen bonding interactions between the 2'-phosphate group of NADP(H) and the K-R-S motif of loop E.

Crystal structure of *R. rubrum* wild-type dIII (PDB ID 1PNO) showing the K-R-S motif and its interactions with the 2'-phosphate of NADP(H). Hydrogen bonds are shown as dashed green lines. This figure was produced using Swiss-PDB Viewer and Povray.

The residues of the K-R-S motif have been targeted in mutagenesis studies using dIII from *E. coli* (Fjellstrom *et al.* 1999a; Hu *et al.* 1999; Bergkvist *et al.* 2000). The equivalent arginine and lysine residues in *E. coli* transhydrogenase, βArg425 and βLys424, were mutated to cysteine residues (Bergkvist *et al.* 2000). The cyclic reaction was measured in dI_2dIII complexes using mutated and wild-type dIII from *E. coli* reconstituted with wild-type dI from *R. rubrum.* Under the conditions used for the purification of dIII the wild-type protein had 92% occupancy with either $NADP^+$ or NADPH bound in its binding site; 8% of the protein was in its apo-protein form. Under the same conditions, the βR425C mutant was present only in its apo-form. The rate of the cyclic reaction ($AcPdAD^+$ reduction by NADH in the presence of $NADP^+$) was 12% compared to that of wild-type dIII. The rate of the reverse reaction (the reduction of $AcPdAD^+$ by NADPH) had an increased rate of 425% compared to that of wild-type dIII. Since $NADP^+$ release from dIII is the rate limiting step of the reverse reaction, this result shows that the rate of $NADP^+$ dissociation from βR425C in dI_2dIII complexes is faster than from wild-type dIII in dI_2dIII complexes. The NADP(H)-content determination and the enzyme assays are evidence that the βR425C mutant has a significantly weakened affinity for NADP(H) compared to wild-type dIII. The βK424C mutant also had a decreased NADP(H) content compared to wild-type dIII, with 63% of it being in its apo-form. The rate of the cyclic reaction was

45% compared to that with wild-type dIII. The rate of the reverse reaction, as with the βR425C mutant, was 425% of that with wild-type dIII, showing that the βK424C mutant also had a weakened affinity for NADP(H).

In mutagenesis studies of the intact enzyme with functional dII components from *E. coli* transhydrogenase, βLys424 and βArg425 were substituted with other residues (Hu *et al.* 1999). Mutants of these two residues (βK424R, βK424G, βR425K, βR425E, βR425G) showed significantly decreased rates of reverse and cyclic transhydrogenation. The apparent K_m was estimated by measuring the rate of the cyclic reaction as a function of $NADP^+$ and NADPH concentrations for the βK424R mutant, and was found to be >1000 fold higher than that of the wild-type protein. This led to the conclusion that the βK424R mutant had a significantly decreased affinity for NADP(H) compared to wild-type dIII.

The enzyme human aldose reductase also has equivalent K-R-S residues (Lys262, Ser263, and Arg268) in its NADP(H)-binding site (Wilson *et al.* 1992; Harrison *et al.* 1994). Although the residues are not consecutive, there are similarities with transhydrogenase dIII since the lysine and serine residues form hydrogen bonds with the 2'-phosphate of NADP(H). Furthermore, the NADP(H)-binding site involves a "holding" loop that is closed over the bound NADPH. This loop is believed to undergo a conformational change to allow the release of the bound nucleotide, providing another parallel with nucleotide release from transhydrogenase. The R268A mutant of aldose reductase was produced and the crystal structure of the apo-protein was solved (Bohren *et al.* 2005). The mutation caused a significant decrease in affinity for NADP(H) and the holding loop was displaced to adopt a more open conformation compared to the wild-type NADPH-bound structure.

1.10.3 The structure of the asymmetric dI_2dIII complex.

When isolated dI and dIII are reconstituted, they spontaneously form a dI_2dIII asymmetric complex, which lacks the second dIII component known to be present in the intact enzyme (Figure 1.12). This has been shown both in solution (Venning *et al.* 2001) and in the crystalline state (Cotton *et al.* 2001; Mather *et al.* 2004; Bhakta *et al.* 2007). Isolated dI forms a dimer in solution; both dI monomers are present in the asymmetric structure. The absence of the second dIII component is possibly due to isolated dIII being locked predominantly in an occluded conformation. Transhydrogenase is thought to have an alternating-site mechanism (see Figure 1.13), where, at any time, one side of the enzyme (*i.e.* one $dI_1dII_1dIII_1$ monomer) is in an occluded conformation while the other side is in an open conformation. For the second dIII monomer to bind to the dI_2dIII complex, it would thus need to be in the open conformation. The production of isolated dIII in its open state has not yet been achieved. Modelling studies have shown that a second dIII component (in its isolated, occluded form) would not be able to bind to the dI_2dIII complex due to side-chain clashing between the two dIII components (Cotton *et al.* 2001). However, NMR experiments have shown that dIII can bind to the dI_2dIII complex, but with a very low affinity (Quirk *et al.* 1999).

The first structure of the asymmetric complex to be solved (Cotton *et al.* 2001) was associated with the nucleotides NAD^+ and $NADP^+$. Good electron density was observed for $NADP^+$ bound to the dIII component, but only for NAD^+ in one of the dI monomers. The electron density of NAD^+ for the dI monomer associated with dIII was very weak. Higher concentrations of NAD(H) were used in the crystallisation conditions and the structures were solved for both the NAD^+/$NADP^+$-bound and the

NADH/NADPH-bound complexes (Mather *et al.* 2004). In these structures, both dI components show electron density for bound NAD(H) as well as for the NADP(H) bound to dIII. They represent catalytically "dead-end" complexes, since both nucleotides were either in their oxidised or their reduced form. If crystallisation experiments had been performed with the dI_2dIII complex and the physiological nucleotides, $NADP^+$ and NADH, hydride transfer would have occurred. Attempts were made to crystallise the asymmetric complex allowing equilibrium to be reached by hydride transfer during crystallisation but with doubtful success (Sundaresan *et al.* 2005). The unit cell in those experiments contained several undefined complexes, which had either NADH and NADPH bound (dead-end complexes) or indiscernible nucleotide content. Catalytically inactive nucleotide analogues 1, 4, 5, 6-tetrahydronicotinamide adenine dinucleotide (H_2NADH) and 1, 4, 5, 6-tetrahydronicotinamide adenine dinucleotide phosphate (H_2NADPH) were used to form complexes with one oxidised and one reduced nucleotide bound (Bhakta *et al.* 2007). In the complex containing bound H_2NADH and $NADP^+$, the charge-distribution on the nucleotides is similar to that with the physiological nucleotides (NADH and $NADP^+$) bound. Thus, the complex was thought more closely to resemble the ground state of the intact enzyme than the earlier dead-end complexes. In the cyrstal structure of the dI_2dIII complex with bound H_2NADH and $NADP^+$, H_2NADH is bound to dI in a proximal position relative to the $NADP^+$ on dIII. Located at the interface of dI and dIII, the hydride transfer site showed the dihydronicotinamide ring of the H_2NADH and the nicotinamide ring of the $NADP^+$ aligned such that the C4 atoms were 3.4 Å apart and apposed to one another. When NADH was modelled into the structure replacing H_2NADH, the *pro-R* hydrogen of

the C4 was in a position to transfer to the *si* face of $NADP^+$. This is in agreement with the stereospecificity of hydride transfer in transhydrogenase described in Section 1.6.

The folds of the individual components of the asymmetric complex (dIII and dI_2) are very similar to those observed in the isolated proteins. Each dI component comprises two domains; dI.1 and dI.2. The dI.1 domains are located on the outside of the complex and the dI.2 domains form a rigid core. The dIII component is in its occluded conformation with loop E closed over the bound nucleotide. Helix D/loop D is in the up position; modelling of dIII with helix D/loop D in the down position resulted in steric clashing between helix D/loop D and the RQD-loop of dI (Sundaresan *et al.* 2003). This is consistent with the involvement of helix D/loop D in a mechanism to transmit conformational change information from dIII to dI.

In the dI_2dIII complex the dIII component makes extensive contacts with dI, mainly with the dI.2 domain. In the intact enzyme it is unlikely that dI interacts with the membrane-spanning dII components. Since nucleotide-binding to dIII is thought to be coupled to proton translocation, extensive contacts are expected between the dIII and dII components.

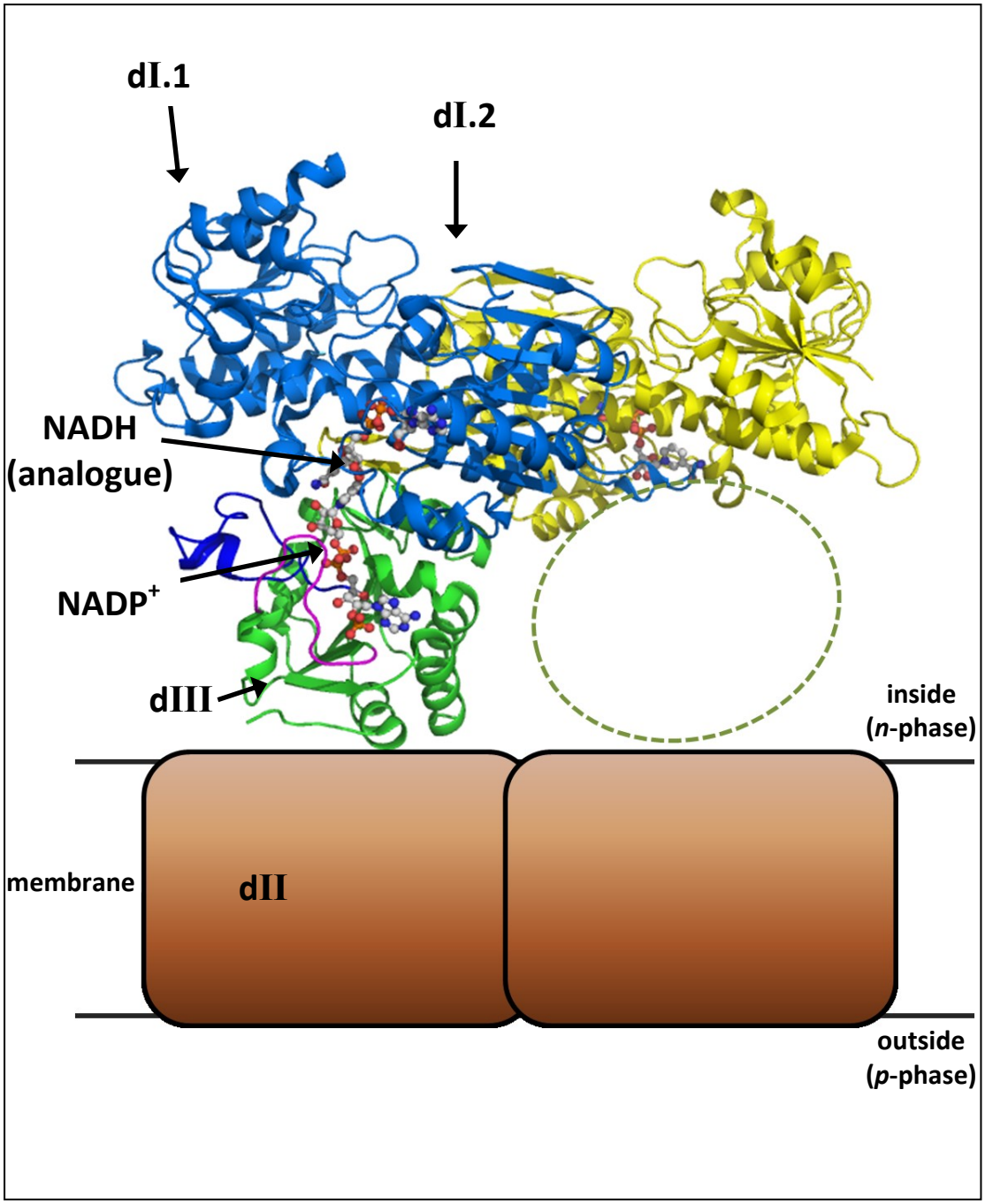

Figure 1.12 Crystal structure of the dI_2dIII asymmetric complex of *R. rubrum* transhydrogenase.

When reconstituted, dI and dIII form an asymmetric complex comprising two dI components (marine blue and yellow) and one dIII component (green). Loop E (magenta), helix D/loop D (deep blue), the expected positions of the two transmembrane dII components and the second dIII component are shown. This figure was produced using Pymol and PDB ID 2OO5.

1.11 The binding-change alternating-site mechanism of transhydrogenase.

During one turnover of the forward reaction of transhydrogenase (left to right in equation 1) one hydride ion is transferred from NADH to $NADP^+$ whilst one proton is translocated across the membrane (Bizouarn *et al.* 1996b). Analysis of the forward, reverse and cyclic reactions and of the rates of NADP(H) binding and release in intact transhydrogenase and in dI_2dIII complexes led to the proposal of a binding-change mechanism for transhydrogenase (Hutton *et al.* 1994). This predicts that dIII can adopt either an open conformation or an occluded conformation. The crystal structure of reconstituted dI and dIII showed that the dI_2dIII complex is asymmetric (Cotton *et al.* 2001) indicating that, in the intact enzyme the two $dI_1dII_1dIII_1$ monomers occupy different conformations, and that these alternate during turnover (Jackson *et al.* 2002). That is, at any time, one $dI_1dII_1dIII_1$ monomer is in the occluded conformation and the other monomer is in the open conformation (Figure 1.13). It was proposed that, in the open conformation, the substrate nucleotides (NADH and $NADP^+$) are able to bind to or dissociate from the enzyme but that hydride transfer is blocked. Once the substrates are bound, the enzyme switches to the occluded conformation. In the occluded conformation the binding and dissociation of nucleotides are prevented but the dihydronicotinamide ring of NADH and the nicotinamide ring of $NADP^+$ are bought together permitting fast hydride transfer ($k_{app} \approx 21000\ s^{-1}$ (Pinheiro *et al.* 2001)). The hydride transfer reaction is direct and does not involve reduced-enzyme intermediates (Venning *et al.* 1997; Venning *et al.* 1999). The dihydronicotinamide ring of NADH and the nicotinamide ring of $NADP^+$ are highly reactive moieties (Van Eikeren *et al.* 1977). Thus, it is essential to keep the two rings apart during nucleotide binding in the

open state. Otherwise, uncontrolled hydride transfer would occur uncoupled from proton translocation.

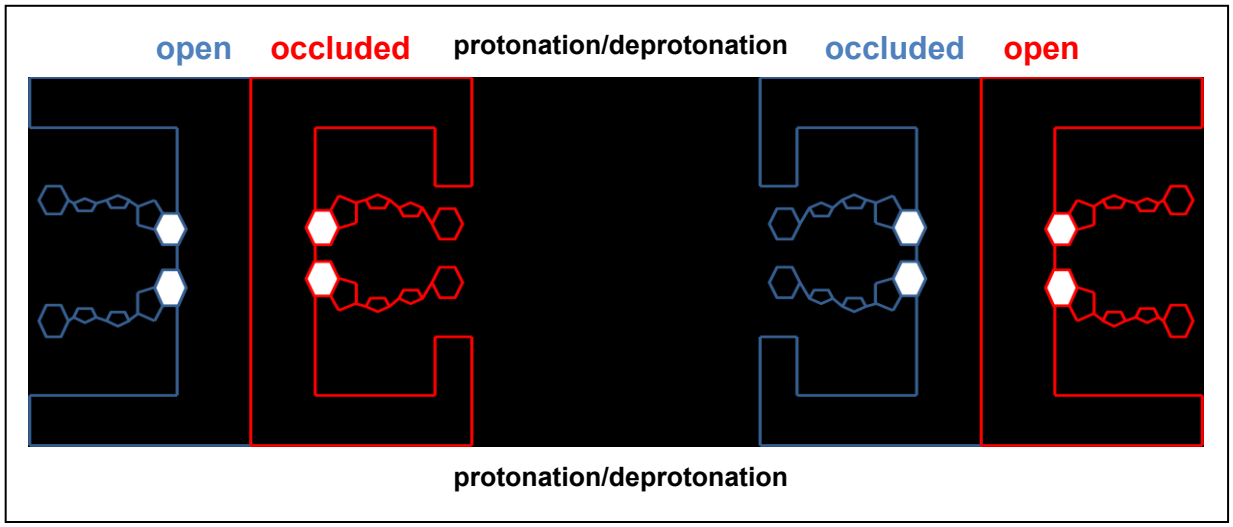

Figure 1.13 Model for the alternating-site mechanism of transhydrogenase.

Taken from (Jackson 2003). At any time, one side of transhydrogenase (*i.e.* one $dI_1dII_1dIII_1$ monomer) will be in an open conformation while the other side is in an occluded conformation. In the open conformation the distance between the nicotinamide and dihydronicotinamide rings is too great for hydride transfer to occur. The two rings are brought together in the occluded conformation to permit hydride transfer. The switch between the open and occluded conformations is a result of a protonation/deprotonation event that is coupled to proton translocation through dII.

For hydride transfer to occur, the enzyme must adopt an occluded state and bring together the dihydronicotinamide and nicotinamide rings of NADH and $NADP^+$, respectively. Crystal structures of isolated dI (Buckley *et al.* 2000; Prasad *et al.* 2002; Johansson *et al.* 2005) indicated that the nicotinamide ring of the bound NAD(H) was able to move significant distances within the protein. Structures of the asymmetric dI_2dIII complex (Cotton *et al.* 2001; Mather *et al.* 2004; Bhakta *et al.* 2007) confirm this and explain its significance. The NADH can adopt a distal position when bound

to dI, in which its dihydronicotinamide ring is 6.5 Å from the nicotinamide ring of $NADP^+$ bound to dIII; the rings are too far apart for hydride transfer. The NADH can also adopt a proximal position in which the dihydronicotinamide ring is closer to the nicotinamide ring of $NADP^+$ such that they are now a distance of 3.6 Å from each other. At this distance van der Waals contacts are formed and hydride transfer becomes possible. Analysis suggested that in the open conformation, the nicotinamide and dihydronicotinamide rings occupy the distal position, and in the occluded conformation they interconvert between the distal and proximal positions (van Boxel *et al.* 2003).

The switch from the open to the occluded conformation, and thus hydride transfer, is coupled to proton translocation through the dII component. The interface between the two substrates, NADH and $NADP^+$, where hydride transfer takes place is a distance of ~30 Å from the dII component. Thus, the coupling is likely to involve a long distance conformational change. NMR experiments have shown that this conformational change is likely to involve interactions between dII and helix D/loop D and loop E of the dIII component (Quirk *et al.* 1999; Jeeves *et al.* 2000) (see Section 1.10.2). It is an essential feature of the binding-change mechanism that the redox state of the nucleotide bound to dIII (*i.e.* $NADP^+$ or NADPH) determines which side of the membrane-spanning dII component protons have access to. When $NADP^+$ is bound to dIII, protons in the *p*-phase (outside) are able to access the proton translocating machinery of dII, and when NADPH is bound to dIII, protons in the *n*-phase (inside) are able access dII (Jackson *et al.* 2002).

1.12 The specificity of nicotinamide nucleotide-binding proteins.

The nicotinamide nucleotides NAD(H) and NADP(H) differ only by a phosphate group on the 2'-hydroxyl group of the adenosine ribose (see Figure 1.4). However, the two nucleotides play very different roles in the cell. NAD^+ usually serves as an oxidant during the reactions of catabolism (glycolysis, fatty acid oxidation and the tricarboxylic acid cycle). Conversely, NADPH is usually used as a reductant, in biosynthetic reactions or in glutathione reduction. That the two nucleotides are structurally similar yet play such different roles in the cell, means that proteins must have mechanisms to distinguish between them.

The specificity of nicotinamide nucleotide-binding proteins has been widely researched (reviewed in Wierenga *et al.* 1985; Baker *et al.* 1992; Bellamacina 1996; Carugo *et al.* 1997). A common fold for nicotinamide nucleotide-binding proteins is the Rossmann fold (Rossmann *et al.* 1974; Eventoff *et al.* 1975), in which βαβ motifs (numbers of strands and helices can differ) form a crevice that houses the nucleotide-binding site. Common features of this fold have been identified as being important for the specific binding of either NAD(H) or NADP(H). In NAD(H)-binding proteins, at the C-terminal of the second β-strand, an aspartate or glutamate residue is often located that hydrogen bonds with the 2'-hydroxyl group of the adenosine ribose. The bulky 2'-phosphate group which replaces the 2'-hydroxyl group in NADP(H) cannot readily fit into this binding pocket. In NADP(H)-binding proteins there is often a cluster of positively charged residues that interact with the negatively charged 2'-phosphate group of NADP(H). This cluster frequently includes an arginine residue that hydrogen bonds to the 2'-phosphate group and stacks with the adenine ring. The specificity of the NAD(H)-binding protein dihydrolipoamide dehydrogenase from *E.*

coli was changed to favour NADP(H)-binding (Bocanegra *et al.* 1993) by replacing a glutamate residue that hydrogen bonds to the 2'-hydroxyl of the adenine ribose group of NAD(H) in the wild-type enzyme with a valine, and introducing four positively charged residues (two arginines, a lysine and a histidine) into the binding site. The removal of the glutamate residue eliminated potential hydrogen bonds to the 2'-hydroxyl group of the adenine ribose of NAD(H), and the introduced positively charged residues provided potential interactions with the 2'-phosphate group of NADP(H), thus switching the specificity of the enzyme from NAD(H) to NADP(H).

Another feature seen in NAD(H)-binding proteins is a GXGXXG fingerprint motif (Wierenga *et al.* 1985), present in a loop located in the nucleotide-binding site between the first β-strand and α-helix of the βαβ motif. The first glycine residue of the GXGXXG motif is highly conserved and allows for a tight turn of the main chain. This turn positions the second glycine residue, whose small side chain is required for the close proximity of the pyrophosphate of the nucleotide with the amino acid residues that interact with it. The third glycine residue is required to provide the close interaction between the β-strands and the α-helix of the βαβ motif. In NADP(H)-binding proteins this is often replaced by a GXGXXA fingerprint motif (Hanukoglu *et al.* 1989) and is thought to be significant for the specificity of nucleotide-binding proteins. Mutation of the alanine residue for a glycine residue in *E. coli* glutathione reductase resulted in a specificity switch from NADP(H) to NAD(H) (Scrutton *et al.* 1990).

1.12.1 Structural description of the specificity of transhydrogenase.

For transhydrogenase to function efficiently dI must be specific for NAD(H) and dIII must be specific for NADP(H).

Crystal structures of the dI component of transhydrogenase (Buckley *et al.* 2000; Prasad *et al.* 2002; Johansson *et al.* 2005) show features that have been identified as important for nucleotide specificity in NAD(H)-binding proteins. Firstly, the NAD(H)-binding site of dI includes a loop between the first β-strand and α-helix of the Rossmann fold which contains a highly conserved GXGXXG fingerprint motif that interacts with the pyrophosphate group of the nucleotide. An invariant aspartate residue, Asp202, is also present in the NAD(H)-binding site, which, in the crystal structures is shown to form hydrogen bonds with the 2'-hydroxyl group of the adenosine ribose of NAD(H).

Crystal structures of the dIII component of transhydrogenase (Prasad *et al.* 1999; White *et al.* 2000; Sundaresan *et al.* 2003) also revealed features identified as important for nucleotide specificity. Thus, the NADP(H)-binding site of dIII contains positively charged residues that interact with the 2'-phosphate group of NADP(H). These include a highly conserved K-R-S motif (Lys164, Arg165, Ser166), in which all three residues form hydrogen bonds with the 2'-phosphate group of NADP(H) and the guanidinium of Arg165 stacks with the adenine ring (see Figure 1.11). The dIII component also includes a loop between the first β-strand and α-helix of the Rossmann fold which contains a highly conserved GXGXXA fingerprint motif that interacts with the pyrophosphate group of the nucleotide. Since the NADP(H) bound to dIII has a flipped conformation compared to other NADP(H)-binding proteins, the

specificity of dIII for NADP(H) is probably predominantly due to the positively charged residues that interact with the 2'-phosphate group of NADP(H).

1.12.2 Review of previous work that has brought into question the specificity of the dIII component for NADP(H).

Previous work has caused the specificity of the dIII component of transhydrogenase to be questioned. In 1994 the cyclic reaction (the reduction of $AcPdAD^+$ by NADH in the presence of NADP(H) (Figure 1.6)) was reported (Hutton *et al.* 1994). As well as this cyclic reaction, a low rate of $AcPdAD^+$ reduction by NADH in intact *E. coli* transhydrogenase was noted in the absence of NADP(H). It was suggested that this was due to low levels of contaminating NADP(H) in the NADH and $AcPdAD^+$ stock solutions.

A higher rate of $AcPdAD^+$ reduction by NADH in the absence of NADP(H) in intact *E. coli* transhydrogenase was reported (Bragg 1996). This was considered too high to be due to contaminating NADP(H). Bragg suggested that the rate of $AcPdAD^+$ reduction by NADH in the absence of $NADP^+$ was due to $AcPdAD^+$ binding in the NADP(H)-binding site on dIII, where it would be directly reduced by NADH bound to dI. In the presence of $NADP^+$, the rate of $AcPdAD^+$ reduction by NADH increased significantly. The promotion of the reaction by $NADP^+$ was attributed to either the displacement of $AcPdAD^+$ by $NADP^+$, or to a second binding site on dIII, in which $NADP^+$ would bind and induce a conformational change that favours the direct reduction of $AcPdAD^+$ by NADH.

Stilwell *et al.* also reported a low rate of $AcPdAD^+$ reduction by NADH in the absence of NADP(H), again in intact *E. coli* transhydrogenase (Stilwell *et al.* 1997).

At pH 6.0, the rate was only a few per cent of that in the presence of $NADP^+$. Effort was made to ensure that there was no contaminating NADP(H) in the stock solutions of NADH and $AcPdAD^+$. The enzyme was also washed extensively in an attempt to remove all bound NADP(H). The conclusion drawn was that either NADP(H) remained tightly bound to dIII throughout the washes and was able to contribute to the reduction of $AcPdAD^+$ by NADH or that NADH or $AcPdAD^+$ bound in the NADP(H)-binding site. Zhang *et al.* (Zhang *et al.* 1997) also found, independently, that intact *E. coli* transhydrogenase catalyses the reduction of $AcPdAD^+$ by NADH in the absence of NADP(H). They came to the same conclusion as Stilwell *et al.*, that NADH or $AcPdAD^+$ could be binding into the NADP(H)-binding site. The explanations put forward by both groups did not require a second binding site on dIII as had been suggested by Bragg (Bragg 1996).

Crystal structures of transhydrogenase dIII were then solved (Prasad *et al.* 1999; White *et al.* 2000; Sundaresan *et al.* 2003) and indicated only one nucleotide binding site rendering unlikely the explanation, put forward by Bragg, of two nucleotide-binding sites on dIII.

In dI_2dIII complexes, the cyclic reaction is mechanistically significant because of its high rate compared to the forward and reverse reactions. The forward and reverse reactions are limited by the very slow dissociation of $NADP^+$ and NADPH from dIII. Within the definition of the cyclic reaction (proposed by Whitehead *et al.* 2009), the alternate reduction of $NADP^+$ by NADH and $AcPdAD^+$ by NADPH take place while $NADP^+$ and NADPH remain tightly bound in the dIII site. An interesting set of experiments was performed by Pedersen *et al.* (Pedersen *et al.* 2003), in which alkaline phosphatase was used to convert most of the NADP(H) in the dIII solution into NAD(H), thus eventually removing most of the NADP(H) (bound to dIII or

unbound). Experiments were conducted using hybrid dI_2dIII complexes formed of reconstituted *E. coli* dIII and *R. rubrum* dI. Remarkably, complexes of dI_2dIII containing phosphatase-treated apo-dIII catalysed $AcPdAD^+$ reduction by NADH in the absence of NADP(H) with a rate of ~75% of that using NADP(H)-bound dIII. Addition of $NADP^+$ to the assay buffer restored full cyclic activity to the phosphatase-treated dIII. It was concluded that for the reaction to proceed, either NADH or $AcPdAD^+$ must be binding into the NADP(H)-binding site on dIII (the "wrong" site) in an orientation that allows hydride transfer with either NADH or $AcPdAD^+$ bound to dI.

1.13 Objectives of this work.

Since NADP(H) binds so tightly to isolated dIII and to dIII in dI_2dIII complexes, it has been difficult to determine the nature of nucleotide binding to the protein. However, this work describes two separate techniques for the removal of bound NADP(H) and the production of apo-dIII. Firstly, the technique was adapted from Pedersen *et al.* (Pedersen *et al.* 2003) using alkaline phosphatase to cleave the 2'-phosphate from NADP(H). Secondly, a mutant dIII was isolated in which the arginine residue from the highly conserved K-R-S motif in the NADP(H)-binding site was substituted by an alanine residue. This mutation eliminates hydrogen bonds between the 2'-phosphate of NADP(H) and the protein, and results in a significantly decreased nucleotide affinity. The production of apo-dIII has enabled us more thoroughly to investigate nucleotide-binding to dIII.

In light of the work presented here, we now have a better understanding of the nucleotide-binding properties of dIII in dI_2dIII complexes. Studies on the kinetics of

nucleotide-binding show a very slow rate of nucleotide association with dIII and provide insight into the mechanism of intact transhydrogenase. NADH is found to bind into the NADP(H)-binding site of dIII with a surprisingly high affinity calling the nucleotide specificity of the enzyme into question. The metabolic significance of this is discussed.

CHAPTER 2

Materials and Methods

2.1 Over-expression of the dI and dIII components of transhydrogenase.

2.1.1 LB (Luria-Bertani) medium.

LB media was used for the growth of *E. coli* (except for the preparation of competent cells). It contained 10 g tryptone, 5 g yeast-extract and 10 g NaCl per litre at pH 7.0 (Sambrook *et al.* 1989). Before use, the medium was sterilised by autoclaving at 121˚C for 20 minutes. To prepare LB agar plates, 1.2 g bacterial agar was added per 100 mL media before autoclaving. Ampicillin was added at a final concentration of 100 μg mL^{-1} when required. The stock solution of ampicillin was sterilised by passage through a 0.45 μm syringe filter prior to use. After the plates had been poured they were either used immediately or stored at 4˚C.

2.1.2 TYM medium.

TYM medium was used during the preparation of competent *E. coli* cells. It contained 20 g tryptone, 5 g yeast-extract, 1 g NaCl and 2.5 g $MgSO_4$ per litre at pH 7.0. The medium was sterilised before use by autoclaving at 121˚C for 20 minutes. To prepare TYM agar plates, 1.2 g bacterial agar was added per 100 mL media before autoclaving. The plates were poured and either used immediately or stored at 4˚C.

2.1.3 Preparation of *E. coli* competent cells.

Competent *E. coli* BL21(DE3) and *E. coli* C600 cells were prepared using the following method. The cells were grown on TYM agar overnight at 37˚C. A single

colony was used to inoculate a 5 mL culture of fresh TYM media and was grown in a shaking incubator overnight at 37˚C. Following this, 200 µL was used to inoculate a 100 mL culture of fresh TYM medium and was grown for ~3 hours, until the optical density reached between 0.5 and 0.9 at 650 nm measured on a Unicam Helios γ spectrophotometer. This culture was then incubated on ice for 5 minutes and the cells harvested by centrifugation at 10,000 *g* for 15 minutes at 4˚C. The cells were re-suspended in 20 mL TfbI buffer (see below) and centrifuged again at 10,000 *g* for 15 minutes at 4˚C. The collected cells were re-suspended in 4 mL TfbII buffer (see below) and kept on ice for 2 minutes. The cells were then dispensed into sterile Eppendorf tubes in 200 µL aliquots and snap frozen in liquid nitrogen. Finally, the cells were stored at -80˚C.

TfbI buffer

30 mM potassium acetate

50 mM $MnCl_2$

100 mM RbCl

10 mM $CaCl_2$

15% glycerol (v/v)

The TfbI buffer was adjusted to pH 5.8 with HCl and sterilised by passage through a 0.45 µm syringe filter prior to use.

TfbII buffer

10 mM MOPS

10 mM RbCl

75 mM $CaCl_2$

15% glycerol (v/v)

The TfbII buffer was adjusted to pH 7.0 with KOH and sterilised by passage through a 0.45 µm syringe filter prior to use.

2.1.4 Site-directed mutagenesis of *R. rubrum* dI and dIII.

The plasmids used in this work are listed in Table 2.1.

pLH1

The mutant plasmid pLH1 harbours a gene which encodes the R165A mutant of dIII from *R. rubrum* transhydrogenase. It was produced and sequenced by Yorkshire Bioscience Ltd. using an undisclosed method.

pLH2

The mutant plasmid pLH2 harbours a gene which encodes the E155W.R165A double mutant of the dIII component from *R. rubrum* transhydrogenase. It was produced using the Stratagene Quikchange kit following the manufacturer's instructions. The template plasmid used was pLH1, (see above) at a concentration of approximately 100 ng. The mutagenic primers were supplied by Alta Bioscience and had the following sequences: -

Forward 5' – CGATCCTTGACGTCTGGAAGGCCGGAACCGTGC – 3'

Reverse 5' – GCACGGTTCCGGCCTTCCAGACGTCAAGGATGC – 3'

pLH4

The mutant plasmid pLH4 harbours a gene which encodes the W72F mutant of the dI component of *R. rubrum* transhydrogenase. Again, it was produced using the Stratagene Quikchange kit following the manufacturer's instructions. The template plasmid used was pCD1 (Diggle *et al.* 1995b) and the mutagenic primers were supplied by Alta Bioscience. They had the following nucleotide sequences: -

Forward 5’ – CCAGGCCGATGTGGTCTTTAAGGTACAGCGCCCGATG – 3’

Reverse 5’ – CATCGGGCGCTGTACCTTAAAGACCACATCGGCCTGG – 3’.

2.1.5 Purification and analysis of plasmids.

Plasmids harbouring genes encoding wild-type and mutant recombinant proteins from *R. rubrum* transhydrogenase (see Table 2.1) were purified using a Qiagen QIAprep Spin Miniprep kit following the manufacturer’s instructions.

plasmid	protein encoded	reference
pNIC2	wild-type dIII	(Diggle *et al.* 1996)
pJDV1	dIII.E155W	(Peake *et al.* 1999a)
pLH1	dIII.R165A	this work
pLH2	dIII.E155W.R165A	this work
pLH3	truncated dIII.R165A	this work (see Chapter 6)
pCD1	wild-type dI	(Diggle *et al.* 1995b)
pLH4	dI.W72F	this work

Table 2.1 Table of plasmids used in this project.

All plasmids were routinely checked by restriction-digest analysis following the manufacturer’s instructions (all restriction enzymes used were from New England Biolabs). In the plasmids pNIC2, pJDV1, pLH1 and pLH2, the dIII gene is harboured in the vector pET11c (Figure 2.1). The dIII gene is inserted in the pET11c vector between the *Bam*HI restriction site (position 319) and the *Nde*I restriction site (position 359) such that the 3’ end of the forward strand of the dIII gene is located at the *Bam*HI site and the 5’ end is located at the *Nde*I site.

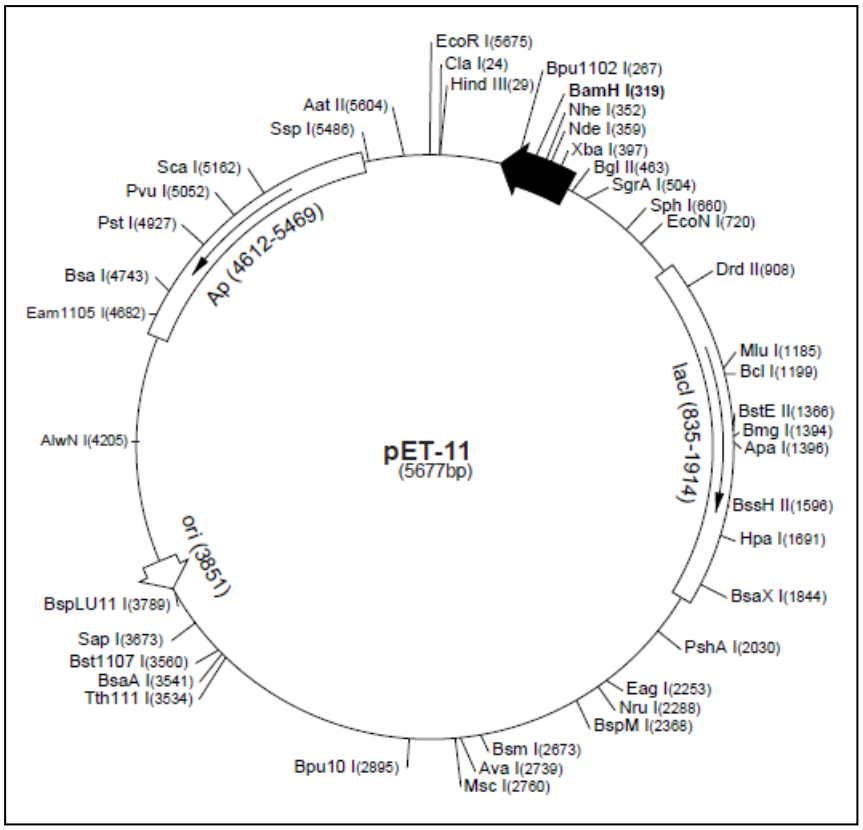

Figure 2.1 Restriction map of the vector pET11c.

The genes encoding wild-type dIII, dIII.E155W, dIII.R165A and dIII.E155W.R165A are harboured in the vector pET11c to produce the plasmids pNIC2, pJDV1, pLH1 and pLH2, respectively.

The sequence of the dIII gene is shown in Figure 2.2. The mutation in pLH1 (to produce dIII.R165A) eliminated an *Afe*I restriction site from pNIC2 (see Table 2.1). Thus, pLH1 was selected by the loss of this site; the sequence of pLH1 was confirmed by DNA sequencing (Yorkshire Bioscience Ltd). To make the E155W mutation in dIII.R165A, the mutagenic primers were designed to introduce an *Aat*II restriction site into pLH1. Thus, pLH2 was selected by the presence of this site; the fidelity of the PCR used in the mutagenesis was confirmed by DNA sequencing (Functional Genomics Laboratory at The University of Birmingham).

In the plasmids pCD1 and pLH4, the dI gene was harboured in the vector pMS119. To make the W72F mutation in wild-type dI, the mutagenic primer (see

previous section) was designed to eliminate an *Eag*I restriction site from pCD1 (see Table 2.1). Thus, pLH4 was selected by the loss of this site; the fidelity of the PCR used in the mutagenesis was confirmed by sequencing (Functional Genomics Laboratory at The University of Birmingham).

```
  1-CATATGAACCGCTCGATCTTCAACGTCATCCTGGGCGGCTTCGGCAGCGAGGGCGGCGTA-60
 61-GCGGCGGCCGGTGGCGCGGCCGGCGATCGTTCGGTCAAGGCCGGCAGCGCCGAAGACGCG-120
121-GCCTTCATCATGAAGAACGCCTCGAAGGTCATCATCGTGCCCGGCTATGGCATGGCGGTG-180
181-GCCCAGGCCCAGCACGCCCTGCGCGAAATGGCCGATGTGCTCAAGAAGGAAGGCGTCGAG-240
241-GTTTCCTACGCCATCCATCCGGTGGCCGGCCGTATGCCCGGGCACATGAACGTGCTGCTG-300
301-GCCGAGGCCAATGTGCCCTATGACGAGGTCTTCGAGCTCGAAGAGATCAACAGCTCGTTC-360
361-CAGACCGCCGATGTCGCCTTCGTCATCGGCGCCAACGACGTGACCAACCCGGCGGCCAAG-420
421-ACCGATCCGTCGAGCCCGATCTACGGCATGCCGATCCTTGACGTTGAAAAGGCCGGAACC-480
481-GTGCTGTTCATCAAGCGCTCGATGGCCTCGGGCTATGCCGGCGTCGAGAACGAACTGTTC-540
541-TTCCGCAACAACACGATGATGCTGTTTGGCGACGCCAAGAAGATGACCGAGCAGATCGTC-600
601-CAGGCGATGAACTGAAGCTCCGGATCC-628
```

Figure 2.2 Sequence of the gene encoding wild-type dIII from *R. rubrum* transhydrogenase.

Highlighted are the *Nde*I restriction site in yellow (including the start codon), the *Bam*HI restriction site in cyan, the stop codon in grey, the bases encoding Glu155 in pink and the bases encoding Arg165 in green.

Following digestion of the plasmid by restriction enzymes, the plasmid fragments were analysed on a 0.8% agarose gel in parallel with a DNA ladder (Bioline HyperLadder I). Samples were prepared by mixing 5 µL of the digested plasmid, 2 µL of "5× loading buffer" (supplied with the DNA ladder) and 3 µL water. To prepare the gel, 0.8% agarose (w/v) was dissolved in 100 mL warm TAE buffer (40 mM tris/HCl, 0.1% acetic acid (v/v), 1 mM EDTA). Ethidium bromide (5 µL) was added and the mixture was poured into a Horizon 58 (Life Technologies Inc.) gel

electrophoresis tank and left to solidify with a comb to create the loading wells. Plasmid samples were loaded into the wells and the gel was run for ~1 hour at 80V. The gel was then visualised using a UV illuminator.

2.1.6 Transformation of *E. coli* cells.

E. coli BL21(DE3) competent cells were transformed with the plasmids pNIC2 (Diggle *et al.* 1996), pJDV1 (Peake *et al.* 1999a), pLH1 (see above) and pLH2 (see above) for over-expression of the genes encoding wild-type dIII of *R. rubrum* transhydrogenase, the E155W mutant of dIII, the R165A mutant of dIII and the E155W.R165A double mutant of dIII, respectively. *E. coli* C600 competent cells were transformed with the plasmid pCD1 (Diggle *et al.* 1995b) and pLH4 (see above) for over-expression of the gene encoding wild-type dI of *R. rubrum* transhydrogenase and the W72F mutant of dI, respectively.

The competent cells were thawed and 50 μL were added to the appropriate plasmid DNA (~20 ng). The mixture was incubated on ice for 30 minutes. It was then subjected to a heat shock at 42˚C for 45 seconds and returned to ice for a further 1 minute. LB medium (500 μL) was then added to the mixture, which was incubated with shaking at 37˚C for 1 hour. Following this, 10 μL and 100 μL aliquots were plated onto LB agar plates containing 100 μg mL^{-1} ampicillin and incubated overnight at 37˚C.

2.1.7 Growth and over-expression of *E. coli* cells.

Following transformation of host *E. coli* cells with plasmid DNA, a single colony was taken from the agar plate and added to 50 mL LB containing 100 μg mL^{-1} ampicillin, and incubated overnight in a shaking incubator at 37˚C. This was then split between 8 flasks, each containing 400 mL fresh LB medium and 100 μg mL^{-1} ampicillin. The cells were grown in a shaking incubator at 37˚C until an optical density of 0.6 to 0.7 was reached at 600 nm on a Unicam Helios γ spectrophotometer. Expression was induced by the addition of 1 mM isopropyl thiogalactoside. The cells were harvested by centrifugation in a Beckman Avanti^{TM} J-25 centrifuge using a JA-10 rotor at 10,000 *g* at 4˚C for 10 minutes. The supernatants were discarded and the pellets were washed with TE buffer (50 mM tris-HCl, 1 mM EDTA, pH 8.0), combined into one tube, and centrifuged again at 10,000 *g* at 4˚C for 10 minutes using the same rotor. The supernatant was discarded and the pellets stored at -20˚C. Cell pellets were then thawed when required. Once thawed, the pellets were re-suspended in TE buffer supplemented with 1 mM DTT for dI and 100 μM $NADP^+$ for dIII. The cells were broken by sonication (5 × 30 second sonications with 60 second intervals) in the presence of 0.5 mM phenylmethanesulfonyl fluoride (PMSF). The cell debris was removed by centrifugation in a Beckman XL-90 ultracentrifuge using a 70 Ti rotor at 150,000 *g* at 4˚C for 1 hour. For the purification of wild-type dIII, dIII.E155W, wild-type dI and dI.W72F, which were predominantly found in the soluble fraction of the cell debris, the respective supernatant was next filtered using a 0.45 μm syringe filter. The isolated proteins were purified using column chromatography as described in following sections. Unlike wild-type dIII, dIII.R165A and dIII.E155W.R165A predominantly formed inclusion bodies, and were present in the pellet after the

centrifugation at 15,000 *g* (Figure 2.3). Thus, a new method of purification was needed for these mutant proteins; existing methods used for wild-type dIII (Diggle *et al.* 1996) were unsuitable.

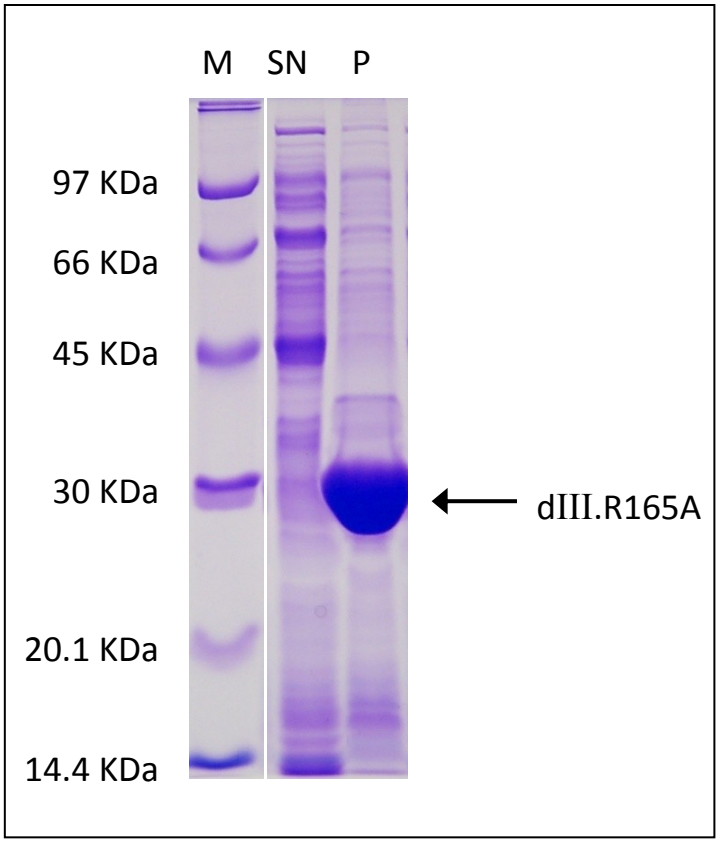

Figure 2.3 SDS PAGE gel showing the expression of recombinant dIII.R165A.

Following the growth and harvesting of the *E. coli* host cells, the cells were re-suspended in 50 mM tris-HCl, pH 8.0, 1 mM EDTA, 100 μM $NADP^+$ and broken by sonication. The broken cells were then subjected to a high-speed centrifugation. The resulting supernatant (SN) and pellet (P) were analysed on a 12% SDS PAGE gel in parallel with a protein marker (M) (GE Healthcare low molecular weight marker), and the gel stained with PAGE blue. It is clear that dIII.R165A forms inclusion bodies and is present predominantly in the pellet.

A method was developed for the purification of dIII.R165A and dIII.E155W.R165A from an existing protocol used for the purification of dI (Obiozo *et al.* 2007),

involving the denaturation and refolding of the proteins. After centrifugation at 150,000 *g*, the supernatant was discarded and the pellet was re-suspended in 20 mM tris-HCl, 40 μM $NADP^+$, 6 M guanidine hydrochloride (GuHCl), pH 8.0. The re-suspended pellet was incubated on ice for 30 minutes and centrifuged in a Beckman XL-90 ultracentrifuge using a 70 Ti rotor at 90,000 *g* at 4˚C for 1 hour. The resulting supernatant was stored at -20˚C. When required, the supernatant was thawed and used for the purification of either dIII.R165A or dIII.E155W.R165A (as described in Section 2.2.4).

2.2 Purification and preparation of the dI and dIII components from *R. rubrum* transhydrogenase.

2.2.1 SDS PAGE.

SDS PAGE is a widely used technique, in which proteins are treated with SDS to denature and dissociate them into their individual subunits. When loaded onto a gel and subjected to an electric current the proteins separate according to their molecular weight; smaller proteins migrate further through the gel than larger proteins (Sambrook *et al.* 1989).

SDS PAGE gels (12%) were prepared using a Bio-Rad Mini-Protean Tetra electrophoresis system. Liquid resolving-gel mixture (3.5 mL) (12% acrylamide (v/v), 375 mM tris/HCl, pH 8.8, 2 mM EDTA, 0.16% SDS (w/v), 0.05% ammonium persulphate (w/v), 0.05% tetramethylethylenediamine (v/v)) was pipetted into the gel cassette, covered by water-saturated butanol to ensure that the top of the gel was level, and allowed to solidify for ~1 hour. The water-saturated butanol was discarded and

liquid stacking-gel mixture (5.5% acrylamide (v/v), 130 mM tris/HCl, pH 6.8, 2 mM EDTA, 0.1% SDS (w/v), 0.05% ammonium persulphate (w/v), 0.1% tetramethylethylenediamine (v/v)) was pipetted onto the resolving gel to fill the remaining space in the cassette. A comb was inserted into the liquid stacking gel to create the loading wells before the gel was allowed to solidify for ~30 minutes.

Protein samples were prepared by adding 20 μL of "2× loading buffer" (125 mM tris/HCl, pH 6.8, 4 mM EDTA, 20% glycerol (v/v), 0.5% bromophenol blue (w/v), 0.5% xylene cyanol (w/v), 5% SDS (w/v), 2% β-mercaptoethanol (v/v)) to 20 μL protein sample. The mixtures were heated to 60˚C for 10 minutes and loaded into the wells of the SDS PAGE gel. The gel was run for ~1 hour at 200 V in running buffer (250 mM tris/HCl, pH 8.3, 144 g L^{-1} glycine, 5 g L^{-1} SDS, 3.72 g L^{-1} EDTA). The gels were then stained by heating to 60˚C in a stain solution of 50% methanol (v/v), 10% acetic acid (v/v), 0.5% PAGE blue (w/v). The gels were then de-stained by heating to 60˚C in a de-stain solution of 10% methanol (v/v), 7% acetic acid (v/v).

2.2.2 Purification of isolated wild-type dIII and dIII.E155W.

The protocol for the purification of wild-type dIII in this work was adapted from an existing protocol (Diggle *et al.* 1996). The filtered supernatant obtained from *E. coli* cells expressing *R. rubrum* dIII (described in Section 2.1.7) was applied to a 300 mL Q-sepharose fast flow ion-exchange column (GE healthcare) pre-equilibrated with 20 mM tris-HCl, 4 μM $NADP^+$, pH 8.0. The column was washed with 50 mL of the same buffer, and then with 150 mL 20 mM tris-HCl, 4 μM $NADP^+$, 200 mM NaCl, pH 8.0. The protein solution was then eluted with 600 mL 20 mM tris-HCl, 4 μM $NADP^+$, 700 mM NaCl, pH 8.0. The presence of dIII was detected using assays

measuring the rate of the cyclic reaction in assays supplemented with purified dI (described in Section 2.3.4), and SDS PAGE. The appropriate fractions were collected and dialysed overnight in 2 L 20 mM tris-HCl, 4 μM $NADP^+$, 0.5 mM PMSF, pH 8.0. The dialysed protein solution was filtered using a 0.45 μm syringe filter, and applied to a 300 mL Q-sepharose high performance ion-exchange column (GE healthcare) pre-equilibrated with 20 mM tris-HCl, 4 μM $NADP^+$, pH 8.0. The column was washed with 40 mL 20 mM tris-HCl, 4 μM $NADP^+$, pH 8.0, and then with 40 mL 20 mM tris-HCl, 4 μM $NADP^+$, 200 mM NaCl, pH 8.0. The protein was eluted with a 600 mL gradient of 20 mM tris-HCl, 4 μM $NADP^+$, 200-600 mM NaCl, pH 8.0. The appropriate fractions were collected and dialysed overnight in 2 L 20mM tris-HCl, 4 μM $NADP^+$, 0.5 mM PMSF, pH 8.0. Solid ammonium sulphate was added to the dialysed protein solution to give a final concentration of 55 g L^{-1}. The protein solution was then filtered using a 0.45 μm syringe filter and was applied to a 300 mL butyl toyopearl hydrophobic interaction column (TOSOH) pre-equilibrated with 20 mM tris-HCl, 4 μM $NADP^+$, 55 g L^{-1} ammonium sulphate, pH 8.0. The column was washed with 40 mL of the same buffer. The protein was eluted with a 600 mL gradient of 20 mM tris-HCl, 4 μM $NADP^+$, 55-0 g L^{-1} ammonium sulphate, pH 8.0. The appropriate fractions were collected, pooled and stored at -20˚C in 25% glycerol (v/v). The procedure described typically produced ~60 mg dIII protein (wild-type dIII or dIII.E155W) from 3.2 L of bacterial culture.

2.2.3 Purification of isolated wild-type dI and dI.W72F.

The protocol for the purification of wild-type dI and dI.W72F in this work was adapted from an existing protocol for the purification of wild-type dI (Diggle *et al.*

1995b). The filtered supernatant obtained from *E. coli* cells expressing *R. rubrum* dI (described in Section 2.1.7) was applied to a 300 mL Q-sepharose fast flow ion-exchange column pre-equilibrated with 20 mM tris-HCl, 1 mM DTT, 1 mM EDTA, pH 8.0. The column was washed with 100 mL of the same buffer and then with 100 mL 20 mM tris-HCl, pH 8.0, 1 mM DTT, 1 mM EDTA, 200 mM NaCl. The protein was eluted with a 600 mL gradient of 20 mM tris-HCl, 1 mM DTT, 1 mM EDTA, 200-400 mM NaCl, pH 8.0. The presence of dI was detected by measuring the rate of the cyclic reaction in assays supplemented with purified dIII (described in Section 2.3.4), and SDS PAGE. The appropriate fractions were collected and dialysed overnight in 2 L 20 mM tris-HCl, 1 mM DTT, 1 mM EDTA, 0.5 mM PMSF, pH 8.0. The dialysed protein solution was filtered using a 0.45 μm syringe filter. Solid ammonium sulphate was added to the dialysed protein solution to give a final concentration of 1.5 M, which was then filtered using a 0.45 μm syringe filter. The protein solution was applied to a 300 mL butyl toyopearl hydrophobic interaction column pre-equilibrated with 20 mM tris-HCl, 1 mM DTT, 1 mM EDTA, 1.5 M ammonium sulphate, pH 8.0. The column was washed with 100 mL of the same buffer. The protein was eluted with a 600 mL gradient of 20 mM tris-HCl, 1 mM DTT, 1 mM EDTA, 1.5-0 M ammonium sulphate, pH 8.0. The appropriate fractions were collected and stored at -20˚C in 25% glycerol (v/v). The procedure described typically produced ~300 mg dI protein (wild-type dI or dI.W72F) from 3.2 L of bacterial culture.

2.2.4 Purification of isolated dIII.R165A and dIII.E155W.R165A.

The protocol described here is for the denaturation and refolding of the protein. This method was adapted from an existing protocol for the purification of dI (Obiozo *et al.* 2007), and developed for the purification of the dIII.R165A and dIII.E155W.R165A mutant proteins. Recall from Section 2.1.7, following centrifugation at 150,000 *g*, the resulting pellet was re-suspended and incubated in a buffer containing 6 M GuHCl, and subjected to another centrifugation step at 90,000 *g*. The resulting supernatant was stored at -20 ˚C. When required, the supernatant was thawed and diluted with 20 mM tris-HCl, 40 μM $NADP^+$, 6 M GuHCl to give a protein concentration of approximately 0.5 mg mL^{-1}. A sample of this (40 mL) was then dialysed overnight in 4 L 30 mM HEPES, 10 μM $NADP^+$, 15% glycerol (v/v), 0.5 mM PMSF, pH 8.0. The dialysed protein solution was centrifuged in a Jouan CR3i centrifuge at 10,000 *g* at 4˚C for 10 minutes to remove any precipitated protein. To concentrate the protein solution, this was applied to a 5 mL HiTrap Q-HP ion-exchange column (GE Healthcare) pre-equilibrated with 20 mM tris-HCl, 4 μM $NADP^+$, pH 8.0. The column was washed with 40 mL of the same buffer, and then with 40 mL 20 mM tris-HCl, 4 μM $NADP^+$, 200 mM NaCl, pH 8.0. The protein was eluted in 1 mL fractions with 20 mL 20mM tris-HCl, 4 μM $NADP^+$, 600 mM NaCl, pH 8.0. The fractions containing the required purified protein were identified by SDS PAGE and pooled.

Following the HiTrap Q-HP ion-exchange column it was usually necessary to remove $NADP^+$ from the protein solution. To this end, 3 mL of the pooled protein was applied using a syringe to two series-connected 5 mL HiTrap desalting columns (GE Healthcare) pre-equilibrated with 20 mM tris-HCl, pH 8.0. The protein was eluted in 1 mL fractions with 10 mL 20 mM tris-HCl, pH 8.0. SDS PAGE showed that the

protein eluted in the first four fractions. These fractions were collected and pooled. The process was repeated, applying 3 mL of the pooled protein to two series-connected HiTrap desalting columns. Again, the first four fractions were collected. The purified, desalted protein was used immediately without storage. The procedure described typically produced ~2 mg dIII.R165A or dIII.E155W.R165A from a 40 mL sample of unfolded protein.

2.2.5 Determination of protein concentration.

All protein concentrations were determined by the microtannin assay (Mejbaum-Katzenellenbogen *et al.* 1959) using bovine serum albumin (BSA) as the standard.

Samples of the purified protein were diluted 20 fold and 50 fold using water. Samples of BSA of known concentration (0-50 $\mu g\ mL^{-1}$) were also prepared. To 1 mL of these samples, 1 mL tannin reagent A (see below) was added. The samples were incubated in a 30˚C water bath for 30 minutes. Tannin reagent B (1 mL) (see below) was then added to each sample and incubated at room temperature for 10 minutes. The absorbance of the samples at 500 nm was measured in a Unicam Helios γ spectrophotometer, which was set to zero using the 0 $\mu g\ mL^{-1}$ BSA sample. A standard curve was constructed from the absorbance values of the BSA samples and used to calculate the concentration of the purified protein.

Tannin reagent A

805 mL deionised water

75 mL concentrated HCl

20 mL phenol

90 g tannic acid

The water and tannic acid were heated to 80˚C before the other components were added. The solution was left to cool before filtering through Whatman #1 filter paper, and was stored at 4˚C.

Tannin reagent B

500 mL deionised water

1 g gum Arabic (acacia)

After combining, the mixture was heated to 80˚C until dissolved. The solution was left to cool before filtering through Whatman #1 filter paper, and was stored at 4˚C.

2.2.6 Gel-filtration of wild-type dIII.

In an attempt to remove bound-$NADP^+$ from dIII, the purified protein solution was applied to two series-connected 5 mL HiTrap desalting columns pre-equilibrated with 20 mM tris-HCl, pH 8.0. The protein was eluted in 1 mL fractions with 10 mL 20 mM tris-HCl, pH 8.0. SDS PAGE showed that the protein eluted in the first four fractions. These fractions were collected and pooled. The process was repeated, applying 3 mL of the pooled protein to two series-connected HiTrap desalting columns. Again, the first four fractions were collected.

2.2.7 Phosphatase-treatment of dIII.

The protocol for the phosphatase-treatment of *R. rubrum* dIII was adapted from a protocol used for the phosphatase-treatment of *E. coli* dIII (Pedersen *et al.* 2003). Prior to phosphatase-treatment, dIII (4 mL) was dialysed overnight against 2 L 20 mM CHES-KOH, pH 9.0. To 50 µL aliquots of the dialysed protein, 10 U calf-intestinal alkaline phosphatase (New England Biolabs) was added, and the solution was incubated at 37˚C for 10 minutes. The phosphatase-treated protein was then

plunged into ice and used within 30 minutes in enzyme assays (see Chapter 3) and fluorescence experiments (see Chapter 4).

Control fluorometric assay experiments were necessary to confirm that essentially all $NADP^+$ and NADPH in the phosphatase-treated dIII had been converted to NAD^+ and NADH, respectively. Fluorescence experiments were performed in parallel with untreated dIII, with an excitation wavelength of 340 nm, an emission wavelength of 460 nm and a half band width of 2 nm. To confirm the absence of $NADP^+$, the phosphatase-treated dIII (0.2 mL) was added to 1.8 mL 20 mM MOPS-KOH, pH 7.0, 5 mM $MgCl_2$, 2 mM isocitrate. The reduction of $NADP^+$ was recorded following the addition of 1 U $NADP^+$-dependent isocitrate dehydrogenase (Sigma Life Science, from porcine heart). To confirm the generation of NAD^+ from the phosphatase treatment of dIII, ethanol was added to give a concentration of 0.1% (v/v) and the reduction of NAD^+ was recorded following the addition of 10 U alcohol dehydrogenase (Sigma Life Science, from baker's yeast).

For the detection of NADPH, the phosphatase-treated dIII (0.2 mL) was added to 1.8 mL 20 mM MOPS-KOH, pH 7.0, 5 mM $MgCl_2$, 2 mM oxidised glutathione before adding 1 U glutathione reductase (Sigma Life Science, from baker's yeast). The oxidation of NADPH by the oxidised glutathione and glutathione reductase was recorded.

2.3 Biochemical methods.

2.3.1 Determination of the $NADP^+$-content of dIII.

The $NADP^+$ content of dIII was assayed using the method described (Klingenberg 1974; Diggle *et al.* 1996). Solutions of known $NADP^+$ concentration (0-50 μM) were used for calibration. To 0.6 mL of each sample of dIII containing approximately 250 μg protein, 0.3 mL 14% perchloric acid (v/v) was added to precipitate the protein, and the mixture was incubated on ice for 10 minutes. The solutions were then neutralised by the addition of 0.45 mL 1 M KOH, 1 M $KHCO_3$, and incubated on ice for 15 minutes before storing at -20˚C for at least an hour. Once thawed, the top clear layer from each sample (0.8 mL) was removed and centrifuged in a Hettich Mikro 20 benchtop centrifuge for 5 minutes to remove any remaining protein precipitate.

The resulting solution (0.8 mL) was then added to 2.2 mL MOPS, pH 7.0, 5 mM $MgCl_2$, 2 mM isocitrate before adding 1 U $NADP^+$-linked isocitrate dehydrogenase (Sigma Life Science, from porcine heart). The reduction of $NADP^+$ by the isocitrate and $NADP^+$-linked isocitrate dehydrogenase was measured at 25˚C as the amplitude of the fluorescence change with an excitation wavelength of 340 nm, an emission wavelength of 460 nm and a half band width of 2 nm. A calibration curve was constructed using the samples of known $NADP^+$ concentration.

2.3.2 Note on the preparation of dialysis tubing used in this project.

In view of some unexpected properties of the dialysis tubing used in this project, it is emphasized that the tubing was routinely pre-prepared by standard procedures

(Bizouarn *et al.* 1996a). Thus, lengths of dialysis tubing (Visking or Spectra/Por, both Medicell) were incubated in 5% $NaHCO_3$ (w/v), 1 mM EDTA at 80˚C for 30 minutes. The tubing was then either used immediately or stored in 20% ethanol (v/v) at 4˚C.

2.3.3 Determination of nucleotide concentration of solutions.

Prior to use, the concentration of nucleotide solutions used in experiments (*e.g.* enzyme assays and fluorescence experiments) was measured for reliable experimental analysis. Nucleotide concentrations were also measured to test passage through dialysis membranes (see Section 3.1.1). To this end, the absorbance of nucleotide solutions (1 mL) was measured on a Unicam Helios γ spectrophotometer at the wavelengths and extinction coefficients given in Table 2.2 using a 1 cm quartz cuvette.

	wavelength (nm)	**extinction coefficient (mM^{-1} cm^{-1})**	**reference**
$NADP^+$	259	18.0	(Boehringer 1987)
NADPH	340	6.2	(Boehringer 1987)
NAD^+	260	17.8	(Boehringer 1987)
NADH	340	6.2	(Boehringer 1987)
$AcPdAD^+$	260	16.2	specification sheet (Sigma)
ADP	259	15.4	(Bock *et al.* 1956)

Table 2.2 Wavelengths and extinction coefficients used to spectroscopically measure the concentration of nucleotide solutions.

2.3.4 Enzyme assays: measurement of the cyclic and reverse transhydrogenation reactions.

Cyclic transhydrogenation

The cyclic reaction is defined (see Section 1.8.3) as the combined reduction of $NADP^+$ by NADH and oxidation of NADPH by $AcPdAD^+$, when both take place without either the $NADP^+$ or the NADPH dissociating from the enzyme (Whitehead *et al.* 2009). The net reaction is the reduction of $AcPdAD^+$ by NADH. The reduction of $AcPdAD^+$ was measured by recording the formation of the product AcPdADH from its absorbance change at 375 nm using an extinction coefficient of 6.1 mM^{-1} cm^{-1} (Palmer *et al.* 1992). The rate of the cyclic reaction was measured using a Shimadzu UV-2401 spectrophotometer at 25˚C. The assay solution for the cyclic reactions under standard conditions in a final volume of 1 mL contained 50 mM MOPS-KOH, pH 7.2, 50 mM KCl, 2 mM $MgCl_2$, 30 nM dIII, 1.0 μM dI and 100 μM NADH. When wild-type dIII was used, no added $NADP^+$ was required because the protein contained tightly bound $NADP^+$; when dIII.R165A or dIII.E155W.R165A was used, the assay solution was supplemented with 100 μM $NADP^+$. After a 2 minute incubation period the reaction was initiated by the addition of $AcPdAD^+$ to give a final concentration of 200 μM.

Reverse transhydrogenation

The reverse reaction was measured as the reduction of $AcPdAD^+$ by NADPH (see Section 1.8.2). The reduction of $AcPdAD^+$ was measured by recording the formation of the product AcPdADH from its absorbance change at 375 nm using an extinction coefficient of 6.1 mM^{-1} cm^{-1} (Palmer *et al.* 1992). Experiments were performed on a

Shimadzu UV-2401 spectrophotometer at 25˚C. The assay solution for the reverse reaction under standard conditions in a volume of 1 mL contained 50 mM MOPS-KOH, pH 7.2, 50 mM KCl, 2 mM $MgCl_2$, 150 nM dIII, 5.0 μM dI and 200 μM NADPH. The reaction was started by the addition of $AcPdAD^+$ to give a final concentration of 200 μM.

2.4 Biophysical methods.

2.4.1 Fluorescence experiments.

Fluorescence experiments were performed either on a Spex Fluoromax fluorimeter or a PTI Quantamaster fluorimeter.

The binding of nucleotides to either dIII.E155W or dIII.E155W.R165A (in complex with dI.W72F) was measured by recording the change in fluorescence at 25˚C using 280 nm excitation, 340 nm emission and a half band width of 4 nm. The assay solution (final volume of 3 mL) contained 20 mM MOPS-KOH, pH 7.0, 0.4 μM dIII and 0.8 μM dI.W72F. The solution was incubated at 25˚C for 5 minutes before nucleotides were added (20 μM).

Fluorescence emission spectra of wild-type dI and dI.W72F were measured using either 275 nm or 290 nm excitation and a half band width of 2.8 nm. The mixture (final volume 3 mL) contained 20 mM MOPS-KOH, pH 7.0, 1.0 μM dI. Emission scans of the buffer solution containing no protein were subtracted to eliminate the water Raman peak.

2.4.2 X-ray crystallography: the crystallisation of dIII.R165A.

Attempts were made to crystallise dIII.R165A. For further details see Chapter 6, where a detailed description is given.

Results and discussion: Part I

CHAPTER 3

The preparation of apo-dIII. Cyclic and aberrant cyclic reactions catalysed by dI_2dIII complexes made with apo-dIII from *R. rubrum* transhydrogenase.

3.1 Removal of NADP(H) from dIII of *R. rubrum* transhydrogenase.

Isolated purified wild-type dIII from *R. rubrum* transhydrogenase contains tightly bound $NADP^+$ (Diggle *et al.* 1996). For this reason, nucleotide-binding studies of the dIII component have been difficult. A method for the removal of NADP(H) from dIII would be useful in experiments designed to understand the binding of nucleotides into the dIII site.

3.1.1 Dialysis of $NADP^+$ from wild-type dIII of *R. rubrum* transhydrogenase.

Attempts were made to remove the bound $NADP^+$ from dIII by dialysis. After more than 3 days of dialysis $NADP^+$ was still present in the dIII. However, it was discovered that $NADP^+$ does not readily pass through dialysis membranes in the way that is expected. Dialysis membranes from Medicell (Visking and Spectra/Por) were prepared as described in Section 2.3.2. A 12-14 KDa cut off is reported (by the manufacturer) for both membranes. Thus, $NADP^+$ with a molecular weight of 765 Da, would be expected to pass effectively through the two membranes. A 1 mL solution containing 1 mM $NADP^+$ in 20 mM tris/HCl, pH 8.0 was dialysed overnight against 1 L 20 mM tris/HCl, pH 8.0 at 4˚C, using Visking and Spectra/Por dialysis membranes. The $NADP^+$ concentrations of the solutions in the dialysis tubing were measured 18 hours later with a spectrophotometer as described in Section 2.3.3. If $NADP^+$ effectively passed through the dialysis membranes (*i.e.* if equilibrium had been reached between the solution in the dialysis tubing and the dialysate), the $NADP^+$ concentration would be 1 μM in both solutions, and 99.9% of the $NADP^+$ in the dialysis tubing would have passed through the membrane. However, after dialysis

the concentration of $NADP^+$ in the Visking dialysis tubing was 525 μM, and in the Spectra/Por dialysis tubing was 460 μM, showing that only about half of the $NADP^+$ had passed through the membranes. Kirkman *et al*. also reported $NADP^+$ to be ineffective at passing through dialysis membranes (Kirkman *et al.* 1986). Similar experiments were set up to test the dialysis of other nucleotides (NADPH, NAD^+, NADH, $AcPdAD^+$ and ADP) through the Visking dialysis membrane. Solutions (1 mL) containing 1 mM nucleotide in 20 mM tris/HCl, pH 8.0 were dialysed separately overnight (18 hours) against 1 L 20 mM tris/HCl, pH8 at 4˚C. Following this, the nucleotide concentrations of the solutions in the dialysis tubing were measured with a spectrophotometer as described in Section 2.3.3. The nucleotide concentrations of the solutions in the dialysis tubing were 545 μM for NADPH, 400 μM for NAD^+, 350 μM for NADH, 150 μM for $AcPdAD^+$ and 15 μM for ADP. These results show that, of the solutions in the dialysis tubing, 44.5% NADPH, 60% NAD^+, 65% NADH, 85% $AcPdAD^+$ and 98.5% ADP had passed through the membrane. Evidently, ADP was the only nucleotide of those tested to dialyse near to equilibrium. The chemical structure of ADP is similar to that of NAD(H), except it lacks the nicotinamide group and the adjacent ribose (see Figure 1.4). Since ADP was the only nucleotide to dialyse nearly to equilibrium, this suggests that properties of the nicotinamide mononucleotide moiety of the $NADP^+$, NADPH, NAD^+, NADH and $AcPdAD^+$ prevent the effective passage of the nucleotides through the dialysis membranes.

3.1.2 Gel-filtration of wild-type dIII from *R. rubrum* transhydrogenase.

It was evident that the removal of $NADP^+$ from the dIII solution could not be achieved using dialysis and that another method was required. Isolated dIII, purified in buffer containing 4 μM $NADP^+$ (as described in Section 2.2.2), contains ~0.75 moles of $NADP^+$ per mole of dIII (Table 3.1). Solutions of dIII were subjected to gel-filtration chromatography using procedures described in Section 2.2.6. After two passages through the gel-filtration columns, essentially all of the $NADP^+$ remained bound to the dIII. This confirms that wild-type dIII has a high affinity for the nucleotide (Diggle *et al.* 1996).

Protein	$NADP^+$ before GF (mol $NADP^+$ mol^{-1} protein)	$NADP^+$ after GF (mol $NADP^+$ mol^{-1} protein)
wild-type dIII	0.71	0.75
	0.79	0.78
	0.73	0.78
dIII.R165A	0.28	0.00
	0.35	0.01
	0.12	0.04

Table 3.1 The $NADP^+$ content of isolated wild-type dIII and dIII.R165A from *R. rubrum* transhydrogenase.

Isolated wild-type dIII and dIII.R165A (samples from 3 separate preparations of each) were passed through a gel-filtration (GF) chromatography column as described in Section 2.2.6 (for more information on dIII.R165A see Section 3.1.4). The nucleotide-content of the proteins before and after gel-filtration was measured by a method involving the denaturation of the protein to extract the bound nucletide, and fluorometrically recording the extent of $NADP^+$ reduction by isocitrate and the enzyme isocitrate dehydrogenase on a Spex Fluoromax fluorimater (as described in Section 2.3.1).

3.1.3 Removal of tightly bound NADP(H) by phosphatase treatment of wild-type dIII from *R. rubrum* transhydrogenase.

The removal of bound NADP(H) from wild-type dIII was achieved using a method adapted from Pedersen *et al.* (Pedersen *et al.* 2003). The dIII protein solution was incubated with calf-intestinal alkaline phosphatase as described in Section 2.2.7. Alkaline phosphatase cleaves the 2'-phosphate group from $NADP^+$ producing NAD^+. Control experiments were performed to detect $NADP^+$ and NAD^+ in untreated and phosphatase-treated solutions of dIII (Figure 3.1). $NADP^+$-dependent isocitrate dehydrogenase (ICDH) catalyses the oxidative decarboxylation of isocitrate, whilst reducing $NADP^+$ to NADPH. In the presence of untreated dIII, which contains bound $NADP^+$, ICDH catalysed its reaction and the production of NADPH could be seen from the fluorescence increase at 340-460 nm (Figure 3.1a). This shows that $NADP^+$ was present in the solution; as the $NADP^+$ slowly dissociated from dIII it was reduced by the ICDH. Alcohol dehydrogenase (ADH) catalyses the oxidation of ethanol whilst reducing NAD^+ to NADH. No fluorescence change was seen when ADH and ethanol were added to the solution of untreated dIII, showing that NAD^+ was not present in the solution. With phosphatase-treated dIII present, ICDH failed to catalyse any detectable oxidative decarboxylation of isocitrate but ADH did catalyse the oxidation of ethanol (Figure 3.1b). This is evidence that $NADP^+$ in the solution had been converted to NAD^+ during the treatment with phosphatase. A "blank" experiment was performed to detect the $NADP^+$ concentration of a solution containing 20 mM MOPS-KOH, pH 7.0, 5 mM $MgCl_2$ (Figure 3.1c). As expected, no detectable reduction of $NADP^+$ was seen, confirming the absence of the nucleotide. Control experiments were also performed to detect NADPH in the dIII solutions using the enzyme glutathione

reductase (also described in Section 2.2.7). Glutathione reductase catalyses the reduction of oxidised glutathione, whilst oxidising NADPH to $NADP^+$. In the presence of untreated dIII, oxidised glutathione was reduced by glutathione reductase and the oxidation of NADPH could be seen (Figure 3.1d). With phosphatase-treated dIII present, no fluorescence change was seen showing that NADPH had been completely removed from the solution during treatment with phosphatase (Figure 3.1e).

The ability of the alkaline phosphatase to cleave the 2'-phosphate from NADP(H) in the protein solution results in the formation of wild-type apo-dIII.

Figure 3.1 (over page) Determination of NADP(H) and NAD^+ levels in solutions of phosphatase-treated wild-type dIII from *R. rubrum* transhydrogenase.

Wild-type dIII was treated with alkaline phosphatase and control experiments were performed to ensure that essentially all NADP(H) had been removed from the protein solution. Fluorescence experiments were performed on a Spex Fluoromax fluorimeter as described in Section 2.2.7. Before recording, the experimental cuvettes contained (a) untreated wild-type dIII and isocitrate, (b) phosphatase-treated wild-type dIII and isocitrate, (c) buffer and isocitrate, (d) untreated wild-type dIII and oxidised glutathione and (e) phosphatase-treated wild-type dIII and oxidised glutathione. Figures (a), (b), and (c) show experiments to detect $NADP^+$ and NAD^+ using $NADP^+$-linked isocitrate dehydrogenase (ICDH) and alcohol dehydrogenase (ADH), respectively. Figures (d) and (e) show experiments to detect NADPH using glutathione reductase (GR). In experiments (a), (b) and (c), the initial rapid fluorescence increase upon addition of ICDH is due to the intrinsic fluorescence of the enzyme.

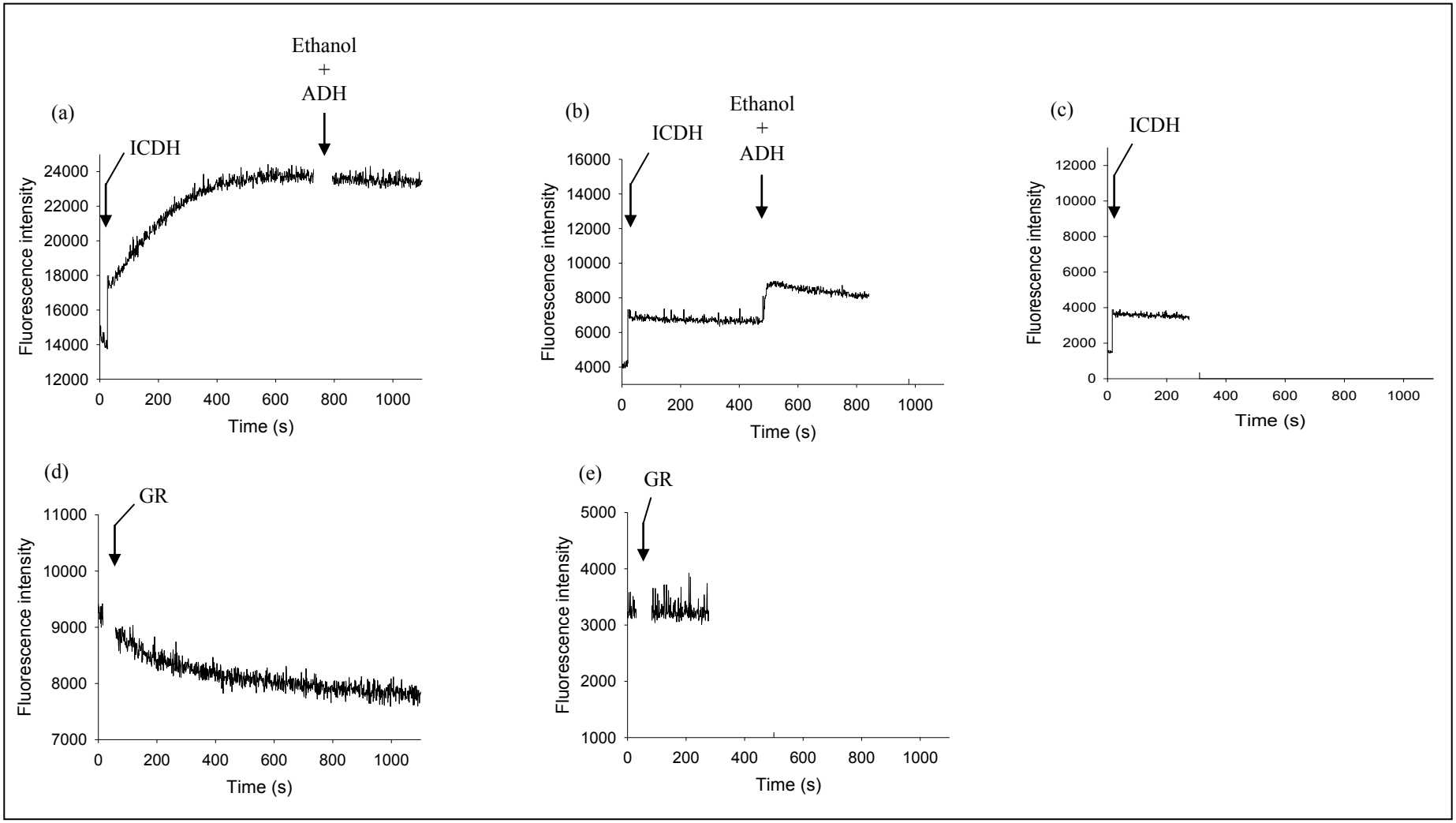
(a)
Ethanol
+
ADH
ICDH
Fluorescence intensity
Time (s)
(b)
ICDH
Ethanol
+
ADH
Fluorescence intensity
Time (s)
(c)
ICDH
Fluorescence intensity
Time (s)
(d)
GR
Fluorescence intensity
Time (s)
(e)
GR
Fluorescence intensity
Time (s)

Figure 3.1

3.1.4 Properties of the mutant dIII.R165A from *R. rubrum* transhydrogenase.

A dIII.R165A mutant from *R. rubrum* transhydrogenase was isolated in which the arginine residue from the highly conserved K-R-S motif in the NADP(H)-binding site was substituted by an alanine. Unlike wild-type dIII, which was expressed mainly in the soluble fraction of the host *E. coli* cells (Diggle *et al.* 1996), dIII.R165A was predominantly expressed in inclusion bodies. Thus, the purification of this mutant protein required a new procedure. Following preliminary work, a successful procedure was developed in which the inclusion bodies containing dIII.R165A were denatured in GuHCl and the protein was subsequently refolded upon removal of the GuHCl by dialysis (see Section 2.2.4). The resulting dIII.R165A was >95% pure. In separate experiments, wild-type dIII was subjected to denaturation and refolding by an equivalent procedure; full activity was recovered with a rate of cyclic transhydrogenation, under standard conditions, of ~2600 mol $AcPdAD^+$ reduced mol^{-1} dIII min^{-1}. This shows that the procedure did not cause inactivation of the wild-type protein, and thus the same was assumed to be true for the mutant.

Previous studies on the equivalent mutation from *E. coli* transhydrogenase (Hu *et al.* 1999; Bergkvist *et al.* 2000) suggest that dIII.R165A from *R. rubrum* transhydrogenase would have a decreased affinity for NADP(H) compared to wild-type dIII. The determination of nucleotide-content showed that dIII.R165A, purified as outlined above, was ~20% occupied by $NADP^+$ (Table 3.1). Samples were subjected to gel-filtration chromatography and the $NADP^+$ content was re-assayed (Table 3.1). The results show that essentially all the bound $NADP^+$ had been removed by the gel-filtration, and suggest that dIII.R165A has a significantly decreased affinity for $NADP^+$ relative to wild-type dIII.

In dI_2dIII complexes formed from *R. rubrum* dI and phosphatase-untreated wild-type dIII, the reverse reaction, as measured by the reduction of $AcPdAD^+$ by NADPH, is limited by the slow dissociation of the product $NADP^+$ from the dIII (see Section 1.8.2). Under the standard conditions described in Section 2.3.4, the reverse reaction was measured in parallel in complexes of wild-type dI and either wild-type dIII (untreated with phosphatase) or dIII.R165A (Figure 3.2). In agreement with earlier results (Diggle *et al.* 1996), the steady-state rate of the reverse reaction was ~1.4 mol $AcPdAD^+$ reduced mol^{-1} dIII min^{-1} in dI_2dIII complexes made with wild-type dIII. In complexes made with dIII.R165A, the rate was much higher (~13 mol $AcPdAD^+$ reduced mol^{-1} dIII min^{-1}). This large increase in rate (~9 fold) is consistent with a faster rate of $NADP^+$ release from dIII.R165A, and a decreased affinity for $NADP^+$ relative to wild-type dIII. However, the rate of the reverse reaction in complexes made with dIII.R165A is still ~1000 fold lower than that of the cyclic reaction (see Section 3.2.5). Thus, the reverse reaction is probably still limited by the release of $NADP^+$.

The methods described above for the formation of the two forms of apo-dIII (phosphatase-treated wild-type dIII or dIII.R165A) are useful to more effectively study nucleotide-binding to dIII.

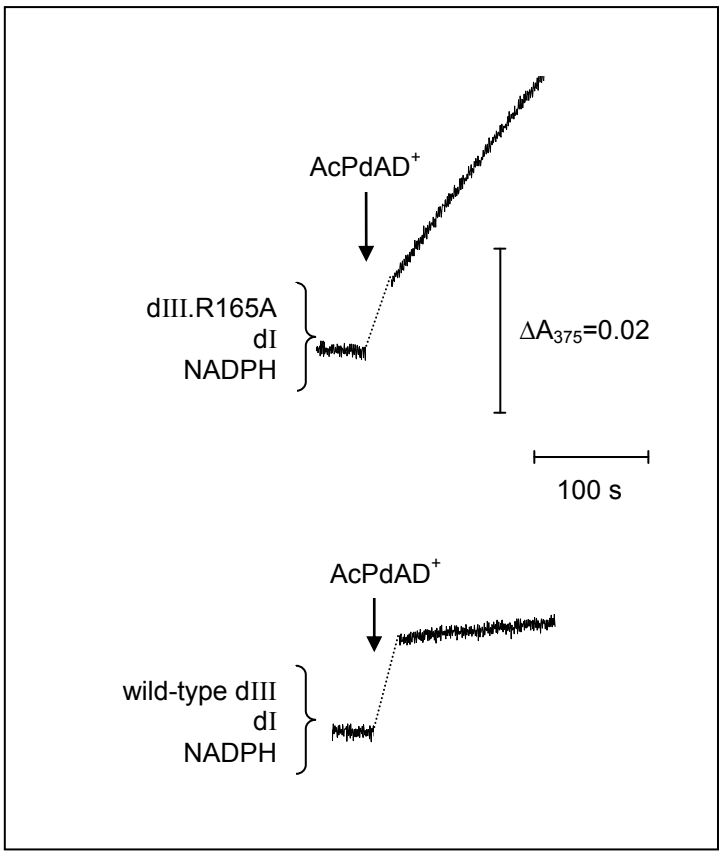

Figure 3.2 The reverse transhydrogenation reaction catalysed by dI_2dIII complexes constructed with dI and either wild-type dIII or dIII.R165A from *R. rubrum* transhydrogenase.

The reduction of $AcPdAD^+$ by NADPH was measured as described in Section 2.3.4. The initial mixture (in curly brackets) was incubated for 5 minutes before recording was started. The reaction was initiated by the addition of $AcPdAD^+$ (shown by the arrows). Disturbances from the mixing procedure have been replaced by dashed lines for clarity.

3.2 The cyclic and aberrant cyclic reactions catalysed by dI_2dIII complexes made from dI and either wild-type apo-dIII or apo-dIII.R165A from *R. rubrum* transhydrogenase.

As described in Section 1.8.3, dI_2dIII complexes constructed with dI and dIII from *R. rubrum* transhydrogenase catalyse the cyclic transhydrogenation reaction. This reaction is defined as the combined reduction of $NADP^+$ by NADH and oxidation of NADPH by NAD^+, without $NADP^+$ or NADPH dissociating from the enzyme (Whitehead *et al.* 2009). The net reaction is the reduction of $AcPdAD^+$ by NADH, and is recorded by measuring the production of AcPdADH from its absorbance change at 375 nm.

3.2.1 The reduction of $AcPdAD^+$ by NADH in the absence of NADP(H) catalysed by dI_2dIII complexes constructed with dI and wild-type apo-dIII from *R. rubrum* transhydrogenase.

Wild-type dIII from *R. rubrum* transhydrogenase was treated with alkaline phosphatase as described in Section 3.1.3. The phosphatase cleaved the 2'-phosphate from the nucleotide, resulting in the formation of the apo-form of dIII. Wild-type apo-dIII was mixed with dI from *R. rubrum* transhydrogenase to form dI_2dIII complexes, which were then used to measure the rate of $AcPdAD^+$ reduction by NADH in the absence of added NADP(H). In the following experiments, the dI and dIII concentrations used (1.0 μM and 30 nM, respectively) were such that essentially all of the dIII was in complex with dI.

In Figure 3.3a, NADH and $AcPdAD^+$ were added simultaneously to dI_2dIII complexes made from dI and wild-type apo-dIII. The reduction of $AcPdAD^+$ by NADH was recorded. The reaction started with a lag phase before reaching its maximum rate after ~30 seconds. In the scheme of the cyclic reaction shown in Figure 1.6, dIII contains tightly bound NADP(H) throughout the reaction. The experiment in Figure 3.3a was conducted ostensibly in the absence of NADP(H). Assuming that both $AcPdAD^+$ and NADH bind exclusively to dI, $AcPdAD^+$ reduction by NADH would not take place without $NADP^+$ or NADPH bound to dIII. However, previous work has suggested that NADH or $AcPdAD^+$ can bind into the $NADP^+$-binding site on dIII (Stilwell *et al.* 1997; Pedersen *et al.* 2003). In the experiment shown in Figure 3.3a, if NADH or $AcPdAD^+$ bound into the dIII site, hydride transfer could occur between the nucleotide bound to dIII and either NADH or $AcPdAD^+$ bound to dI. Thus, a rate of $AcPdAD^+$ reduction by NADH would be observed (a scheme for this reaction is shown in Figure 3.4). The conclusion can be drawn that either NADH or $AcPdAD^+$, or indeed both nucleotides, are binding into the dIII site (the "wrong" site). Since NADH and $AcPdAD^+$ bind rapidly to dI (Venning *et al.* 1999; Venning *et al.* 2000) and hydride transfer between bound nucleotides is fast (Pinheiro *et al.* 2001), the presence of the lag phase shows that the unspecific binding of NADH and/or $AcPdAD^+$ to dIII is very slow. Moreover, the presence of the lag phase enables experiments to be performed to identify which nucleotide, NADH, $AcPdAD^+$ or both can bind into the dIII site. To this end, the dI_2dIII complexes formed with dI and wild-type apo-dIII were incubated with $AcPdAD^+$ for 2 minutes before the reaction was started by the addition of NADH (Figure 3.3b). The reaction started with a lag phase before reaching a maximum rate. From this result, it can be concluded that during the 2 minute incubation period, the $AcPdAD^+$ had not bound into the dIII site and that the

lag phase was probably due to the slow binding of NADH to dIII. If $AcPdAD^+$ had bound to dIII during the incubation period, the dIII binding-sites would have been occupied by $AcPdAD^+$ when the reaction was initiated, and the reaction would not have started with a lag phase, but with a prompt rate. The experiment shown in Figure 3.3b was repeated, except the order of $AcPdAD^+$ and NADH was switched (Figure 3.3c). Thus, dI_2dIII complexes formed from dI and wild-type apo-dIII were incubated for 2 minutes with NADH before the reaction was initiated by the addition of $AcPdAD^+$. The reaction began with a prompt rate of ~2270 mol $AcPdAD^+$ reduced mol^{-1} dIII min^{-1}; there was no lag phase. The absence of a lag phase in this experiment shows that during the 2 minute incubation period NADH had fully occupied the dIII binding-sites and the reaction was able to proceed immediately at its maximum rate once initiated with $AcPdAD^+$.

The reduction of $AcPdAD^+$ by NADH in the absence of NADP(H), where NADH binds into the dIII site (the "wrong" site), is here defined as the "aberrant" cyclic reaction, as shown by the scheme in Figure 3.4. It should be emphasised at this point that, when experiments similar to those shown in Figure 3.3 were performed with complexes of dI and wild-type dIII untreated with phosphatase (*i.e.* with bound $NADP^+$) carrying out the "normal" cyclic reaction, no lags were observed (data not shown).

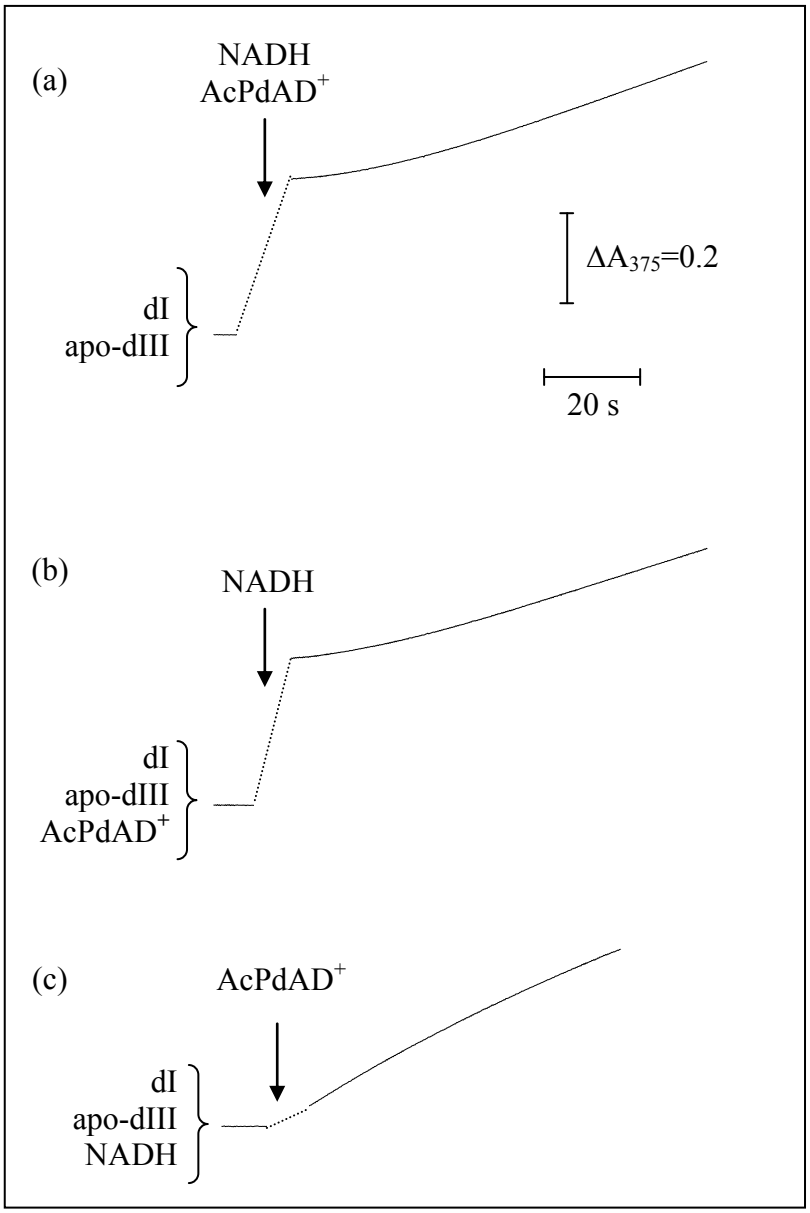

Figure 3.3 Experiments showing the aberrant cyclic reaction catalysed by dI_2dIII complexes formed with dI and wild-type apo-dIII from *R. rubrum* transhydrogenase.

The aberrant cyclic reaction was measured as the reduction of $AcPdAD^+$ by NADH (as described in Section 2.3.4) in the absence of NADP(H). In experiment (a), recording was started immediately after the initial mixture (in curly brackets) had been added to the cuvette. In experiments (b) and (c) the initial mixture was incubated in the cuvette for 2 minutes before recording was started. The reactions were initiated by the addition of nucleotides (shown by the arrows). Disturbances from mixing are replaced by dashed lines for clarity. Concentrations were 30 nM for dIII; 1.0 μM for dI; 200 μM for NADH and 200 μM for $AcPdAD^+$.

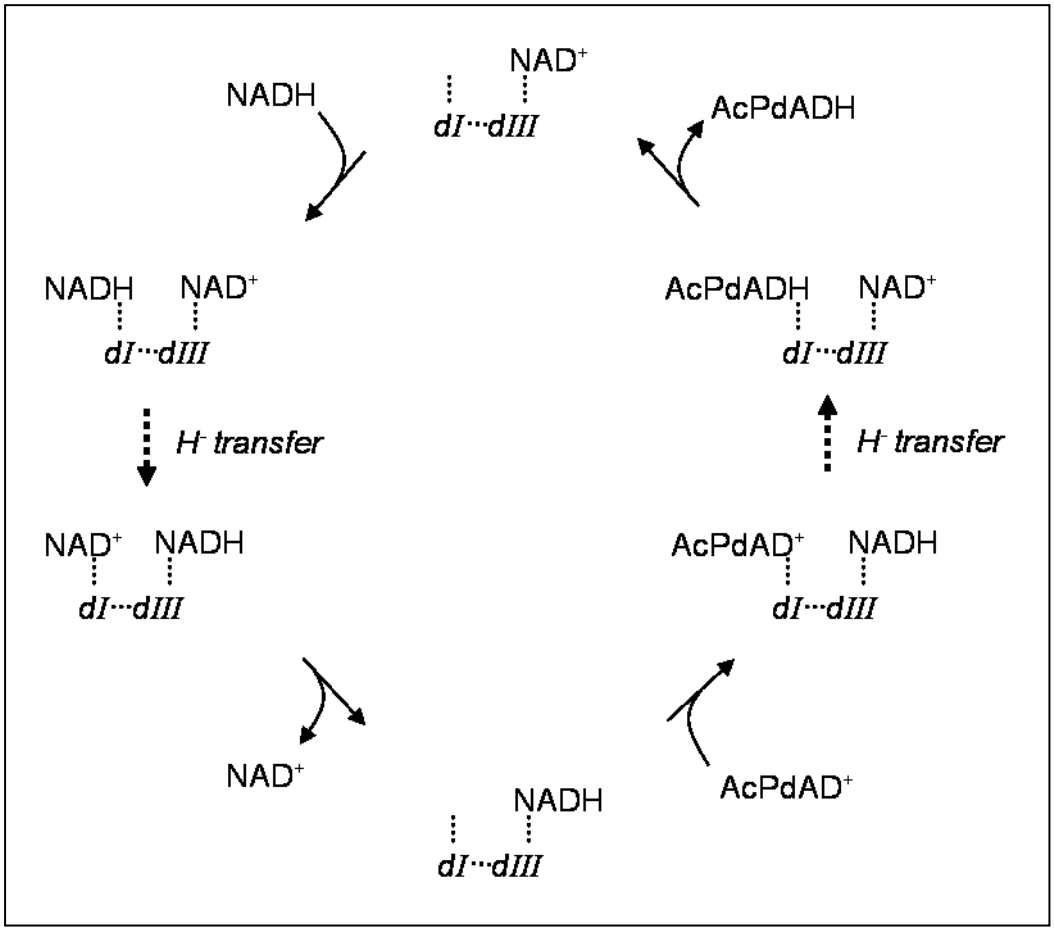

Figure 3.4 Scheme of the aberrant cyclic reaction.

In this scheme, the dotted lines indicate interactions between dI and dIII, and between the protein components and bound nucleotides. The dashed arrows show the two hydride transfer steps in the cyclic reaction. Only one of the two dI subunits is depicted. Overall, the aberrant cyclic reaction is the reduction of $AcPdAD^+$ by NADH in the absence of NADP(H), where NAD^+ and NADH remain bound to dIII. When dI and apo-dIII are mixed they spontaneously form dI_2dIII complexes. NADH binds slowly to dIII in these complexes. When $AcPdAD^+$ is added, it rapidly binds to dI and is reduced by the NADH bound to dIII. The resulting AcPdADH dissociates from dI whilst the NAD^+ remains bound to dIII. NADH then binds to dI and reduces the NAD^+ on dIII. The resulting NAD^+ dissociates from dI whilst NADH remains bound to dIII. Another molecule of $AcPdAD^+$ binds to dI and the cycle is repeated.

3.2.2 Binding properties of dI_2dIII complexes constructed with dI and either wild-type dIII or dIII.R165A from *R. rubrum* transhydrogenase.

Following the experiments described in the previous section (where the rate of the aberrant cyclic reaction, catalysed by dI_2dIII complexes was measured), similar experiments were designed using apo-dIII.R165A instead of wild-type apo-dIII. When dI and wild-type dIII from *R. rubrum* transhydrogenase are mixed, they rapidly form dI_2dIII complexes (Venning *et al.* 2001). The same cannot be assumed for dI and dIII.R165A. Prior to enzyme assays, it was necessary to ensure that the affinity of dIII.R165A for dI was not affected by the R165A mutation. To this end, the cyclic reaction (*i.e.* the reduction of $AcPdAD^+$ by NADH in the presence of $NADP^+$) catalysed by dI_2dIII complexes formed with dI and either wild-type dIII (untreated with phosphatase) or dIII.R165A was measured under standard conditions (described in Section 2.3.4) as a function of dI concentration (Figure 3.5). The concentration of dIII was kept constant throughout and the concentration of dI was varied. The concentration of dI required to reach the half-maximal rate was ~40 nM for wild-type dIII and ~100 nM for dIII.R165A. The former value is consistent with previous results of calorimetry experiments where the K_d for the binding of dIII to dI_2 was found to be ≤60 nM (Venning *et al.* 2001). These results show that the affinity of dIII.R165A for dI has decreased ~2 fold relative to wild-type dIII. However, the concentrations of dI (1.0 μM) and dIII (30 nM) used in the experiments described in this project ensure that essentially all dIII, wild-type or dIII.R165A, will exist as dI_2dIII complexes.

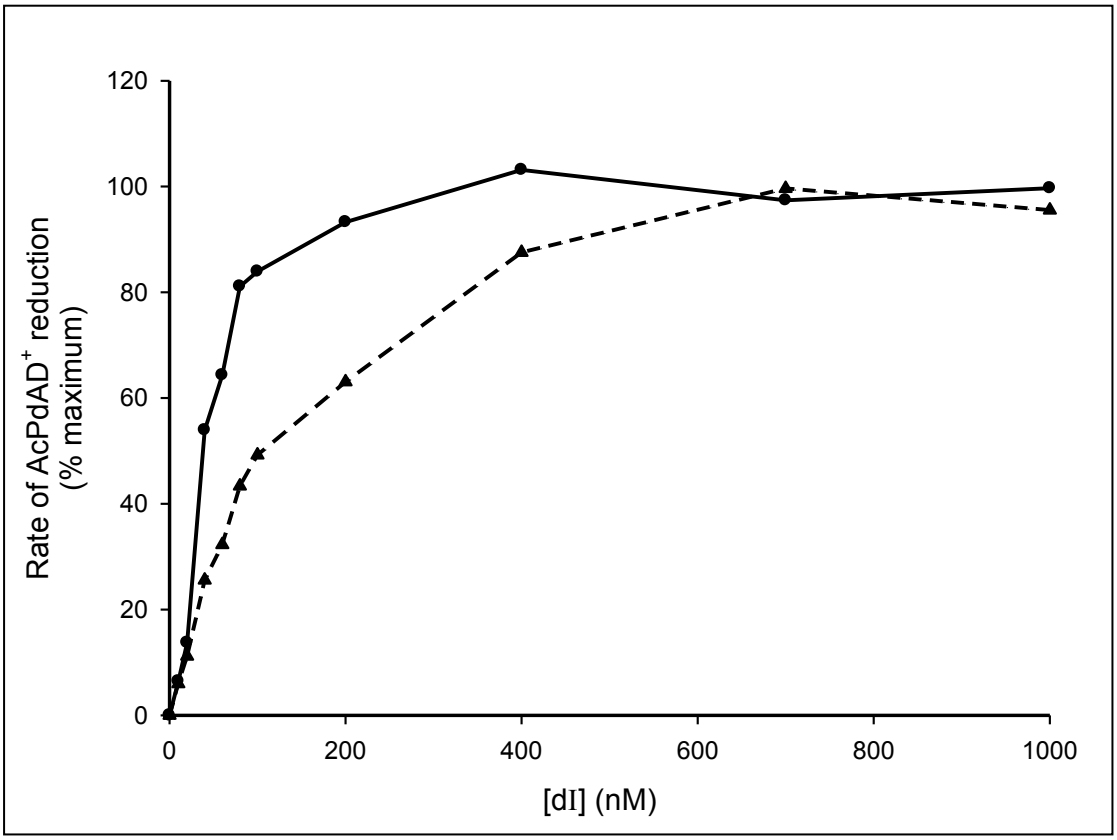

Figure 3.5 Effect of dI concentration on the rate of the cyclic reaction catalysed by dI_2dIII complexes constructed with dI and either wild-type dIII or dIII.R165A from *R. rubrum* transhydrogenase.

The rate of $AcPdAD^+$ reduction by NADH in the presence of $NADP^+$ was measured under standard conditions (described in Section 2.3.4). The reactions were catalysed by dI_2dIII complexes formed by mixing dI with either wild-type dIII (solid lines, circles) or dIII.R165A (dashed lines, triangles). The dIII concentration was kept constant (30 nM) while the dI concentration was varied. The data plotted are of single measurements.

3.2.3 The reduction of $AcPdAD^+$ by NADH in the absence of NADP(H) catalysed by dI_2dIII complexes constructed with dI and apo-dIII.R165A from *R. rubrum* transhydrogenase.

The experiments shown in Figure 3.3, which revealed the aberrant cyclic reaction catalysed by dI_2dIII with wild-type dIII, were repeated using dI_2dIII complexes formed with dIII.R165A (Figure 3.6). The dIII.R165A used in these experiments had been passed through a gel-filtration chromatography column prior to use (see Section 2.2.4) to remove bound NADP(H); thus it was in its apo-form. Overall, the results were very similar for dI_2dIII complexes formed with apo-dIII.R165A compared with those formed with wild-type apo-dIII.

Firstly, NADH and $AcPdAD^+$ were simultaneously added to dI_2dIII complexes made from dI and apo-dIII.R165A from *R. rubrum* transhydrogenase (Figure 3.6a). The reaction started with a lag phase similar to that seen with dI_2dIII complexes formed with wild-type apo-dIII. The reaction reached a maximum rate only after ~30 seconds. From this result, it can be concluded that NADH and/or $AcPdAD^+$ binds into the NADP(H)-binding site on dIII.R165A. Since both NADH and $AcPdAD^+$ bind rapidly to dI (Venning *et al.* 1999; Venning *et al.* 2000) and hydride transfer between bound nucleotides is fast (Pinheiro *et al.* 2001), the lag phase can be attributed to the very slow binding of either NADH or $AcPdAD^+$ to dIII.R165A.

Secondly, experiments were designed to determine which nucleotide (NADH and/or $AcPdAD^+$) binds to dIII.R165A in the dI_2dIII complexes. To this end, $AcPdAD^+$ was incubated for 2 minutes with dI_2dIII complexes formed with dI and apo-dIII.R165A, before the reaction was started by the addition of NADH (Figure 3.6b). Again, the reaction started with a lag phase before reaching the maximum rate.

This shows that during the 2 minute incubation period, $AcPdAD^+$ did not bind into the dIII.R165A site. If $AcPdAD^+$ had bound to dIII.R165A during the incubation period, the dIII.R165A binding sites would have been occupied by $AcPdAD^+$ when the NADH was added, causing the reaction to start promptly without a lag. Thus, it can be concluded that $AcPdAD^+$ does not bind to dIII.R165A, and that the lag phase must be due to the slow binding of NADH to into the dIII.R165A sites. To confirm this, NADH was incubated with dI_2dIII complexes formed with apo-dIII.R165A for 2 minutes before the reaction was started by the addition of $AcPdAD^+$ (Figure 3.6c). The reaction began promptly at a rate of ~1380 mol $AcPdAD^+$ reduced mol^{-1} dIII min^{-1}; there was no lag phase. This shows that during the 2 minute incubation period the dIII.R165A sites had been fully occupied with NADH, such that when $AcPdAD^+$ was added the reaction could proceed immediately at a maximum rate. The rate of the aberrant cyclic reaction observed using complexes with dIII.R165A was about 20% lower than that observed using complexes with wild-type dIII.

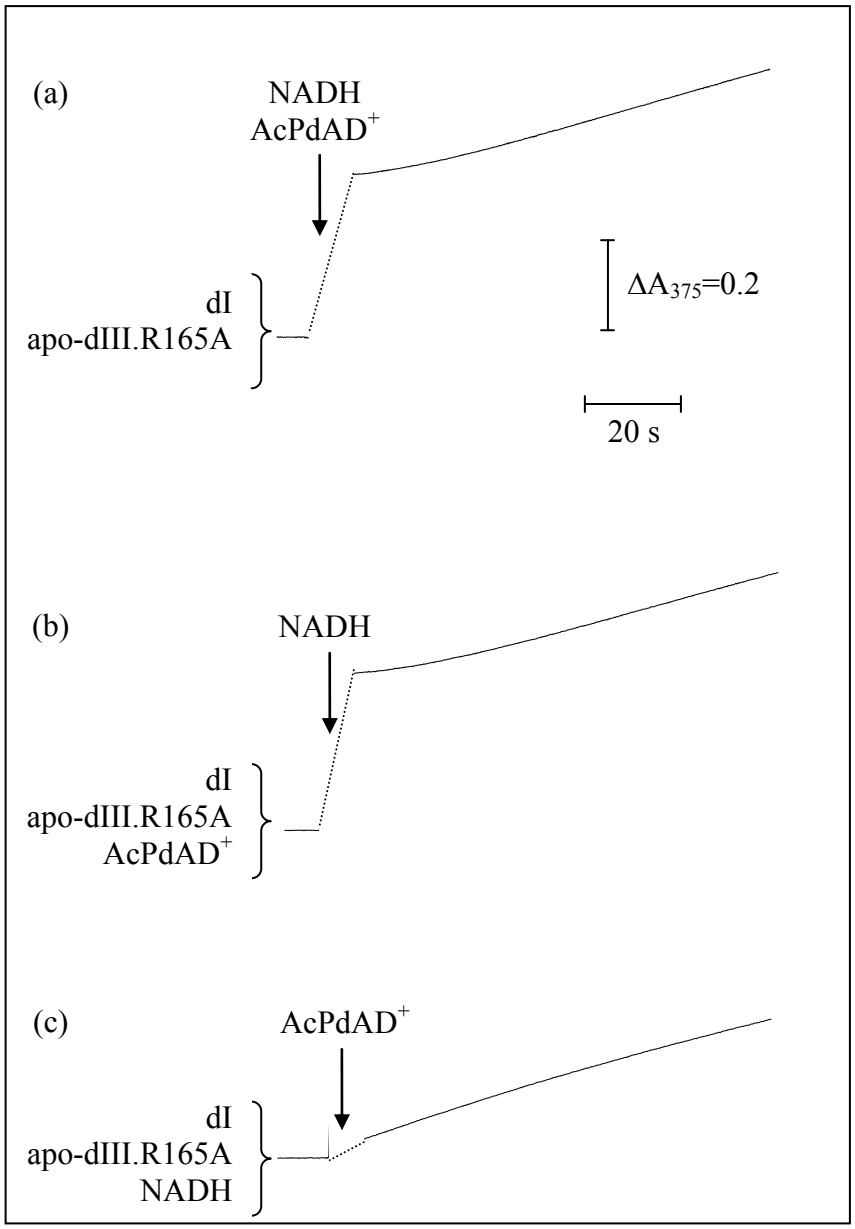

Figure 3.6 Experiments measuring the aberrant cyclic reaction catalysed by dI_2dIII complexes constructed with dI and apo-dIII.R165A from *R. rubrum* transhydrogenase.

The aberrant cyclic reaction was measured as the reduction of $AcPdAD^+$ by NADH (as described in Section 2.3.4) in the absence of NADP(H). In experiment (a), recording was started immediately after the initial mixture (in curly brackets) was added to the cuvette. In experiments (b) and (c), the initial mixture was incubated for 2 minutes before recording was started. The reactions were initiated by the addition of nucleotides (shown by the arrows). Disturbances from mixing are replaced by dashed lines for clarity. Concentrations were 30 nM for apo-dIII.R165A; 1.0 μM for dI; 200 μM for NADH and 200 μM for $AcPdAD^+$.

3.2.4 The reduction of $AcPdAD^+$ by NADH in the presence of $NADP^+$ catalysed by dI_2dIII complexes constructed with dI and wild-type apo-dIII from *R. rubrum* transhydrogenase.

As explained in Section 3.1.3, treatment of wild-type dIII with alkaline phosphatase resulted in the formation of apo-dIII. Previously, it has proved difficult to study the binding of $NADP^+$ and NADPH to dIII due to the very high affinity of the protein for the nucleotides. The formation of the apo-form of wild-type dIII enables experiments to observe NADP(H)-binding to dIII to be designed. To this end, the cyclic reaction, catalysed by dI_2dIII complexes formed with dI and wild-type apo-dIII from *R. rubrum* transhydrogenase, was recorded as the reduction of $AcPdAD^+$ by NADH with added $NADP^+$.

Firstly, NADH, $AcPdAD^+$ and $NADP^+$ were simultaneously added to dI_2dIII complexes formed with dI and wild-type apo-dIII (Figure 3.7a). The reaction started with a lag phase and reached the maximum rate only after ~30 seconds. Since NADH and $AcPdAD^+$ bind rapidly to dI (Venning *et al.* 1999; Venning *et al.* 2000) and hydride transfer between bound nucleotides is fast (Pinheiro *et al.* 2001), the presence of the lag phase in this experiment shows that nucleotide-binding to dIII in dI_2dIII complexes is very slow. Recall from Section 3.2.1 that NADH is able to bind aberrantly into the dIII site. Thus, the lag phase can be attributed to either the slow binding of $NADP^+$ and/or NADH to dIII. If $NADP^+$ were binding to dIII, it would be rapidly reduced by NADH on dI during a "normal" cyclic reaction; if NADH were binding to dIII it would be rapidly oxidised by $AcPdAD^+$ on dI during an aberrant cyclic reaction.

In a second experiment, dI was incubated with NADH, $AcPdAD^+$ and $NADP^+$ for 1 minute before the reaction was started by the addition of wild-type apo-dIII (Figure 3.7b). The reaction again started with a lag phase before it reached its maximum rate. This confirms that the lag is not due to NADH or $AcPdAD^+$ binding slowly to dI. The incubation period provided sufficient time for the nucleotides to bind to dI, yet the lag phase remained. This confirms that NADH and $AcPdAD^+$ bind rapidly to dI (Venning *et al.* 1999; Venning *et al.* 2000).

In the next experiment, dI_2dIII complexes formed with dI and wild-type apo-dIII, were incubated for 2 minutes with $AcPdAD^+$ before the reaction was initiated by the simultaneous addition of NADH and $NADP^+$ (Figure 3.7c). The reaction started with a lag phase and only after ~30 seconds reached its maximum rate. The incubation period provided sufficient time for dI and dIII to associate to form dI_2dIII complexes (Venning *et al.* 2001), and also for $AcPdAD^+$ to bind to the enzyme (Venning *et al.* 1999), but the lag phase remained. This result confirms that the lag phase is due to the slow binding of either NADH or $NADP^+$ to dIII.

In the experiments described in this section, it has been assumed that $NADP^+$ can bind into the empty site on dIII. The experiment shown in Figure 3.7d strongly supports the assumption. Thus, dI_2dIII complexes formed with dI and wild-type apo-dIII were incubated with $AcPdAD^+$ and $NADP^+$ for 2 minutes before the reaction was initiated by the addition of NADH. The reaction began promptly at a rate of ~2360 mol $AcPdAD^+$ reduced mol^{-1} dIII min^{-1}; without any detectable lag. Recall from experiments described in Section 3.2.1, that $AcPdAD^+$ is unable to bind into the dIII site. Thus, it can be concluded that during the incubation period the $NADP^+$ bound into the empty sites of dIII. When NADH was added, the dIII sites were occupied by $NADP^+$ and the reaction could proceed immediately at the maximum rate. If $NADP^+$

had not bound to dIII, the reaction would have started with a lag phase. This confirms that the lag phase in the experiments described in this section was at least partly due to the slow binding of $NADP^+$ to dIII. However, it cannot be ruled out in these experiments that the lag phase was also partly due to the slow binding of NADH into the dIII site.

Figure 3.7 (over page) Experiments measuring the cyclic reaction catalysed by dI_2dIII complexes formed with dI and wild-type apo-dIII from *R. rubrum* transhydrogenase.

The cyclic reaction was recorded as the reduction of $AcPdAD^+$ by NADH with added $NADP^+$ as described in Section 2.3.4. In experiment (a), recording was started immediately after the initial mixture (in curly brackets) was added to the cuvette. In experiment (b), the initial mixture was incubated in the cuvette for 1 minute before recording was started, and in experiments (c) and (d) the initial mixture was incubated for 2 minutes before recording was started. The reactions were initiated in each experiment by the addition of nucleotides or proteins (shown by the arrows). Disturbances from mixing are replaced by dashed lines for clarity. Concentrations were 30 nM for phosphatase-treated dIII; 1.0 μM for dI; 200 μM for NADH; 200 μM $NADP^+$ and 200 μM for $AcPdAD^+$.

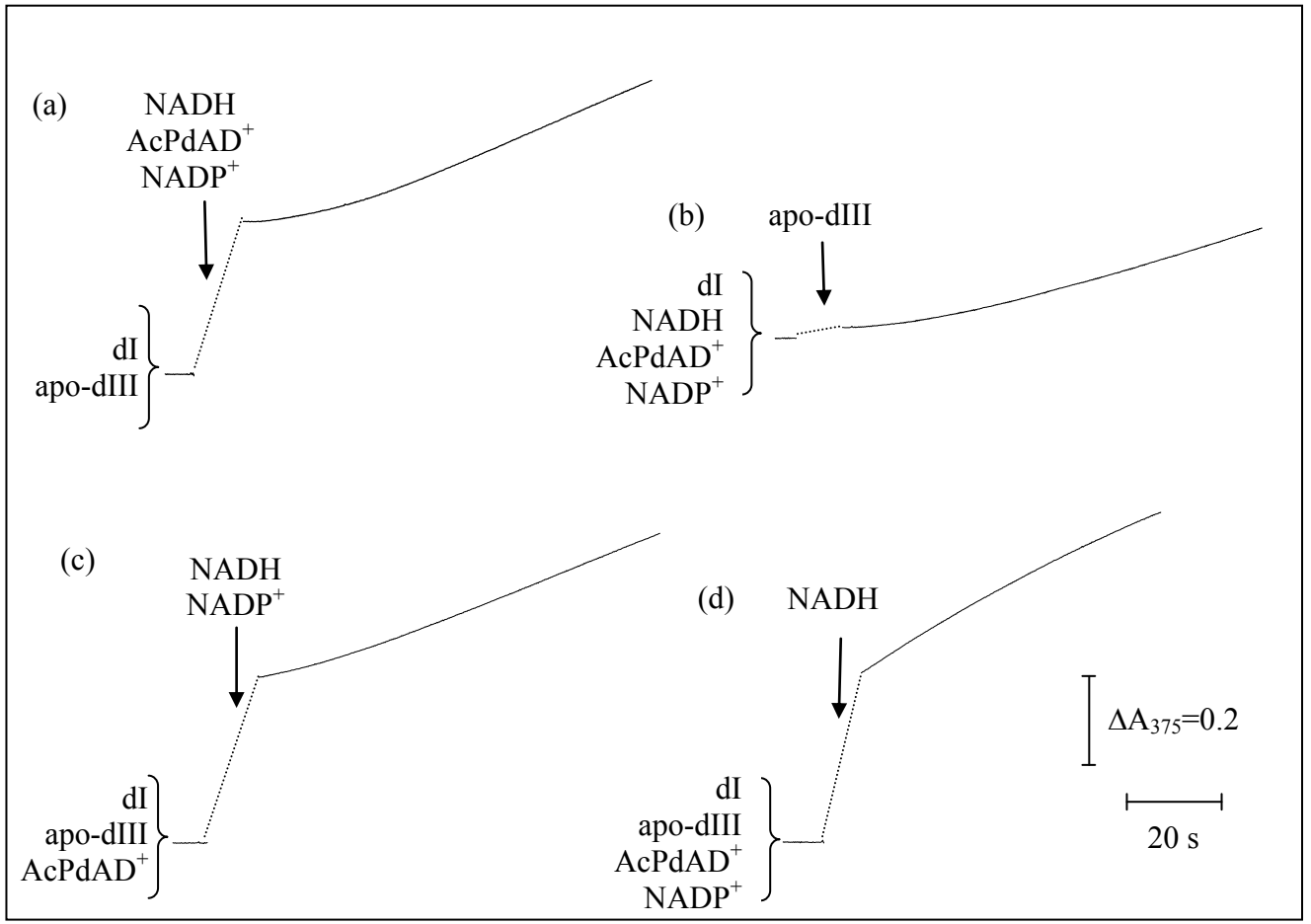
(a)
NADH
AcPdAD+
NADP+
dI
apo-dIII
(b)
apo-dIII
dI
NADH
AcPdAD+
NADP+
(c)
NADH
NADP+
dI
apo-dIII
AcPdAD+
(d)
NADH
dI
apo-dIII
AcPdAD+
NADP+
ΔA375=0.2
20 s

Figure 3.7

3.2.5 The reduction of AcPdAD$^+$ by NADH in the presence of NADP$^+$ catalysed by dI$_2$dIII complexes constructed with dI and apo-dIII.R165A from *R. rubrum* transhydrogenase.

The mutant dIII.R165A has been shown to have a significantly decreased affinity for NADP$^+$ compared to wild-type dIII. Thus, experiments were designed to measure the binding of NADP$^+$ to apo-dIII.R165A in dI$_2$dIII complexes. The results of experiments to measure the reduction of AcPdAD$^+$ by NADH in the presence of NADP$^+$ with dI$_2$dIII complexes formed with apo-dIII.R165A, were very similar to those with dI$_2$dIII complexes formed with wild-type apo-dIII.

Firstly, NADH, AcPdAD$^+$ and NADP$^+$ were simultaneously added to dI$_2$dIII complexes formed with dI and apo-dIII.R165A (Figure 3.8a). The reaction started with a lag phase and reached its maximum rate only after ~30 seconds. Again, since NADH and AcPdAD$^+$ bind rapidly to dI (Venning *et al.* 1999; Venning *et al.* 2000) and hydride transfer between bound nucleotides is fast (Pinheiro *et al.* 2001), the presence of the lag phase shows that the binding of nucleotides to apo-dIII in dI$_2$dIII complexes is very slow.

Next, NADH, AcPdAD$^+$ and NADP$^+$ were incubated for 1 minute with dI before the reaction was initiated by the addition of apo-dIII.R165A (Figure 3.8b). The reaction started with a lag phase and reached a maximum rate only after ~30 seconds. This shows that the lag cannot be attributed to nucleotides binding slowly to dI, since the incubation period provided sufficient time for binding, yet the lag phase remained. It can be concluded that the lag phase is due to the very slow binding of NADP$^+$ and/or NADH to the dIII.R165A. In another experiment, complexes of dI$_2$dIII formed from dI and apo-dIII.R165A were incubated with AcPdAD$^+$ for 2 minutes before the

reaction was initiated by the simultaneous addition of NADH and $NADP^+$ (Figure 3.8c). The reaction started with a lag phase before reaching a maximum rate only after ~30 seconds. It was established that $AcPdAD^+$ does not bind into the dIII site of dI_2dIII formed with dI and either wild-type apo-dIII (in Section 3.2.1) or apo-dIII.R165A (in Section 3.2.3). The result here supports the view that $AcPdAD^+$ does not bind into the dIII site on dIII.R165A. If $AcPdAD^+$ did bind, the reaction would have started immediately at a maximum rate with no lag phase; *i.e.* the $AcPdAD^+$ would have bound to dIII in the incubation period and hydride transfer would have begun immediately. However, this was not the case: the lag is due to the slow binding of $NADP^+$ and/or NADH to dIII.

In the experiments described in figures 3.7a, b and c, the lag phase could be attributed to the slow binding of either NADH or $NADP^+$ to dIII. Given that dIII.R165A has a significantly decreased affinity for $NADP^+$ relative to wild-type dIII it was investigated whether $NADP^+$ is able to bind to dIII under the conditions of the experiments. To this end, dI_2dIII complexes formed with dI and apo-dIII.R165A were incubated for 2 minutes with $AcPdAD^+$ and $NADP^+$ (Figure 3.8d). The reaction started immediately at a maximum rate of ~1420 mol $AcPdAD^+$ reduced mol^{-1} dIII min^{-1}. Recall that $AcPdAD^+$ does not bind into the dIII site of dI_2dIII formed with dI and either wild-type apo-dIII or apo-dIII.R165A. This result therefore shows that $NADP^+$ does bind to dIII.R165A during the incubation period such that the dIII.R165A binding-sites were occupied by $NADP^+$ when the reaction was initiated with NADH. The reaction could then proceed promptly at the maximum rate. If $NADP^+$ had not bound to dIII.R165A, an initial lag phase would have been observed, attributable to the slow binding of NADH to dIII.R165A. The rate of the cyclic

reaction observed using dI_2dIII complexes with dIII.R165A was about 35% lower than that observed in complexes with wild-type dIII.

In summary, the results in this section show that the lag phase at the onset of the cyclic reaction can be attributed to the slow binding of $NADP^+$ into the dIII.R165A site. Some slow binding of NADH probably also takes place in these experiments and leads to a contribution from an aberrant cyclic reaction.

Figure 3.8 (over page) Experiments measuring the cyclic reaction catalysed by dI_2dIII complexes formed with dI and apo-dIII.R165A from *R. rubrum* transhydrogenase.

The cyclic reaction was recorded as the reduction of $AcPdAD^+$ by NADH with added $NADP^+$ as described in Section 2.3.4. In experiment (a), recording was started immediately after the initial mixture (in curly brackets) was added to the cuvette. In experiment (b) the initial mixture was incubated in the cuvette for 1 minute before recording was started, and in experiments (c) and (d) the initial mixture was incubated for 2 minutes before recording was started. The reactions were initiated in each experiment by the addition of nucleotides or proteins (shown by the arrows). Disturbances from mixing are replaced by dashed lines for clarity. Concentrations were 30 nM for dIII.R165A; 1.0 μM for dI; 200 μM for NADH; 200 μM $NADP^+$ and 200 μM for $AcPdAD^+$.

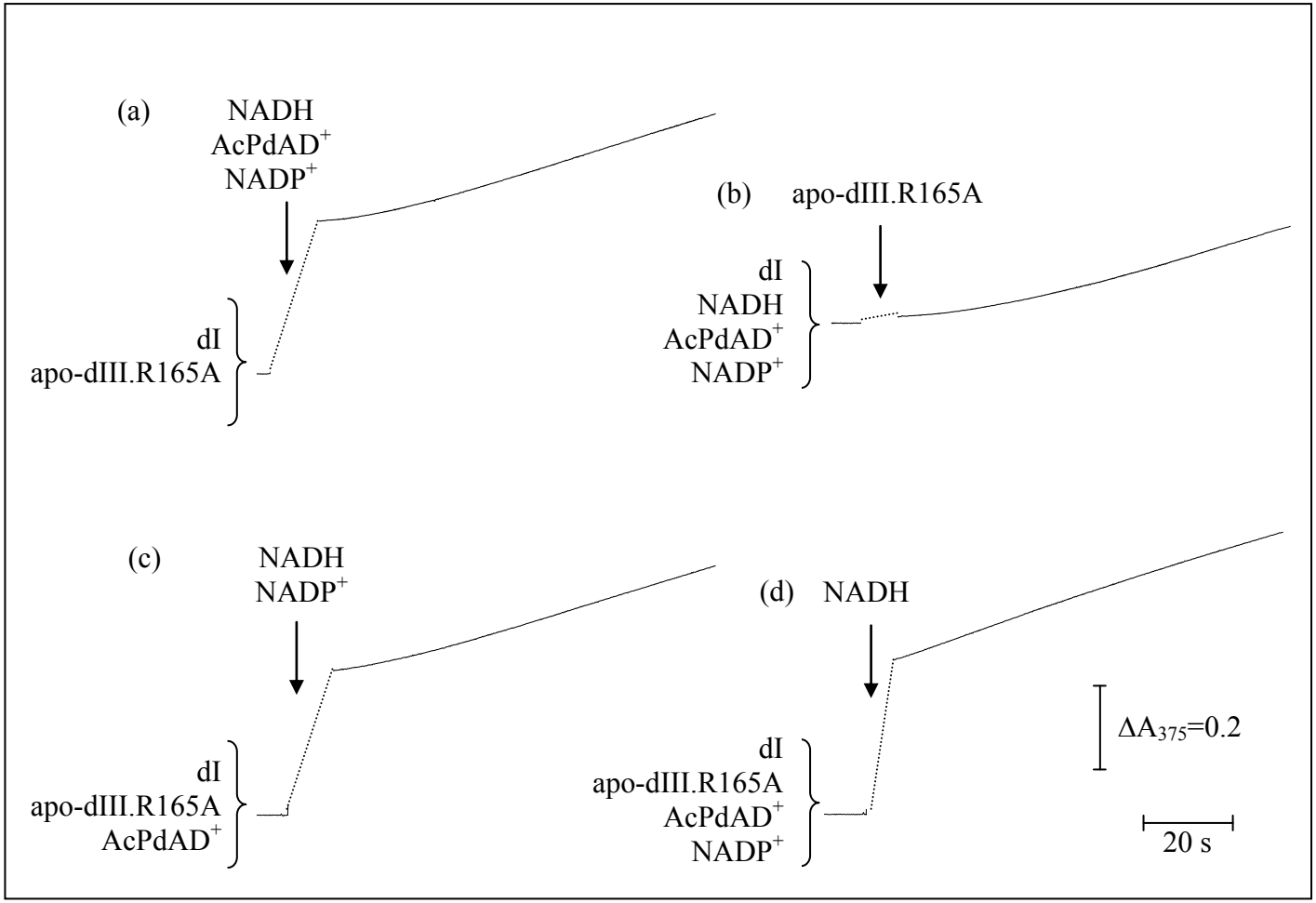
(a)
NADH
AcPdAD+
NADP+
dI
apo-dIII.R165A
(b)
apo-dIII.R165A
dI
NADH
AcPdAD+
NADP+
(c)
NADH
NADP+
dI
apo-dIII.R165A
AcPdAD+
(d)
NADH
dI
apo-dIII.R165A
AcPdAD+
NADP+
ΔA375=0.2
20 s

Figure 3.8

3.3 Analysis of the lag phase to determine the kinetics of nucleotide-binding to dIII in dI_2dIII complexes from *R. rubrum* transhydrogenase.

The lag phase at the onset of the cyclic and aberrant cyclic reactions was analysed to determine the kinetics of nucleotide-binding to dIII in dI_2dIII complexes constructed with dI and either wild-type apo-dIII or apo-dIII.R165A. In the first set of experiments, a protocol similar to that shown in figures 3.3b and 3.5b, for the aberrant cyclic reaction was adopted. In this protocol dI_2dIII complexes were incubated with $AcPdAD^+$ before the reaction was initiated by the addition of NADH. The reactions started with a lag phase. The rate of $AcPdAD^+$ reduction during this lag phase was plotted against time (Figure 3.9). Since the binding of NADH to dIII is slow, and the rates of other component reactions are fast, the rate of $AcPdAD^+$ reduction during the lag phase is proportional to the degree of occupancy of the dIII site. The plots therefore show the filling of the dIII site with NADH. Assuming that all the sites are filled when the maximum rate of reaction is reached, the time taken to fill half the sites ($t_{½}$) was ~10 s. In a second set of experiments, using a protocol similar to that shown in figures 3.6c and 3.7c, dI_2dIII complexes were incubated with $AcPdAD^+$ before the reaction was initiated by the simultaneous addition of NADH and $NADP^+$. Again, the reactions started with a lag phase and the rate of $AcPdAD^+$ reduction during this lag phase was plotted against time (Figure 3.9A). Here, the NADH and $NADP^+$ compete for dIII binding sites to produce a population of complexes catalysing the cyclic reaction and a population catalysing the aberrant cyclic reaction.

The plots show that the kinetics of nucleotide-binding to dIII were similar in both sets of experiments. Thus, the kinetics of NADH-binding and of $NADP^+$-binding to dIII in dI_2dIII complexes are similar. The kinetics were also similar for the binding

of nucleotides to the dIII component of the complexes, whether using wild-type dIII or dIII.R165A. Further analysis of the data is consistent with nucleotide binding to dIII (wild-type dIII or dIII.R165A) being first-order in dI_2dIII complexes (Figure 3.9B).

Figure 3.9 (over page) Kinetics of the lag phase in experiments measuring the cyclic and aberrant cyclic reactions catalysed by dI_2dIII complexes constructed with dI and either wild-type apo-dIII or apo-dIII.R165A from *R. rubrum* transhydrogenase.

The apo-form of wild-type dIII was prepared by phosphatase treatment (see Section 2.2.7), and of dIII.R165A, by two passages down a gel-filtration chromatography column (see Section 2.2.4). Rates of $AcPdAD^+$ reduction were measured from experiments with complexes of wild-type dI and either wild-type apo-dIII (solid lines, closed symbols) or apo-dIII.R165A (dashed lines, open symbols). In the first set of experiments, using the protocol shown in figures 3.3b and 3.5b, the reaction was initiated by the addition of 200 μM NADH (blue lines, circles). In a second set of experiments, using the protocol from figures 3.6c and 3.7c, the reaction was initiated by the simultaneous addition of 200 μM $NADP^+$ and 200 μM NADH (red lines, triangles). Rates were calculated from tangents to the absorbance change at 375 nm, and were plotted as a function of time after initiating the reaction (Panel A). The plots from the two sets of experiments were normalised to the same maximum rate (at the end of the lag phase). Results of duplicate experiments from each experimental condition are presented to illustrate scatter on the data.

The rate of $AcPdAD^+$ reduction during the lag phase is proportional to the degree of occupancy of dIII. Points were taken from one data set of the graph shown in Panel A. From these data points the concentration of apo-dIII was calculated at various time intervals (assuming that the concentration of apo-dIII at 100% of the maximum rate of $AcPdAD^+$ reduction was 0 nM, and at 0% of the rate was 30 nM, which is the total concentration of dIII added to the reaction). Plotting ln[apo-dIII] against time gave a straight line graph (Panel B); this is consistent with nucleotide binding to dIII being first-order in dI_2dIII complexes (see Figure 5.2).

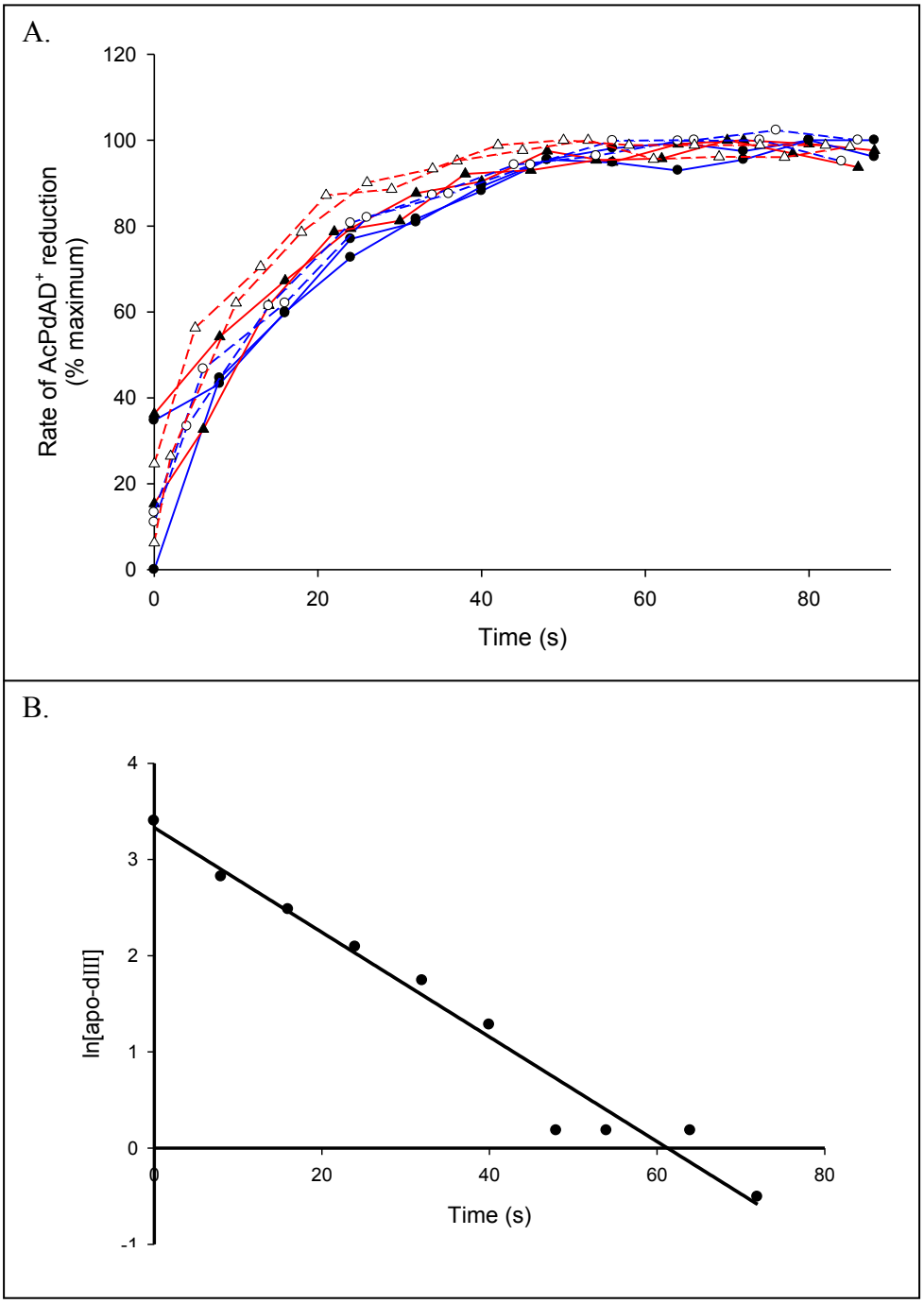
A.
Rate of AcPdAD+ reduction (% maximum)
120
100
80
60
40
20
0
0
20
40
60
80
Time (s)
B.
ln[apo-dIII]
4
3
2
1
0
-1
0
20
40
60
80
Time (s)

Figure 3.9

3.4 Estimation of nucleotide-binding affinities of wild-type dIII and dIII.R165A in dI_2dIII complexes from *R. rubrum* transhydrogenase by measuring the rates of the cyclic and aberrant cyclic reactions.

Experiments, in which the rates of the cyclic and aberrant cyclic reactions were measured, were extended in attempts to estimate K_d values of wild-type dIII and dIII.R165A in dI_2dIII complexes for $NADP^+$, NADPH and NADH.

Firstly, to estimate binding affinities for $NADP^+$ and NADPH, dI_2dIII complexes constructed with dI and either wild-type apo-dIII or apo-dIII.R165A were incubated for 5 minutes with $AcPdAD^+$ and varying concentrations of either $NADP^+$ or NADPH before the reaction was initiated by the addition of NADH. Recall that $AcPdAD^+$ is unable to bind to the dIII in these complexes, thus the initial rate of reaction should be proportional to the amount of dIII occupied by either $NADP^+$ or NADPH. The concentration required to reach the half-maximal rate in complexes with wild-type dIII was ~5 μM for $NADP^+$ (Figure 3.10A) and ~1 μM for NADPH (Figure 3.10B). In complexes with dIII.R165A the concentration required to reach the half-maximal rate was ~40 μM for $NADP^+$ (Figure 3.10A) and ~1 μM for NADPH (Figure 3.10B).

Secondly, experiments were performed to estimate the binding affinity of wild-type dIII and dIII.R165A in dI_2dIII complexes for NADH. Complexes constructed with dI and either wild-type apo-dIII or apo-dIII.R165A were incubated for 5 minutes with varying concentrations of NADH before the reaction was initiated by the addition of $AcPdAD^+$. In the incubation period the NADH bound to the dIII to an extent dependent on binding affinity. Thus, the initial rate of reaction should be proportional to the amount of dIII occupied by NADH when the reaction is initiated.

The concentration of NADH needed to reach the half-maximal rate in dI_2dIII complexes was ~40 μM in complexes formed with wild-type dIII and with dIII.R165A (Figure 3.10C).

There are a number of difficulties in relating the experimental values from Figure 3.10 to nucleotide-binding affinities. Firstly, the substrate concentration required to give a half-maximal rate of an enzyme-catalysed reaction (the K_m when other substrates are saturating) is only a measure of the K_d for some kinetic schemes (Fersht 1999). Secondly, in both the cyclic and aberrant cyclic reactions, catalysed by dI_2dIII complexes, NADH and $AcPdAD^+$ compete for the same site on dI causing substrate inhibition (Bizouarn *et al.* 1995). This leads, for example, to the decrease in reaction rate at high concentrations of NADH in Figure 3.10C and will complicate the analysis. Thirdly, there is a problem in experiments shown in Figure 3.7 and 3.8 that NADH and $NADP^+$ both compete for the same site on dIII, giving rise to a mixture of cyclic and aberrant cyclic reactions. It is concluded that the above estimates of the nucleotide concentrations which give half-maximal rates of reaction are only loosely indicative of the K_d values.

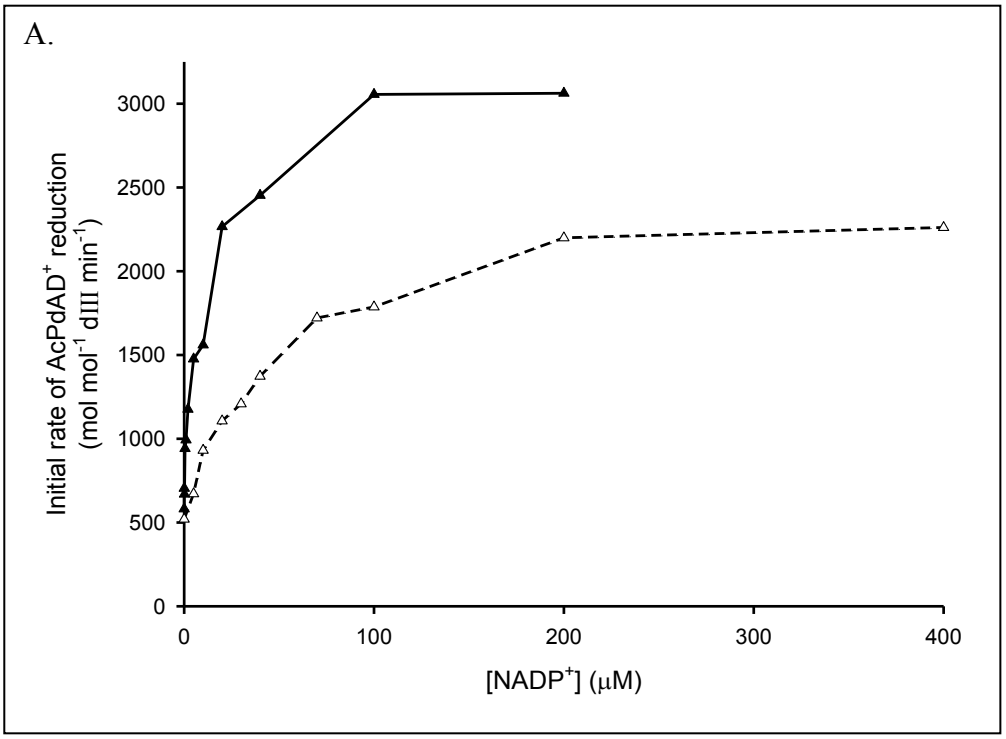

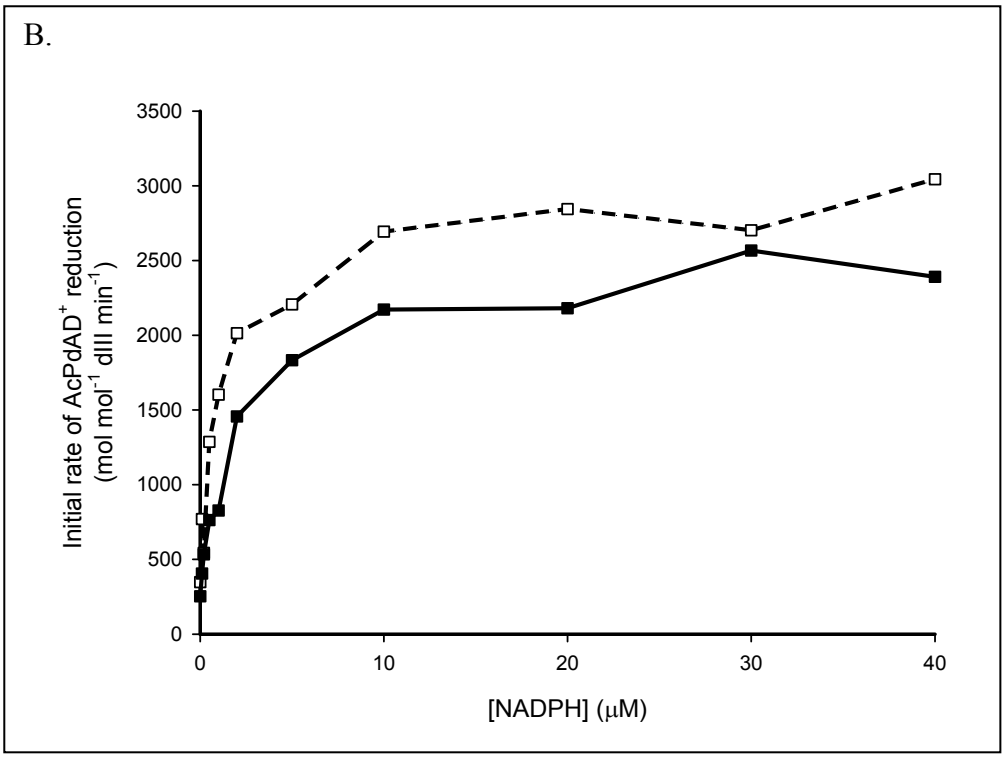

Figure 3.10 continued over page

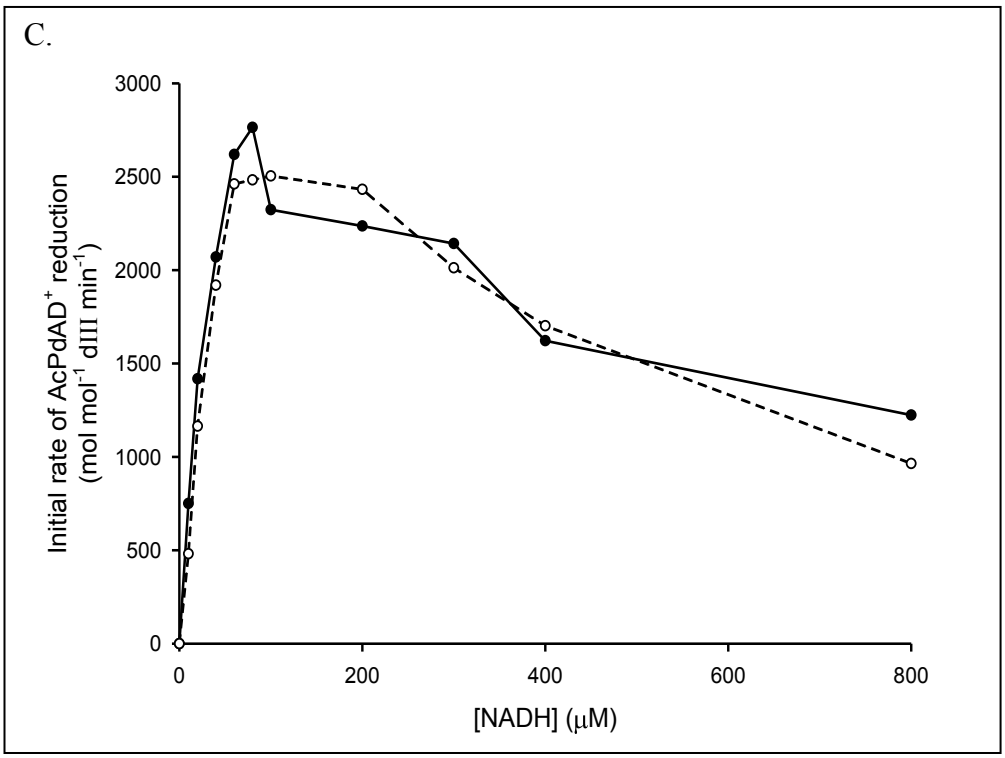

Figure 3.10 Effect of nucleotide concentration on the initial rate of the cyclic or aberrant cyclic reactions catalysed by dI_2dIII complexes from *R. rubrum* transhydrogenase.

To estimate binding affinities of wild-type dIII (solid lines, closed symbols) or dIII.R165A (dashed lines, open symbols) in dI_2dIII complexes for $NADP^+$ and NADPH, the initial rate of the cyclic reaction (*i.e.* the rate of $AcPdAD^+$ reduction by NADH in the presence of NADP(H)) was measured as a function of $NADP^+$ concentration (A, triangles) or NADPH concentration (B, squares). To estimate binding affinities of wild-type dIII or dIII.R165A in dI_2dIII complexes for NADH, the initial rate of the aberrant cyclic reaction (*i.e.* the rate of $AcPdAD^+$ reduction by NADH in the absence of NADP(H)) was measured as a function of NADH concentration (C, circles). The reaction conditions were as described in Section 2.3.4 except that the initial mixture was incubated for 5 minutes before the reaction was initiated. The data plotted are of single measurements.

CHAPTER 4

The nucleotide-binding properties of the dIII component of dI_2dIII complexes from *R. rubrum* transhydrogenase determined by fluorescence experiments.

4.1 Fluorescence properties of dIII.E155W from *R. rubrum* transhydrogenase.

The fluorescence of the single tryptophan residue (βTrp415) in *E. coli* dIII is affected by the redox state of the bound nucleotide (Fjellstrom *et al.* 1997; Fjellstrom *et al.* 1999b). The equivalent residue in *R. rubrum* dIII is Glu155 and it was replaced by a tryptophan (Peake *et al.* 1999a). Complexes of *R. rubrum* dI and dIII.E155W had rates of cyclic transhydrogenation that were undiminished from those of wild-type dI_2dIII complexes. However, the fluorescence of the lone Trp155 was sensitive to the redox state of the bound nucleotide; it was greater when $NADP^+$ was bound than when NADPH was bound (Peake *et al.* 1999a; Venning *et al.* 2000; Pinheiro *et al.* 2001; Rodrigues *et al.* 2001; Venning *et al.* 2001). This provides a useful system for studying nucleotide binding.

In previous studies, when excess NADPH was added to a solution containing $NADP^+$-bound dIII.E155W, a slow fluorescence quenching was observed (Rodrigues *et al.* 2001). It was reasoned that NADPH in excess would bind rapidly into the dIII site once the $NADP^+$ had dissociated. This enabled the first-order rate constant for $NADP^+$ release to be calculated. Conversely, when excess $NADP^+$ was added to a solution containing NADPH-bound dIII.E155W, a very slow fluorescence increase was seen. The rate was attributed to the dissociation of NADPH and the first-order rate constant for NADPH release was calculated. At neutral pH, the first-order rate constants for $NADP^+$ and NADPH release were 0.018 s^{-1} and 0.00045 s^{-1}, respectively (Rodrigues *et al.* 2001). This was evidence not only that nucleotide release from dIII is very slow, but also indicated that isolated dIII binds NADPH with a higher affinity than $NADP^+$.

4.2 Properties of dI.W72F, in which the single Trp of wild-type dI from *R. rubrum* transhydrogenase has been replaced by a Phe.

Wild-type dI from *R. rubrum* transhydrogenase has a single tryptophan at position 72 with an intense fluorescence at an unusually short wavelength (Broos *et al.* 2003; Tveen Jensen *et al.* 2008). The fluorescence from Trp72 is quenched when dI binds NADH. The objective of the work described in this chapter was to investigate the properties of nucleotide binding to the dIII component of dI_2dIII complexes. To this end it was necessary to replace Trp72 of dI with a non-fluorescent amino acid residue. The fluorescence of dI_2dIII complexes made of this protein and dIII.E155W would then arise only from the lone tryptophan in dIII.E155W.

The mutant dI.W72F was isolated as described in Section 2.1.4, and was purified by the same procedure as was effective for wild-type dI (see Section 2.2.3). Complexes made from dI.W72F and dIII.E155W catalysed cyclic transhydrogenation at a rate of ~3170 mol $AcPdAD^+$ reduced mol^{-1} dIII min^{-1}, which was comparable to rates of reaction catalysed by complexes made from wild-type dI and dIII.E155W (~2560 mol $AcPdAD^+$ reduced mol^{-1} dIII min^{-1}). This shows that the W72F mutation of the dI component has no inhibitory effect on catalysis.

In a set of experiments (Figure 4.1) it was found that the dependence of the rate of cyclic transhydrogenation on the dI.W72F concentration at a fixed concentration of dIII.E155W was similar to that observed with wild-type dI. The dI concentration required to reach the half-maximal rate was ~55 nM for complexes with dI.W72F and ~70 nM for complexes with wild-type dI. These results are comparable to equivalent experiments using complexes of wild-type dI and wild-type dIII (Diggle

et al. 1996). This indicates that dI.W72F forms complexes with dIII.E155W with a similar affinity to wild-type dI.

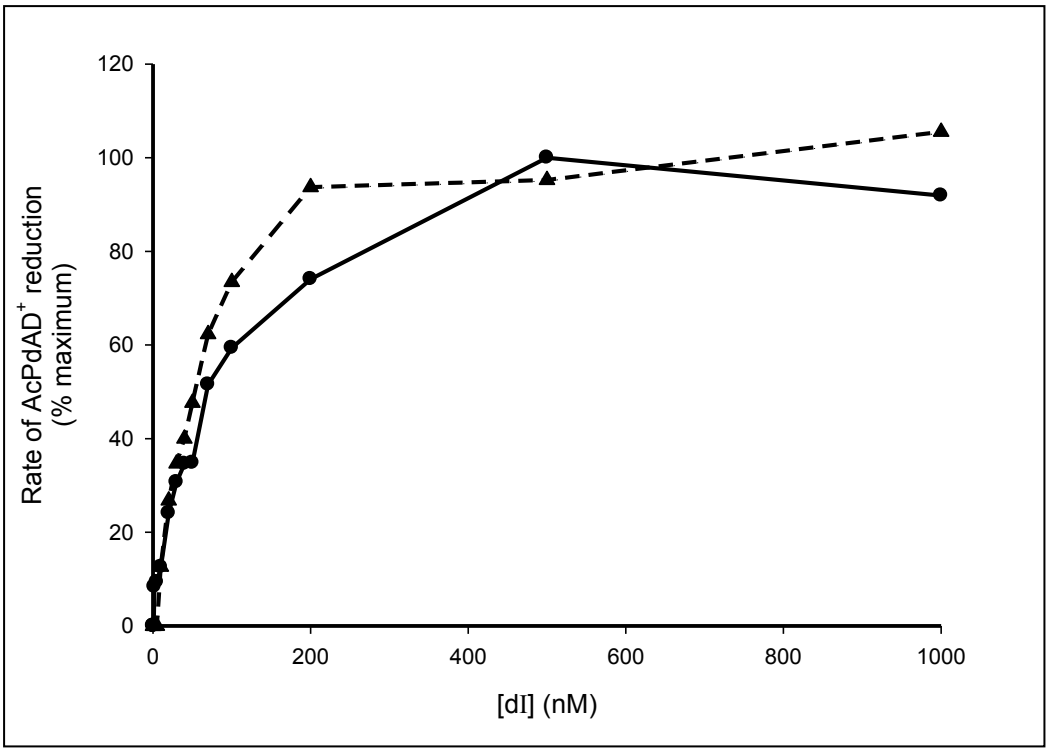

Figure 4.1 Effect of dI concentration on the rate of cyclic transhydrogenation catalysed by complexes constructed with dIII.E155W and either wild-type dI or dI.W72F from *R. rubrum* transhydrogenase.

The initial rate of $AcPdAD^+$ reduction by NADH in the presence of $NADP^+$ was measured under standard conditions (described in Section 2.3.4). The reactions were catalysed by complexes constructed from dIII.E155W and either wild-type dI (solid line, circles) or dI.W72F (dashed line, triangles). The dIII concentration was kept constant (30 nM) while the dI concentration was varied. The data plotted are of single measurements.

4.2.1 Fluorescence properties of dI.W72F.

The fluorescence emission spectra of wild-type dI and dI.W72F using excitation wavelengths of 275 nm and 290 nm are shown in Figure 4.2. At both excitation wavelengths the intense emission at 308 nm is considerably reduced by the mutation, consistent with the view that the fluorescence in the wild-type protein originates from Trp72.

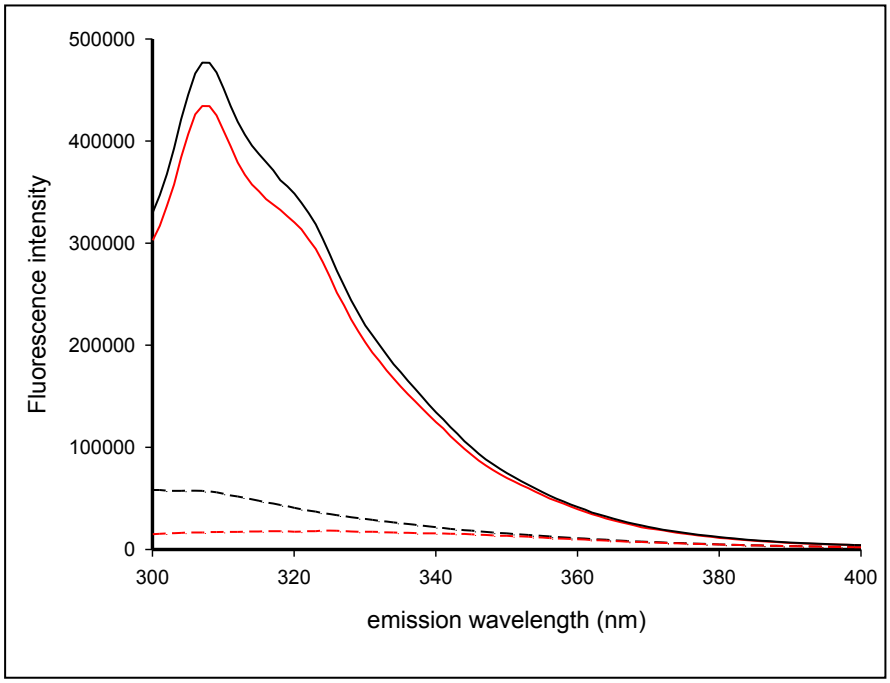

Figure 4.2 Fluorescence emission spectra of isolated wild-type dI and dI.W72F from *R. rubrum* transhydrogenase.

Fluorescence emission scans were performed on a PTI Quantamaster fluorimeter as described in Section 2.4.1. The experimental cuvette contained 20 mM MOPS-KOH, pH 7.0 and 1.0 µM of either isolated wild-type dI (solid lines) or dI.W72F (dashed lines) in a final volume of 3 mL. The excitation wavelength was 275 nm (black line) or 290 nm (red line).

Tryptophan emission is excited strongly by light at both 275 nm and 290 nm (Lakowicz 2004); thus, the fluorescence from the wild-type dI is only slightly less intense using 290 nm excitation. However, tyrosine emission is much reduced when excited at 290 nm (Lakowicz 2004). The fluorescence emission of dI.W72F at around 300-310 nm when excited at 290 nm is rather less than when excited at 275 nm. This suggests that the low fluorescence in dI.W72F originates from the 8 tyrosine residues in the protein. This low fluorescence was unaffected by the addition of NADH to the protein (data not shown).

4.3 The binding of nucleotides to the dIII.E155W component of dI_2dIII complexes from *R. rubrum* transhydrogenase.

4.3.1 The binding of nucleotides to dIII.E155W in complexes constructed with dI.W72F and apo-dIII.E155W from *R. rubrum* transhydrogenase.

Experiments were designed to measure the binding of nucleotides to the dIII component of dI_2dIII complexes constructed with dI.W72F and apo-dIII.E155W (Figure 4.3). The dIII.E155W used in these experiments had been treated with phosphatase to produce apo-dIII.E155W. In each experiment there was an initial rapid fluorescence quenching upon addition of nucleotides which was due to an inner-filtering effect (the reabsorption of emission light and/or the absorption of excitation light by the nucleotide). It is assumed that the slow fluorescence changes following this inner-filtering effect were the result of the binding of nucleotides to dIII.E155W. The Trp155 fluorescence was then measured during the addition of various nucleotides, all at 20 μM. Following the inner-filtering effect, the addition of $NADP^+$

gave rise to a slow increase in fluorescence (Figure 4.3a), and the addition of the reduced nucleotides NADPH (Figure 4.3b) and NADH (Figure 4.3c) gave rise to a slow decrease in fluorescence. These fluorescence changes can be attributed to the slow binding of the nucleotides to the dIII component of the complexes. It should be recalled that the addition of NADH to isolated dI.W72F did not cause any change in fluorescence. Replicate experiments showed that the addition of NAD^+ (for example Figure 4.3d) led to a small but reproducible increase in fluorescence, but that the addition of $AcPdAD^+$ (Figure 4.3e) did not cause any significant fluorescence change.

Figure 4.3 (over page) Fluorescence experiments showing the binding of nucleotides to dIII.E155W in complexes formed with dI.W72F and apo-dIII.E155W from *R. rubrum* transhydrogenase.

Fluorescence experiments were performed on a PTI Quantamaster fluorimeter as described in Section 2.4.1. For each experiment, the initial mixture (3 mL), containing 20 mM MOPS-KOH, pH 7.0, 0.4 μM apo-dIII.E155W and 0.8 μM dI.W72F, was incubated for 5 minutes before recording was started. Nucleotides (20 μM) were added as shown by the arrows. The change in fluorescence intensity resulting from nucleotide-binding to dIII.E155W in the complexes was recorded. The initial rapid fluorescence quenching was due to the inner-filtering effect.

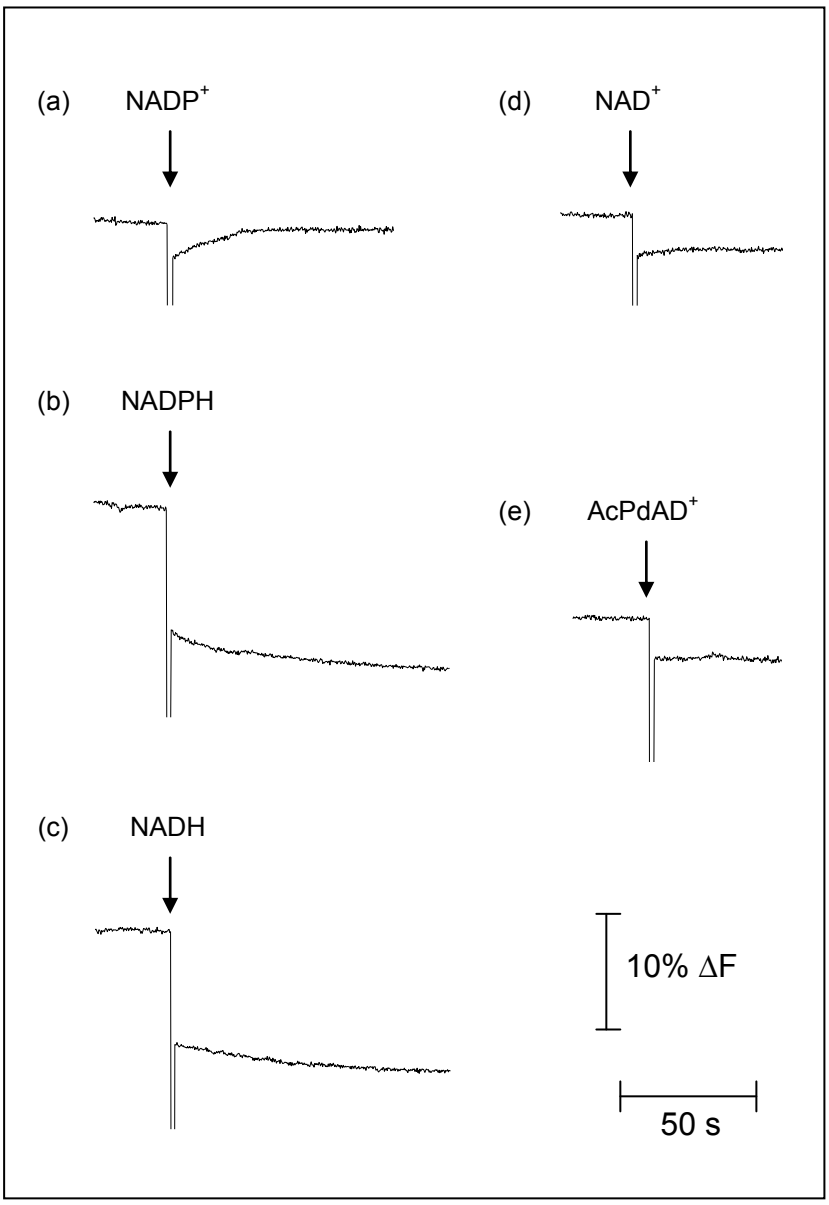

Figure 4.3

4.3.2 Properties of the double mutant dIII.E155W.R165A from *R. rubrum* transhydrogenase.

A double mutant of the dIII component of *R. rubrum* transhydrogenase, dIII.E155W.R165A, was isolated (as described in Section 2.1.4), in which Arg165 from the K-R-S motif in the dIII binding-site was mutated to an alanine residue, and Glu155 was replaced by a tryptophan. The double mutant was purified by the same

procedure as was effective for dIII.R165A (see Section 2.2.4), and the apo-form of the protein was produced by subjecting the protein to gel-filtration.

Complexes made from dI and dIII.E155W.R165A catalysed cyclic transhydrogenation at a rate of 1750 ± 380 mol $AcPdAD^+$ reduced mol^{-1} dIII min^{-1}, which was comparable to rates of reaction catalysed by complexes made from dI and dIII.R165A (1770 ± 130 mol $AcPdAD^+$ reduced mol^{-1} dIII min^{-1}) (both values are the average of 3 preparations). This confirms earlier reports (Peake *et al.* 1999a) that the E155W mutation has no inhibitory effect on catalysis. In a set of experiments it was found that the dependence of the rate of the cyclic reaction on $NADP^+$ (Figure 4.4A) or NADPH (Figure 4.4B) concentrations were similar to those observed with dIII.R165A (see Figure 3.5). The concentrations of $NADP^+$ and NADPH needed to reach the half-maximal rate using complexes made with dI and dIII.E155W.R165A were ~20 μM and ~1 μM, respectively. This indicates that, when in complex with dI, dIII.E155W binds nucleotides with a similar affinity to dIII.R165A.

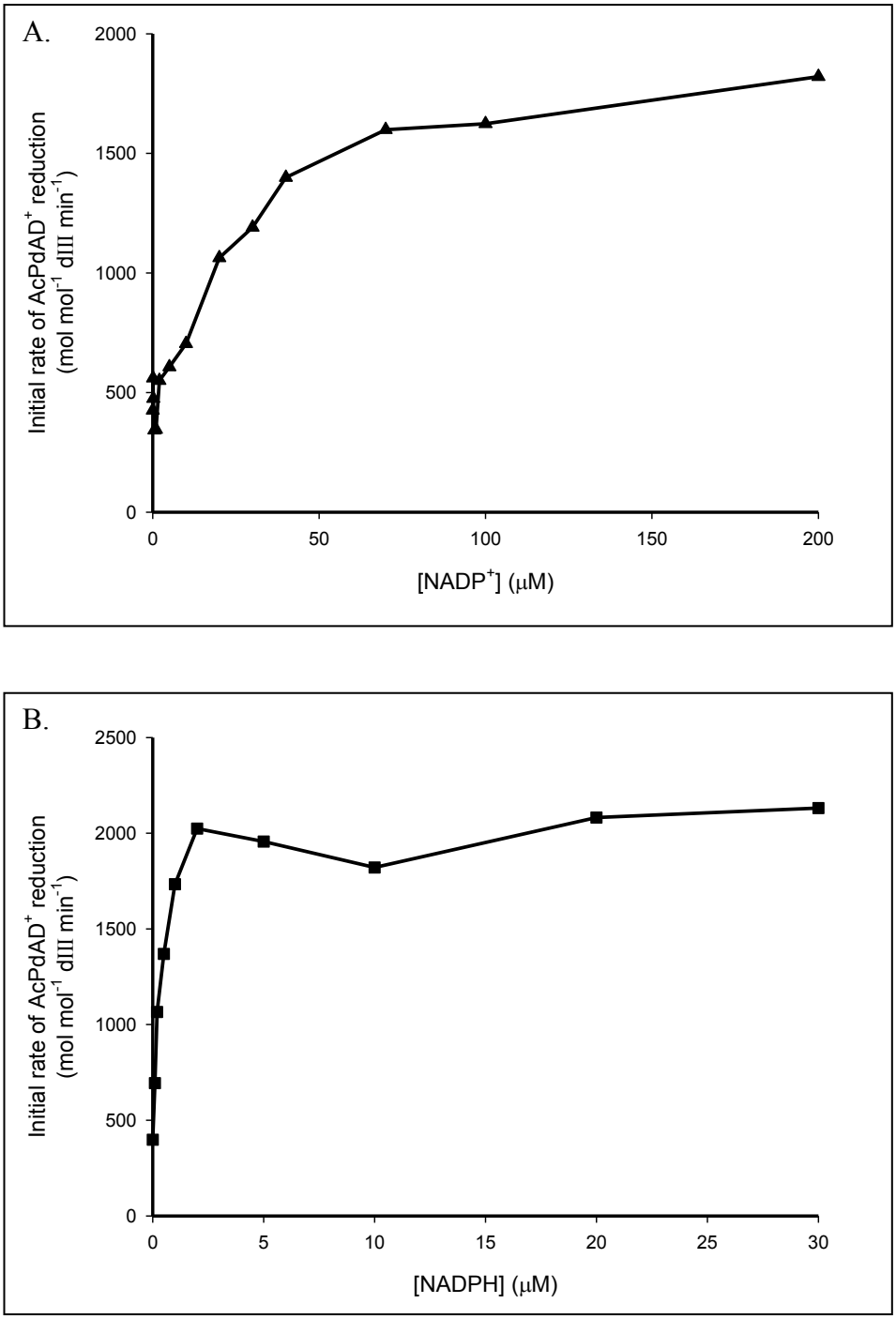

Figure 4.4 Effect of NADP(H) concentration on the rate of cyclic transhydrogenation catalysed by complexes made with dI and dIII.E155W.R165A from *R. rubrum* transhydrogenase.

To estimate binding affinities of dIII.E155W.R165A in dI_2dIII complexes for $NADP^+$ and NADPH, the initial rate of $AcPdAD^+$ reduction by NADH was measured as a function of $NADP^+$ concentration (A, triangles) or NADPH concentration (B, squares). The reaction conditions were as described in Section 2.3.4. The data plotted are of single measurements.

4.3.3 The binding of nucleotides to dIII.E155W.R165A in complexes constructed with dI.W72F and apo-dIII.E155W.R165A from *R. rubrum* transhydrogenase.

Fluorescence experiments, similar to those shown in Figure 4.3, were designed to observe the binding of nucleotides to the dIII component of complexes made with dI.W72F and apo-dIII.E155W.R165A (Figure 4.5). The Trp155 fluorescence was measured during the addition of various nucleotides (20 μM) to these complexes. The addition of $NADP^+$ gave rise, following the inner-filtering effect, to a slow increase in fluorescence (Figure 4.5a). The addition of the reduced nucleotides NADPH (Figure 4.5b) and NADH (Figure 4.5c) gave rise to a slow decrease in fluorescence. These fluorescence changes signify the binding of the nucleotides to the dIII component of the complexes. Replicate experiments showed that the addition of NAD^+ (Figure 4.5d) led to a small but reproducible increase in fluorescence, but the addition of $AcPdAD^+$ (Figure 4.5e) did not cause any significant fluorescence change.

The fluorescence changes shown in these experiments are similar to those observed when nucleotides were added to complexes made with dI.W72F and apo-dIII.E155W (see Figure 4.3).

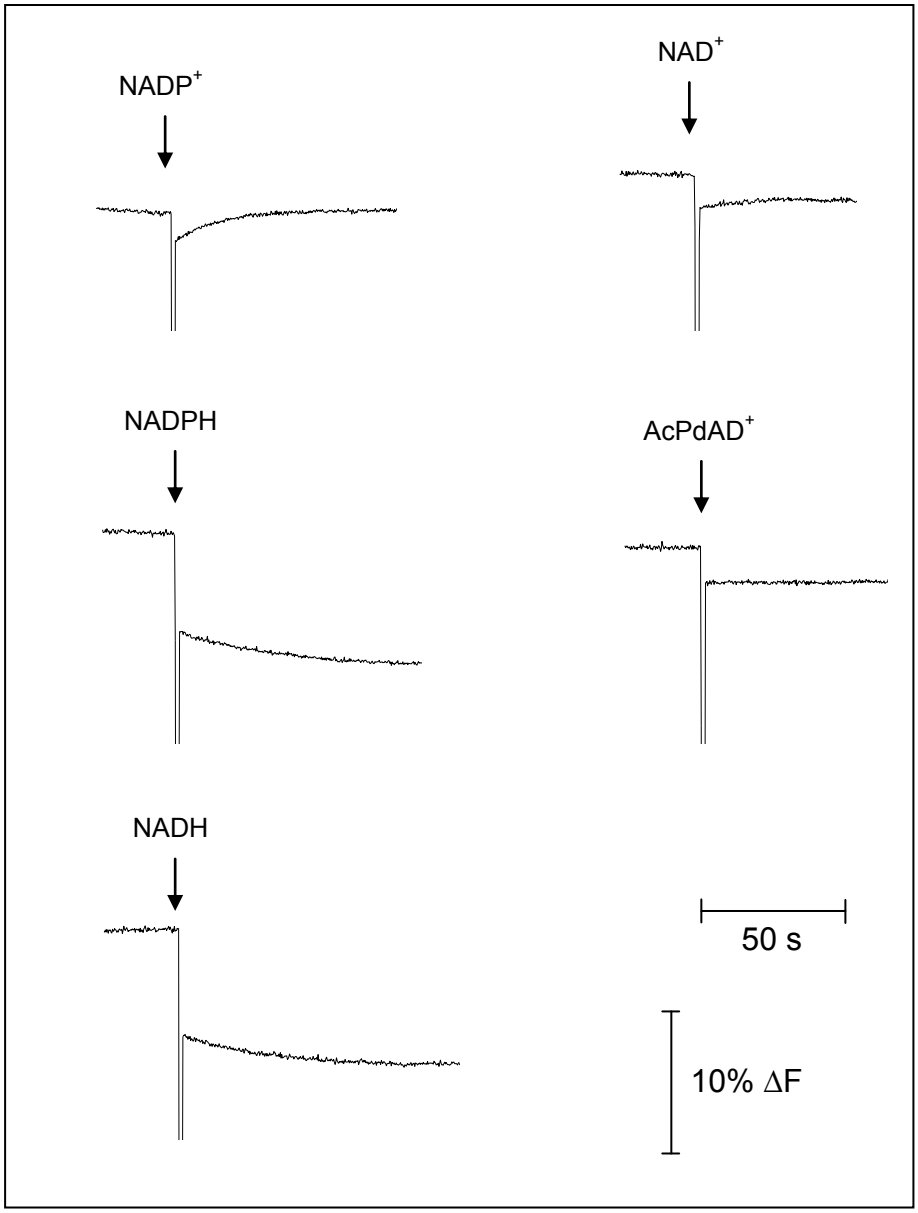

Figure 4.5 Fluorescence experiments showing the binding of nucleotides to dIII.E155W.R165A in complexes formed with dI.W72F and apo-dIII.E155W.R165A from *R. rubrum* transhydrogenase. Fluorescence experiments were performed on a PTI Quantamaster fluorimeter as described in Section 2.4.1. The initial mixture (3 mL) containing 20 mM MOPS-KOH, pH 7.0, 0.4 μM apo-dIII.E155W.R165A and 0.8 μM dI.W72F was equilibrated for 5 minutes in the experimental cuvette. Nucleotides (20 μM) were then added (as shown by the arrows) while the fluorescence intensity was measured. The initial rapid fluorescence decrease was due to the inner-filtering effect.

4.4 Kinetics of nucleotide-binding to dIII.E155W and dIII.E155W.R165A in complexes with dI.W72F from the fluorescence experiments.

The slow fluorescence changes produced by nucleotide addition to complexes made with dI.W72F and either dIII.E155W or dIII.E155W.R165A (see figures 4.3 and 4.5) can be attributed to nucleotide-binding into the dIII site. The amplitude of the fluorescence change was measured at various time intervals after the addition of the nucleotide and plotted as a function of time (Figure 4.6). The amplitude of the fluorescence change is assumed to be proportional to the degree of occupancy of dIII. Figure 4.6 and other experiments (not shown) establish that the kinetics of $NADP^+$-binding, NADPH-binding and NADH-binding to dIII.E155W or dIII.E155W.R165A, in complexes with dI.W72F, were similar within the scatter on the data (*i.e.* the rate of nucleotide-binding is not affected by the chemical nature of nicotinamide nucleotide or by its oxidation state). In previous work it was shown that the exchange of $NADP^+$ for NADPH bound to dIII.E155W (in complexes with wild-type dI) led to a decrease in fluorescence (Peake *et al.* 1999a; Rodrigues *et al.* 2001; Venning *et al.* 2001). The fluorescence decrease was attributed to resonance energy transfer from Trp155 to the NADPH. However, here we have shown that the binding of oxidised nucleotides ($NADP^+$ and NAD^+) to dIII.E155W in complexes with dI.W72F causes a fluorescence increase and the binding of reduced nucleotides (NADPH and NADH) causes a fluorescence decrease. This suggests that the environment around Trp155 is altered by the binding of nucleotides, and that the changes in the Trp155 environment caused by reduced nucleotides are different from those caused by oxidised nucleotides.

The rate of the fluorescence change was also unaffected by varying the concentration of the added nucleotide. If the binding of nucleotides were a simple,

second-order reaction, the initial rate of the fluorescence change (following the inner-filtering effect) would be directly proportional to the nucleotide concentration. However, at least with $NADP^+$, NADPH and NADH in complexes formed with dI.W72F and dIII.E155W.R165A, and with NADH in complexes formed with dI.W72F and dIII.E155W, this was not the case. An increase in nucleotide concentration led to a less than proportionate increase in the initial rate. Because of its high affinity, this was most readily seen with NADPH. Thus, above 1 μM (where the binding-sites were fully occupied at equilibrium) and below 50 μM (where the inner-filtering effect was still manageably small), the initial rate of fluorescence change was independent of nucleotide concentration. This suggests that the binding of nucleotides to dIII in dI_2dIII complexes is not a simple, second-order process but that binding is likely to involve a conformational change of the protein.

Within error, the kinetics of nucleotide-binding to the dIII component of dI_2dIII complexes determined from the analyses of the lag phases of the cyclic and aberrant cyclic reactions (see Figure 3.9) are similar to those determined from the amplitudes of the fluorescence change. Although the scatter on the data is large, the half times (t½) for nucleotide-binding (Figures 3.9 and 4.6) were all in the order of 25 s.

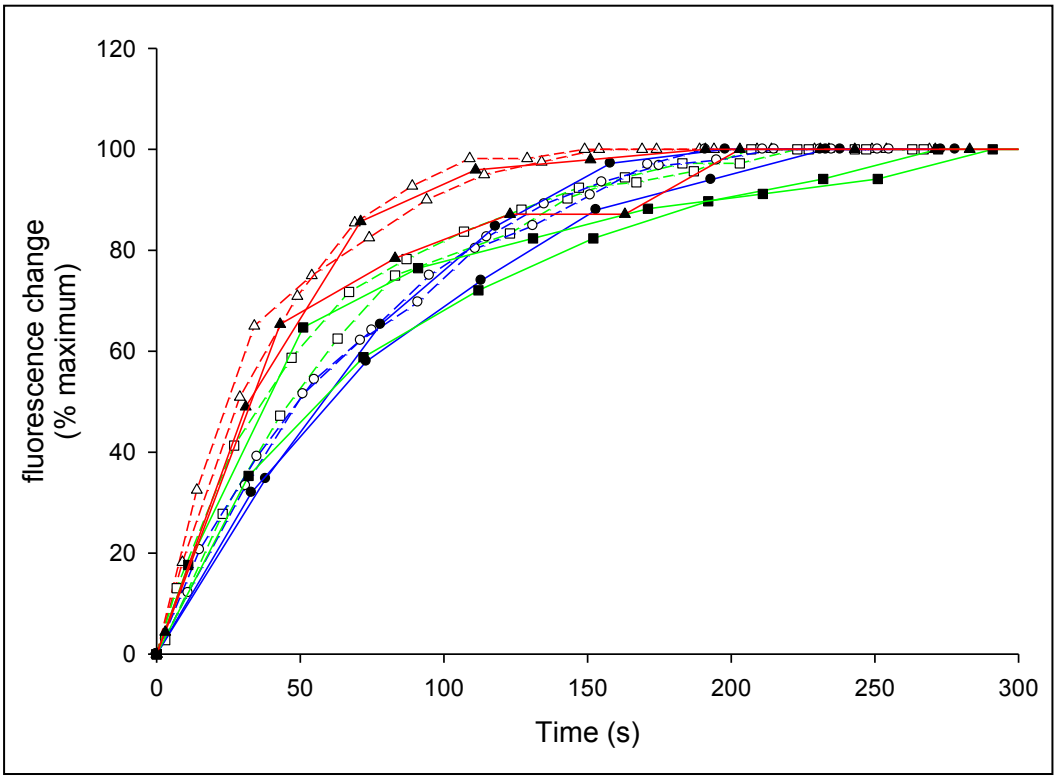

Figure 4.6 Kinetics of nucleotide-binding to either apo-dIII.E155W or apo-dIII.E155W.R165A in complexes with dI.W72F from *R. rubrum* transhydrogenase.

Nucleotides were added to complexes constructed with dI.W72F and either apo-dIII.E155W (solid lines, closed symbols) or apo-dIII.E155W.R165A (dashed lines, open symbols). The amplitude of the resulting fluorescence change (following the inner-filtering effect) was measured as a function of time. Experiments are shown using two concentrations of each nucleotide; the concentrations were 1 μM and 40 μM for NADPH (green lines, squares) and 5 μM and 50 μM for both $NADP^+$ (red lines, triangles) and NADH (blue lines, circles).

4.5 Nucleotide-binding affinities of dIII.E155W and dIII.E155W.R165A from *R. rubrum* transhydrogenase estimated from fluorescence experiments.

A set of experiments was designed to estimate K_d values of dIII.E155W and dIII.E155W.R165A for nucleotides when in complex with dI.W72F. Complexes were

generated from dI.W72F and either apo-dIII.E155W or apo-dIII.E155W.R165A, and the Trp155 fluorescence was measured during the addition of nucleotides (varying concentrations). Following the inner-filtering effect, slow fluorescence changes were observed (similar to those shown in Figures 4.3 and 4.5) that can be attributed to the slow binding of nucleotides to the dIII component of the complexes. The amplitude of this fluorescence change was assumed to be proportional to the occupation of the dIII component and was plotted as a function of nucleotide concentration (Figure 4.7).

Figure 4.7 (over page) The dependence of the Trp fluorescence change on nucleotide concentration in complexes constructed with dI.W72F and either apo-dIII.E155W or apo-dIII.E155W.R165A from *R. rubrum* transhydrogenase.

Fluorescence experiments were performed on a PTI Quantamaster fluorimeter as described in Section 2.4.1. Nucleotide at the concentrations shown was added to solutions containing complexes generated with 0.8 μM dI.W72F and either 0.4 μM apo-dIII.E155W (solid lines, closed symbols) or 0.4 μM apo-dIII.E155W.R165A (dashed lines, open symbols). The amplitude of the Trp fluorescence change was assumed to be proportional to the occupancy of the dIII component in the complexes. Thus, the amplitude was measured as a function of $NADP^+$ concentration (A, triangles), NADPH concentration (B, squares) or NADH concentration (C, circles). The data plotted are of single measurements.

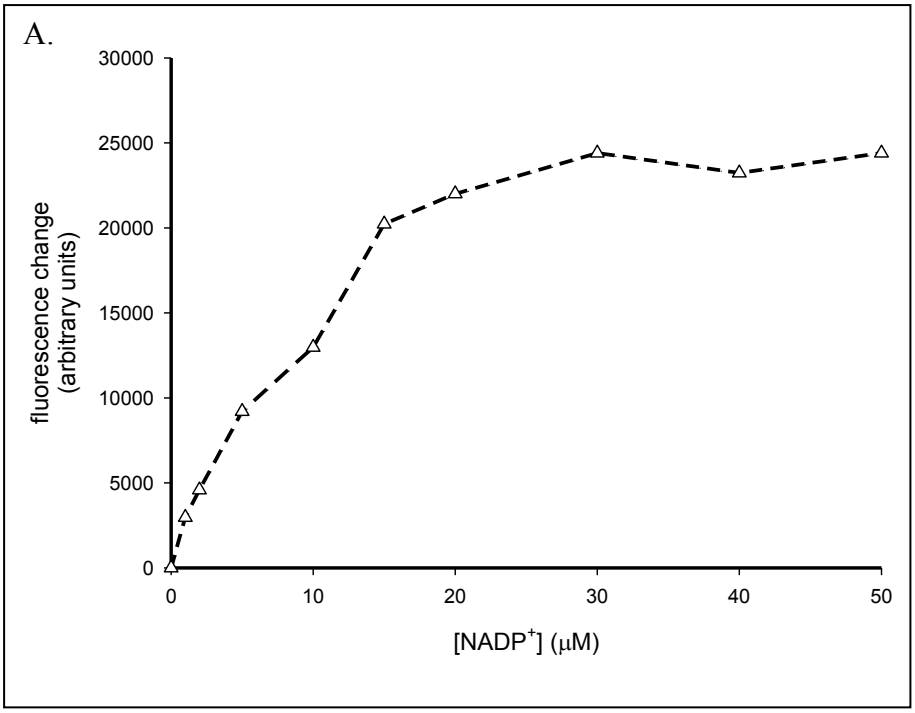

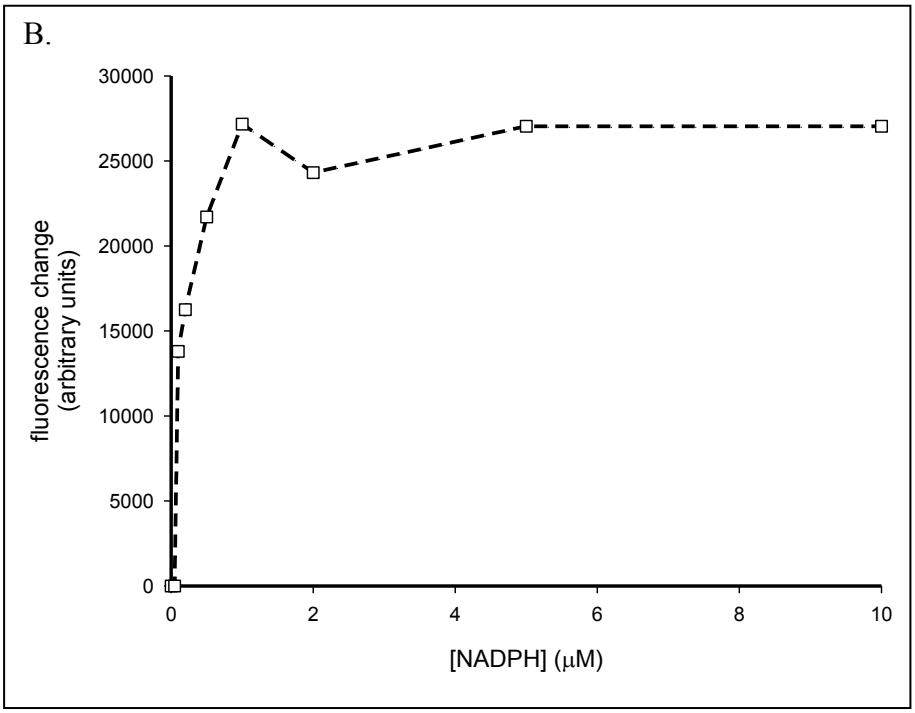

Figure 4.7 continued over page

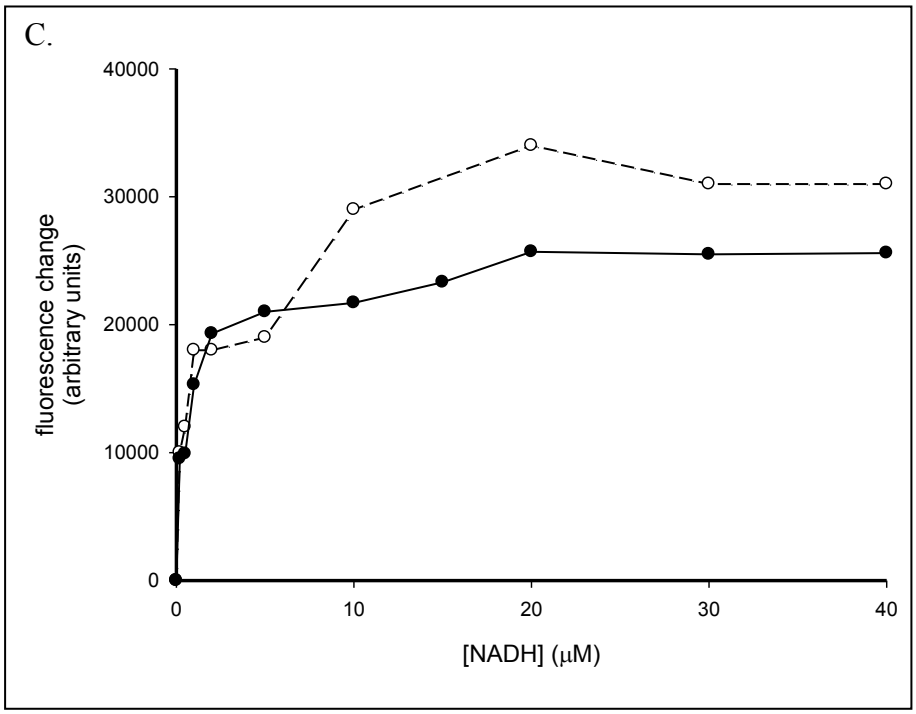

Figure 4.7 continued

Since the concentration of the dIII component in these experiments is in the same order as the nucleotide concentrations, the K_d values could not simply be calculated from the graphs in Figure 4.7 as the nucleotide concentration needed to reach the half-maximal fluorescence change. The equation $K_d = [E][nuc]/[E.nuc]$ (where [E.nuc] is the concentration of enzyme with bound nucleotide, [nuc] is the concentration of free nucleotide and [E] is the concentration of unbound enzyme) can be expanded to $[E.nuc] = ([E]_0[nuc])/([nuc] + K_d)$ where $[E]_0$ is the total enzyme concentration) and then to $[E.nuc] = [E]_0 - \frac{[E.nuc]}{[nuc]}K_d$ (Fersht 1999). Plotting [E.nuc] vs $[E.nuc]/[nuc]$ gave straight line graphs (Figure 4.8), of which the gradients were equal to $-K_d$. Thus, the K_d of dIII.E155W in complex with dI.W72F for NADH was ~4 μM (Figure 4.8D). The K_d of dIII.E155W.R165A in complex with dI.W72F for NADPH was ~0.1 μM (Figure 4.8B), for $NADP^+$ was ~12 μM (Figure 4.8A) and for

NADH was ~8 μM (Figure 4.8C). The K_d values of dIII.E155W in the complexes for $NADP^+$ or NADPH could not be reliably estimated in this way due to carry-over of phosphatase into the fluorescence cuvette. The concentration of the carried-over phosphatase was such that the 2'-phosphate of a significant fraction of the added $NADP^+$ or NADPH would have been cleaved during the assay.

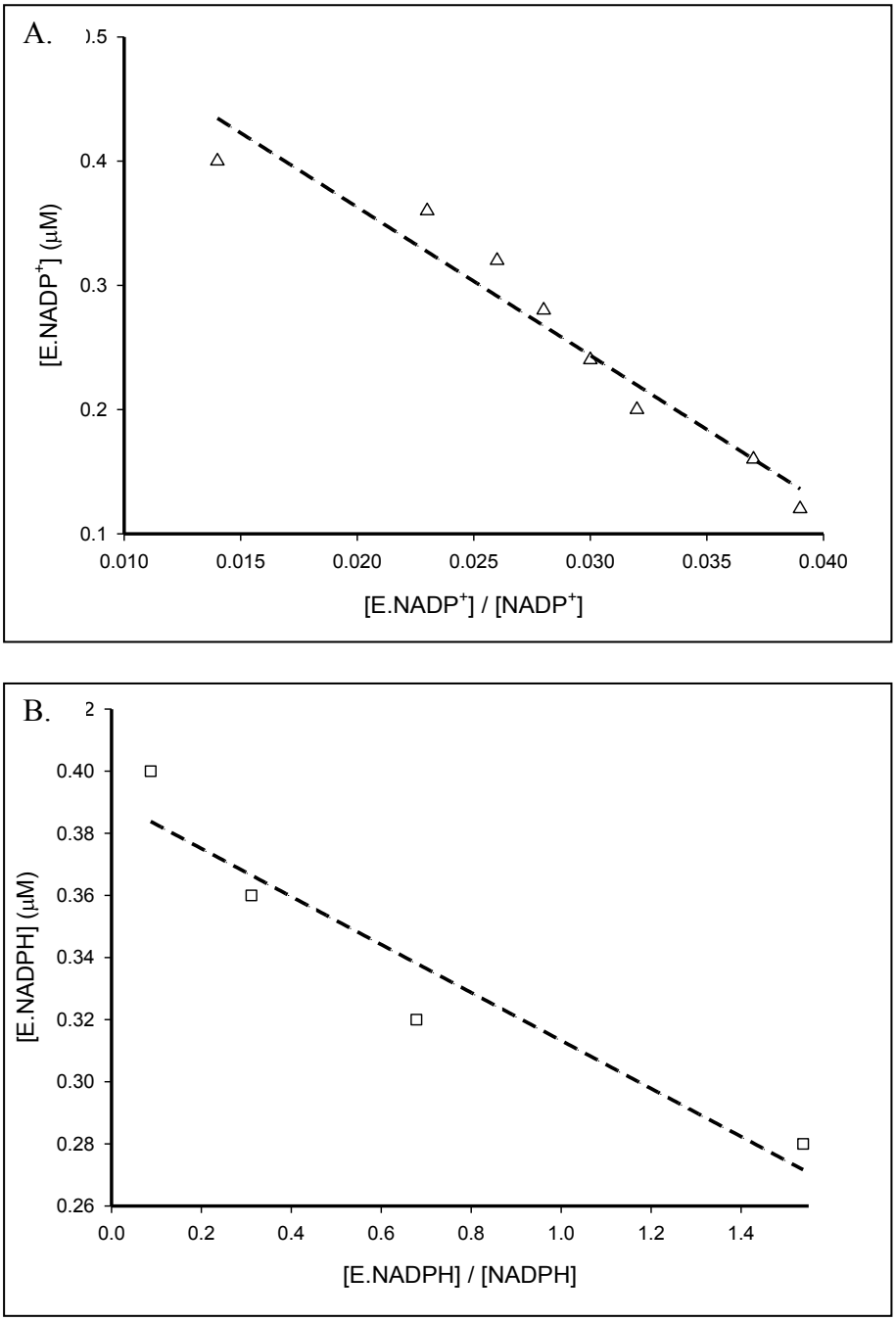

Figure 4.8 continued over page

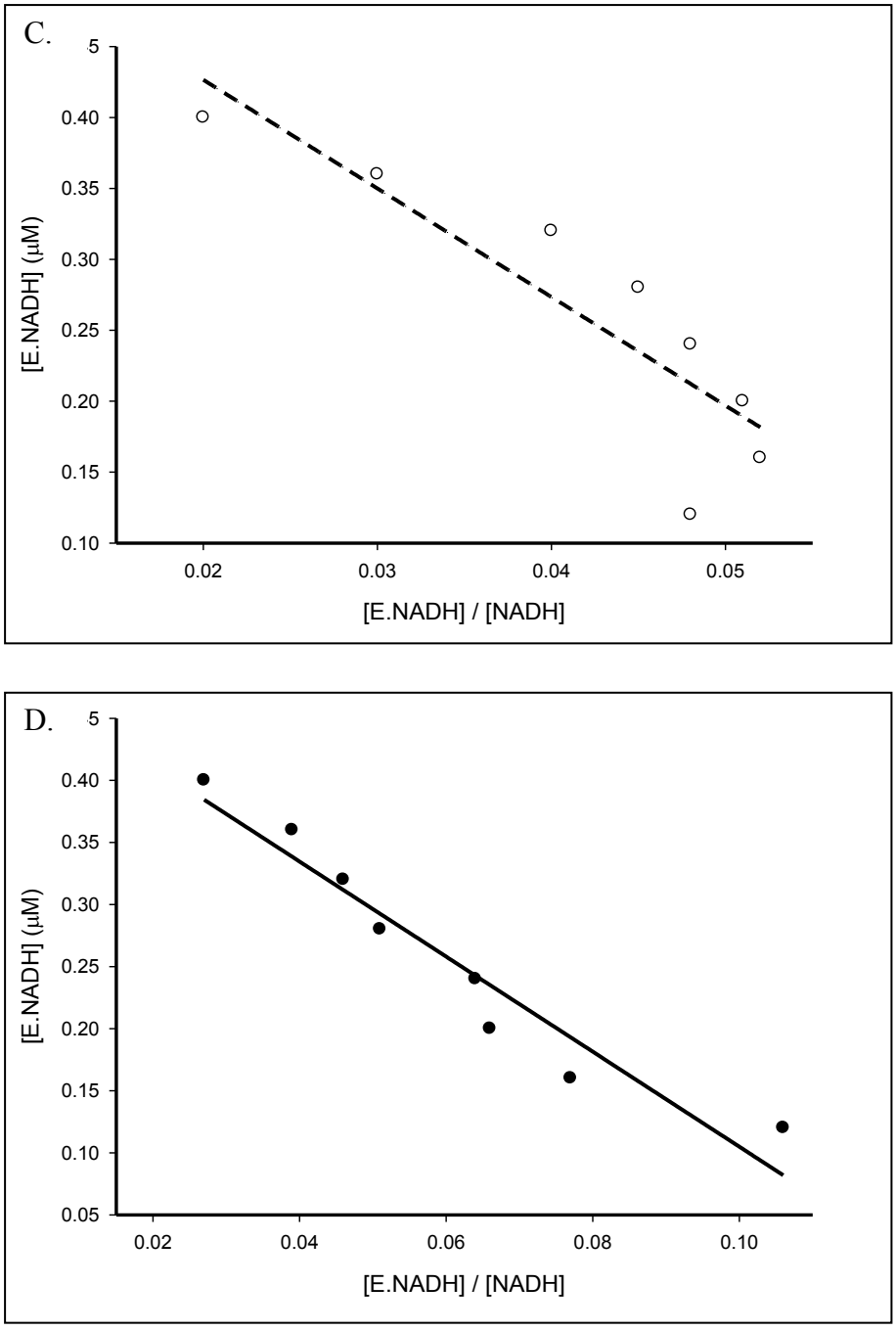

Figure 4.8 Plots to estimate the K_d values of either dIII.E155W or dIII.E155W.R165A in complex with dI.W72F for nucleotides.

Using various data points from the graphs in Figure 4.7, [E.nuc] and [nuc] were calculated. Plots of [E.nuc] vs [E.nuc]/[nuc] gave straight line graphs with a gradient of $-K_d$. Thus, the K_d values for either dIII.E155W (solid lines, closed symbols) or dIII.E155W.R165A (dashes lines, open symbols) in complex with dI.W72F for $NADP^+$ (A, triangles), NADPH (B, squares) and NADH (C and D, circles) were calculated.

CHAPTER 5

Discussion

5.1 Nucleotide-binding affinities of the dIII component of *R. rubrum* transhydrogenase: overall conclusions.

The nucleotide-binding affinities of the dIII component in dI_2dIII complexes were estimated either by measuring the rates of the cyclic and aberrant cyclic reactions (Chapter 3), or by measuring the amplitude of fluorescence changes caused by nucleotide addition (Chapter 4). A summary of the results is given in Table 5.1. The indications are that in dI_2dIII complexes wild-type dIII has nucleotide-binding affinities in the order NADPH > $NADP^+$ > NADH > NAD^+ > $AcPdAD^+$, and dIII.R165A has nucleotide-binding affinities in the order NADPH > $NADP^+$ ≈ NADH > NAD^+ > $AcPdAD^+$.

Wild-type dIII binds its reduced substrate NADPH with a higher affinity than that of its oxidised substrate $NADP^+$. NMR experiments have shown that there are structural differences between dIII in its NADPH-bound form and in its $NADP^+$-bound form (Quirk *et al.* 1999). However, these structural differences have not been observed in any of the published crystal structures that include the dIII component (Prasad *et al.* 1999; White *et al.* 2000; Cotton *et al.* 2001; Sundaresan *et al.* 2003; Mather *et al.* 2004; Bhakta *et al.* 2007). Wild-type dIII also binds the reduced nucleotide NADH with a higher affinity than that of the oxidised nucleotide NAD^+. The weaker binding of NADH than NADPH, and of NAD^+ than $NADP^+$, to wild-type dIII is probably due to the replacement of the 2'-phosphate group of NADP(H) for the 2'-hydroxyl group of NAD(H). The absence of the 2'-phosphate group will lead to the elimination of hydrogen bonds between the residues in the NADP(H)-binding site (*e.g.* the K-R-S motif) and the nucleotide. Interestingly, dIII.R165A was found to bind NADH and $NADP^+$ with a similar affinity. As well as decreasing the affinity for

$NADP^+$, the R165A mutation also eliminated some specificity of dIII for $NADP^+$. Clearly, Arg165 (together with Lys164 and Ser166 of the K-R-S motif) and the set of interactions involving the 2'-phosphate moiety of the NADP(H), play important roles in both nucleotide-binding and nucleotide-specificity.

experiment type	**protein**	**apparent K_d [a] (μM)**		
		NADPH	**$NADP^+$**	**NADH**
enzyme assays	wild-type dIII	1	5	40
enzyme assays	dIII.R165A	1	40	40
enzyme assays	dIII.E155W.R165A	1	20	ND[b]
fluorescence	dIII.E155W	ND[b]	ND[b]	4
fluorescence	dIII.E155W.R165A	0.1	12	8

Table 5.1 Summary of apparent K_d values of dIII components in dI_2dIII complexes for nucleotides.

[a] Apparent K_d values were either estimated from enzyme assays as the nucleotide concentration required to reach the half-maximal rate (see Chapter 3), or calculated from fluorescence experiments (see Chapter 4).

[b] ND = not determined.

The NAD^+ analogue, $AcPdAD^+$, was unable to bind to the dIII component of dI_2dIII complexes under the conditions of the experiments described in this thesis. $AcPdAD^+$ has an acetyl group in place of the carboxamide at the C3 position of the nicotinamide ring of NAD^+. The crystal structure of *R. rubrum* dIII with bound $NADP^+$ (Sundaresan *et al.* 2003), shows that the NH_2 group of the carboxamide forms

hydrogen bonds with the highly conserved residues Val87, Ala88 and Met91 (Figure 5.1). There are also potential hydrogen bonds between these residues and the NH_2 group of the carboxamide in the crystal structures of dIII from *H. sapiens* (White *et al.* 2000) and *B. taurus* (Prasad *et al.* 1999). These hydrogen bonds will clearly be lost when $AcPdAD^+$ binds into the site in place of $NADP^+$. This will account for the failure to observe a significant degree of binding of $AcPdAD^+$ in the experiments described in Chapters 3 and 4.

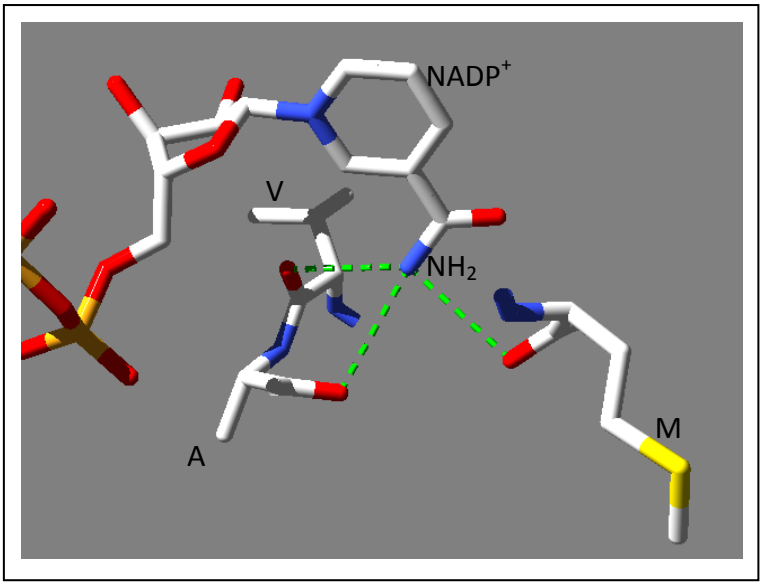

Figure 5.1 Crystal structure showing the importance of the carboxamide group of the nicotinamide moiety of $NADP^+$ in binding to dIII.

Hydrogen bonds between the NH_2 of the carboxamide group and residues Val87, Ala88 and Met91 of *R. rubrum* dIII are shown as dashed green lines. This figure was produced using Swiss-PDB Viewer and Povray using PDB ID 1PNO.

5.2 The mechanistic significance of the slow binding of nucleotides to the dIII component of dI_2dIII complexes from *R. rubrum* transhydrogenase.

As described in Section 1.11, transhydrogenase is thought to function by way of a binding-change mechanism involving open and occluded conformations of the enzyme. Nucleotides can bind to or dissociate from dI in either conformation. However, nucleotides can only bind to or dissociate from dIII when in the open conformation. In the occluded conformation, the (dihydro)nicotinamide rings of the nucleotides are brought together and hydride transfer is permitted. The switch between the open and occluded conformations is thought to be central in the coupling mechanism of hydride transfer and proton translocation. Loop E of dIII has been identified as an important structural element involved in this switch. Crystal structures show loop E closed over the bound nucleotide when dIII adopts an occluded conformation (White *et al.* 2000; Sundaresan *et al.* 2003; Bhakta *et al.* 2007). Although no crystal structures of dIII in the open conformation have been solved, it is thought that loop E retracts to allow the conversion from the occluded to the open state (Rodrigues *et al.* 2002). Analyses of the results presented in this thesis not only support the proposed binding-change mechanism of transhydrogenase, but also give a kinetic and structural insight into the conversion between the open and occluded conformations.

It was shown by enzyme assays (Chapter 3) and fluorescence experiments (Chapter 4) that nucleotide-binding to the dIII component of dI_2dIII complexes is very slow. Furthermore, the initial rates of fluorescence changes caused by nucleotide-binding to dIII in the complexes were independent of the concentration of the nucleotide. This led to the suggestion that the binding of nucleotides to the dIII

component of dI_2dIII complexes is not a simple, second-order process but that binding is likely to involve a conformational change of the protein (see Section 4.4). The new data can be readily explained by the model for nucleotide-binding in Figure 5.2. This model is consistent with the finding that the rate of nucleotide binding is governed by a step (*i.e.* that described by k_1), which is first-order in dI_2dIII complexes (see Figure 3.9B).

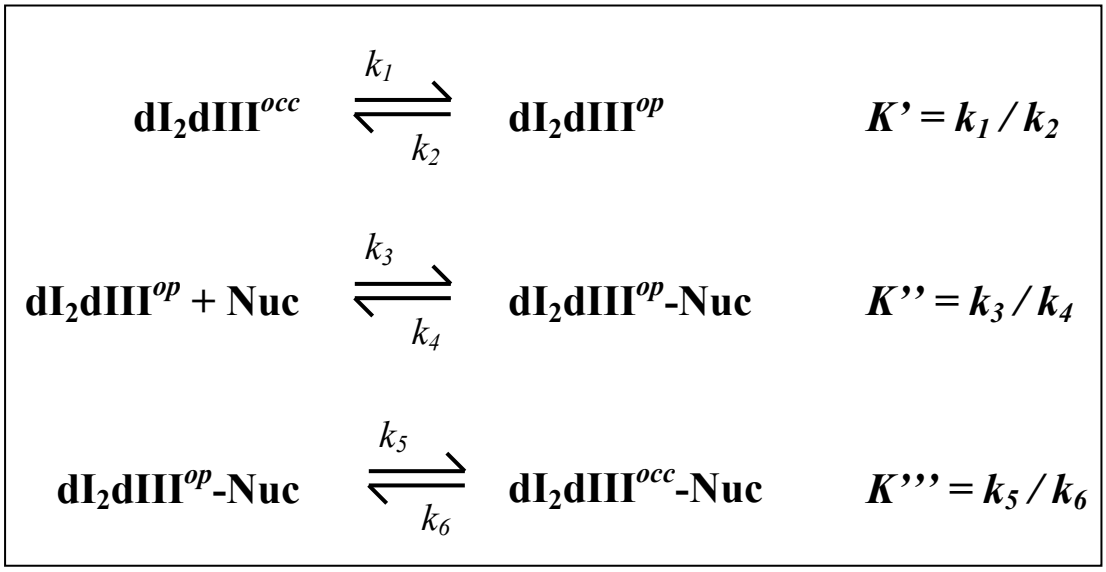

Figure 5.2 Model of nucleotide-binding to wild-type apo-dIII or apo-dIII.R165A in dI_2dIII complexes from *R. rubrum* transhydrogenase.

The dIII component of dI_2dIII complexes can adopt an open (*op*) or occluded (*occ*) conformation. In solution, it predominantly adopts the occluded conformation (*i.e. K'* is small and *K'''* is large). In the open conformation, nucleotide (Nuc)-binding to dIII can occur readily. The protein can then switch to the occluded conformation where hydride transfer can take place. For clarity, the binding of nucleotides to dI is not shown. Rate constants for each step are represented by k_1 through k_6.

In the model, apo-dIII in the dI_2dIII complex exists predominantly in its occluded conformation; *K'* is small. For nucleotide binding to take place, dIII must

adopt its open conformation. The switch from the occluded to the open conformation is slow; thus k_1 is small. Typically, the second-order rate constants for the binding of substrates to enzymes are large and in the order of 10^7 M^{-1} s^{-1} (Fersht 1999). Thus, once in its open conformation, dIII is expected to bind nucleotides rapidly; k_3 in the model is large (perhaps ≈ 10^7 M^{-1} s^{-1}). The nucleotide-bound form of dIII also favours the occluded conformation; K''' is large.

Within the context of the model, the rate of nucleotide-binding to dIII is limited by the conversion of apo-dIII from the occluded to the open conformation (the first-order rate constant k_1). Since t½ ≈ 25 s for nucleotide-binding to dIII in dI_2dIII complexes (see Chapters 3 and 4), the value of k_1 can be calculated as ~0.03 s^{-1} (using the first-order rate equation t½ = ln2/k).

Rodrigues *et al.* (Rodrigues *et al.* 2001) calculated first-order rate constants for $NADP^+$ and NADPH release from isolated dIII. The rate constant for NADPH release (0.00045 s^{-1}) was significantly slower than that for $NADP^+$ release (0.018 s^{-1}) suggesting a higher affinity of dIII for the reduced nucleotide. In the experiments of Rodrigues *et al.*, excess $NADP^+$ was added to solutions of NADPH-bound dIII.E155W and the rate of the fluorescence increase was measured. The rate of $NADP^+$ binding was thought to be limited by the rate of NADPH release from the protein. In other experiments, NADPH was added to a solution of $NADP^+$-bound dIII.E155W and the rate of the fluorescence decrease was measured. The rate of NADPH binding was thought to be limited by the rate of release of $NADP^+$. In light of the model proposed in this thesis (Figure 5.1) the results of Rodrigues *et al.* need to be re-interpreted. There are two possibilities. Firstly, the conversion from the occluded to the open conformation of nucleotide-bound dIII (k_6) limits the binding reaction, and is dependent on the chemical nature of the bound nucleotide (*i.e.* k_6 is

smaller with NADPH-bound dIII than with $NADP^+$-bound dIII). Recall that, in contrast, the rate of nucleotide binding to apo-dIII was similar for both $NADP^+$ and NADPH because it was limited in both cases by the conversion of the occluded apo-form to the open apo-form (see Chapter 4). An alternative explanation for the results of Rodrigues *et al*. is that the rate constants k_4 and k_6 are in the same order, and therefore the rate of nucleotide release is limited both by the conversion from the occluded to open conformation of the protein (k_6), and by the dissociation of the protein-nucleotide complex when in the open conformation (k_4) - NADPH dissociates more slowly from dIII than $NADP^+$ (*i.e.* k_4 is smaller with NADPH-bound dIII than with $NADP^+$-bound dIII).

The kinetics of nucleotide binding to apo-dIII.R165A in dI_2dIII complexes were similar to those of wild-type apo-dIII. It was shown that $NADP^+$ dissociates from dIII.R165A much more readily than from wild-type dIII (see Table 3.1). In terms of the model shown in Figure 5.2, this could result from an increase in k_4. That the kinetics of nucleotide binding to dIII.R165A and wild-type dIII are similar is consistent with the view that the R165A mutation had no effect on the rate constant (k_1) for the conversion from the occluded to the open conformation. The residues of the K-R-S motif (including Arg165) are located at the N-terminus of loop E. The unchanged value of k_1 perhaps therefore indicates that the R165A mutation does not greatly affect the rate of opening of loop E during the switch between the occluded to the open conformations.

Crystal structures of dIII, bound to either $NADP^+$ or NADPH, show the protein in its occluded conformation where loop E is closed over the bound nucleotide (Prasad *et al.* 1999; White *et al.* 2000; Sundaresan *et al.* 2003; Bhakta *et al.* 2007). There are numerous interactions between the bound nucleotide and the protein that

were thought to be important in stabilising dIII in its occluded conformation. Although no structural data of dIII in its apo-form currently exists, it was thought that loop E might adopt an open conformation in the absence of bound nucleotide. However, the results presented in this thesis suggest that like NADP(H)-bound dIII, apo-dIII predominantly adopts its occluded conformation, in which loop E is expected to be closed over the nucleotide-binding site. Obviously, in the absence of bound nucleotide, interactions between the nucleotide and the protein would be lost. These interactions are clearly not as important for stabilising dIII in its occluded state as once thought. The question then arises: what stabilises loop E in its occluded conformation in the absence of bound nucleotide? The crystal structures of dIII in its occluded state also show several intramolecular hydrogen bonds between residues of loop E and helix D/loop D of dIII. These residues include Asp132 (via its side chain), Glu155 (side chain), Thr134 (peptide carbonyl) and Asn135 (side chain) in helix D/loop D, and Ala172 (peptide amine), Arg181 (side chain), Asn176 (side chain) and Glu175 (peptide carbonyl) in loop E. Most of these residues are at least partially conserved, and Asp132 has previously been identified as being important for nucleotide binding (Meuller *et al.* 1996; Fjellstrom *et al.* 1999a). Even in the absence of bound nucleotide, these hydrogen bond interactions between residues of helix D/loop D and loop E may be essential for stabilising dIII in its occluded conformation. A crystal structure of apo-dIII would determine the intramolecular interactions that stabilise the protein, and indeed loop E, in an occluded conformation. Crystallisation trials were attempted with apo-dIII.R165A but were unsuccessful (see Chapter 6).

It remains unclear how the conversion between the occluded and open conformations, and thus coupling between hydride transfer and proton translocation in

the intact enzyme, is modulated. Further structural information of dIII in its open conformation would be particularly revealing and would give an insight into the expected conformational change of loop E relative to dIII in its occluded conformation. Indeed a crystal structure of the intact enzyme (including the membrane-spanning dII components) would answer many unresolved issues regarding the coupling mechanism of transhydrogenase. For example, identifying the interactions between the dII and dIII components would give us a better understanding of how the switch between the open and occluded conformations of the protein is modulated during proton translocation, and what interactions cause loop E of dIII to favour either its open or occluded conformation.

5.3 The metabolic significance of NADH binding in the "wrong" site of transhydrogenase.

Wild-type dIII in dI_2dIII complexes binds NADH with a surprisingly high affinity. Furthermore, the occurrence of the aberrant cyclic reaction shows that NADH binds to dIII in the correct orientation to undergo hydride transfer with nucleotide bound to dI. The cyclic and aberrant cyclic reactions are only observed experimentally with the non-physiological nucleotide, $AcPdAD^+$. The equivalent reactions in the intact enzyme with physiological nucleotides would involve the reduction of NAD^+ by NADH; thus resulting in no net change of redox state of the nucleotides and no net proton translocation. These equivalent reactions would probably not occur at any significant rate in the living cell because turnover of the intact enzyme is driven by Δp and involves switching between the occluded and open states. When dIII is converted into the open state it can rapidly release its product nucleotides and bind substrate

nucleotides; thus breaking the cycling. This said, the phenomenon of NAD(H) binding to the dIII site (the "wrong" site) brings into question the efficiency of transhydrogenase. If NAD(H) were able to bind to dIII in the intact enzyme in the living cell, hydride transfer would occur between NAD^+ and NADH causing the enzyme to slip. There are two possible scenarios for the aberrant binding of NAD(H) to dIII in the living cell. Firstly, if NADH bound to dIII and NAD^+ bound to dI, then hydride transfer (not resulting in any overall change of redox state of the nucleotides) would lead to outward proton translocation from the *n*-phase to the *p*-phase. Since there is no free energy available from the redox reaction, this would only take place if the proton electrochemical potential was greater inside the bacterial cell compared to outside (*i.e.* $\Delta p > 0$) to drive the reaction. This would be an unlikely occurrence under physiological conditions. A more likely scenario (Figure 5.3) would be, if NAD^+ bound to dIII and NADH bound to dI. Hydride transfer (again not resulting in any overall change in redox state of the nucleotides) would lead to inward proton translocation from the *p*-phase to the *n*-phase. For this to occur, the proton electrochemical potential would need to be greater outside the bacterial cell relative to the inside (*i.e.* $\Delta p < 0$). In this situation, transhydrogenase would dissipate Δp, uncoupling the respiratory chain from ATP-synthesis. For NAD^+ to bind to dIII in the cell, the NAD(H) pool would need to be predominantly in its oxidised form, and the free NADP(H) concentration would need to be very low compared to that of NAD^+. Measuring the concentrations of nicotinamide nucleotides in the cell is difficult (Krebs *et al.* 1969) and knowledge of $NAD(P)^+$/NAD(P)H ratios and concentrations is limited. Therefore, it is difficult to predict whether the conditions, resulting in NAD^+ binding to dIII, would ever be met.

It cannot be ruled out that, in the living cell, the concentrations and redox states of the nicotinamide nucleotides are such that transhydrogenase does not slip. NADP(H) concentrations may be too high ever to allow the binding of NAD(H) to dIII. In the experiments described in this thesis, NAD(H) was shown to bind to the dIII component of dI_2dIII complexes; in the intact enzyme with functional dII components, the affinity of dIII for NAD(H) may be too low for NAD(H) to bind to a significant degree. Thus, it is possible that the aberrant binding of NAD(H) to dIII may not occur at any significant rate in the cell and impinge on metabolism.

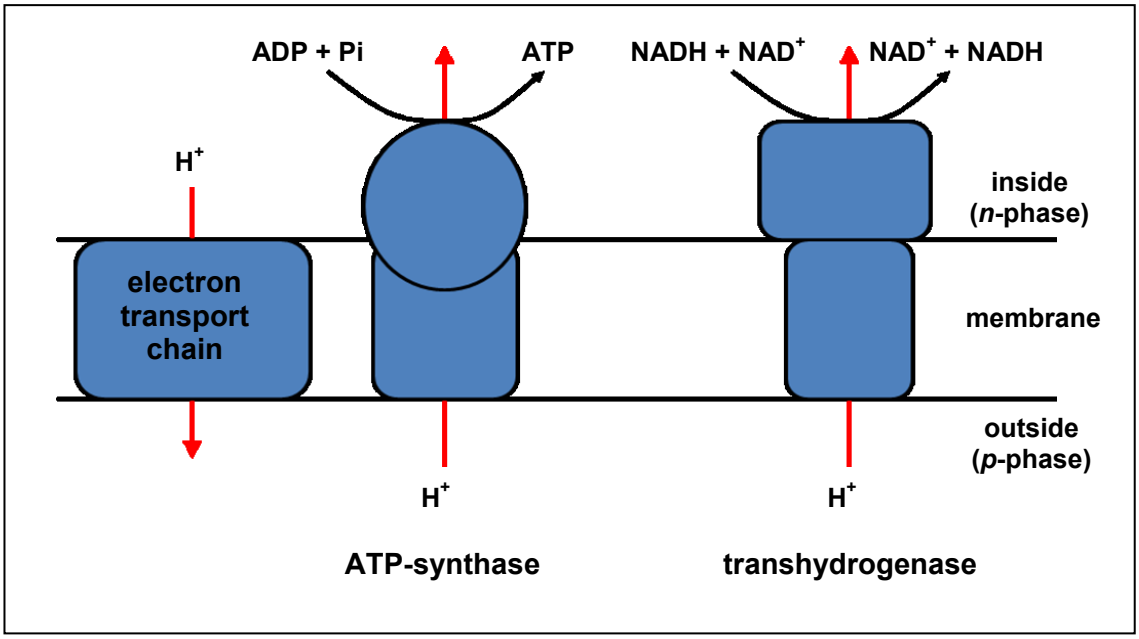

Figure 5.3 Cartoon of the chemiosmotic proton circuit showing the transhydrogenation reaction that would occur if NAD^+ bound to dIII in the living cell.

If NAD^+ bound to dIII in the living cell, proton translocation would be coupled to the hydride transfer reaction producing NAD^+ and NADH from NADH bound to dI and NAD^+ bound to dIII. This would dissipate Δp, decreasing the energy available to ATP-synthase to produce ATP. However, the rate of electron transport through the electron transport chain, and hence proton pumping into the *p*-phase, would continue at a high rate. This would uncouple the electron transport chain from ATP synthesis.

Results and discussion: Part II

CHAPTER 6

Crystallisation of *R. rubrum* dIII.R165A.

6.1 Introduction

Several high-resolution structures of various components of transhydrogenase have been determined previously (Table 6.1). However, because of the tight binding of NADP(H) to dIII, a structure of apo-dIII is not available. In light of the results presented earlier in this work, the crystal structure of apo-dIII would be invaluable to provide information about the conformation of apo-dIII. The results predict that apo-dIII would adopt an occluded conformation, in which loop E is closed over the empty nucleotide-binding site. Thus, a crystal structure would give an insight into the interactions between residues surrounding the NADP(H)-binding site which may stabilise dIII, and indeed loop E, in its occluded conformation.

Previous work on transhydrogenase (Hu *et al.* 1999; Bergkvist *et al.* 2000) has shown that mutating residues in the highly conserved K-R-S motif decreases the affinity of the protein for NADP(H) (see Section 1.10.2.2). As described earlier in this work (Chapter 3), a mutant of the dIII component from *R. rubrum* transhydrogenase, dIII.R165A, was isolated in which the arginine from the highly conserved K-R-S motif was substituted for an alanine residue. Enzyme and fluorescence assays as well as direct nucleotide-content determination experiments confirmed that dIII.R165A did indeed have a significantly decreased affinity for $NADP^+$ relative to wild-type dIII. Moreover, the apo-form of dIII.R165A was produced by subjecting the protein to gel-filtration. Following these results, it was considered possible to crystallise apo-dIII.R165A. To this end, crystallisation trials were prepared as described in this chapter.

Table 6.1 Table of published crystal structures of transhydrogenase.

protein complex	organism	resolution (Å)	space group	unit cell parameters a×b×c (Å) α, β, γ (°)	(reference) PDB ID
dI-NAD^+	*R. rubrum*	2.0	$P2_1$	65.9×116.6×102.0 90.0, 104.2, 90.0	(Buckley *et al.* 2000) 1F8G
dI-NADH	*R. rubrum*	1.9	$P2_1$	64.1×116.7×92.6 90.0, 106.3, 90.0	(Prasad *et al.* 2002) 1L7E
apo-dI	*R. rubrum*	1.8	$P2_1$	67.0×117.1×94.2 90.0, 108.3, 90.0	(Prasad *et al.* 2002) 1L7D
dI-NAD^+	*E. coli*	1.9	P1	38.8×67.0×76.6 67.1, 80.7, 81.0	(Johansson *et al.* 2005) 1X14
dI-NADH	*E. coli*	2.0	P1	38.7×67.1×76.8 67.2, 80.2, 81.6	(Johansson *et al.* 2005) 1X15
apo-dI	*E. coli*	1.9	P1	38.8×66.9×76.3 67.1, 80.7, 81.2	(Johansson *et al.* 2005) 1X13
dIII-$NADP^+$	*R. rubrum*	2.1	$P6_122$	117.9×117.9×211.3 90.0, 90.0, 120.0	(Sundaresan *et al.* 2003) 1PNO
dIII-$NADP^+$	*H. sapiens*	2.0	$P4_122$	58.1×58.1×250.8 90.0, 90.0, 90.0	(White *et al.* 2000) 1DJL
dIII-$NADP^+$	*B. taurus*	1.2	P1	33.7×36.7×38.5 68.4, 88.0, 74.8	(Prasad *et al.* 1999) 1D4O
dIII-NADPH	*H. sapiens*	2.2	$P4_122$	57.8×57.8×250.9 90.0, 90.0, 90.0	(Mather *et al.* 2004) 1U31
dIII-NADPH	*R. rubrum*	2.4	$P6_122$	118.3×118.3×212.8 90.0, 90.0, 120.0	(Sundaresan *et al.* 2003) 1PNQ
dI_2dIII (NAD^+/$NADP^+$)	*R. rubrum*	2.5	$P2_12_12_1$	71.5×74.2×205.1 90.0, 90.0, 90.0	(Cotton *et al.* 2001) 1HZZ

dI_2dIII ($NAD^+/NADP^+$)	*R. rubrum*	2.3	$P2_12_12_1$	71.7×74.0×204.2 90.0, 90.0, 90.0	(Mather *et al.* 2004) 1U28
dI_2dIII (NADH/NADPH)	*R. rubrum*	3.0	$P2_12_12_1$	72.3×74.6×204.2 90.0, 90.0, 90.0	(Mather *et al.* 2004) 1U2D
dI_2dIII (NAD^+/H_2NADPH)	*R. rubrum*	2.3	$P2_12_12_1$	72.2×74.4×204.8 90.0, 90.0, 90.0	(Bhakta *et al.* 2007) 2OOR
dI_2dIII ($H_2NADH/NADP^+$)	*R. rubrum*	2.6	$P2_12_12_1$	71.2×101.0×131.7 90.0, 90.0, 90.0	(Bhakta *et al.* 2007) 2OO5

6.2 A brief overview of protein x-ray crystallography.

X-ray crystallography is a widely used technique to determine the secondary and tertiary structure of proteins at high resolution. To begin with, the protein to be crystallised must be highly purified and concentrated; the required protein concentration depends on the individual protein but is typically around 10-20 mg mL^{-1}.

The crystallisation of the protein is often the most difficult part of the crystallographic process. A diagrammatic summary of the process is given in Figure 6.1. Once crystallised, the protein crystal is placed in an x-ray beam where it diffracts the x-rays onto a detector to produce a diffraction pattern. From this diffraction pattern an electron density map can be calculated and subsequently the three-dimensional structure of the protein can be determined.

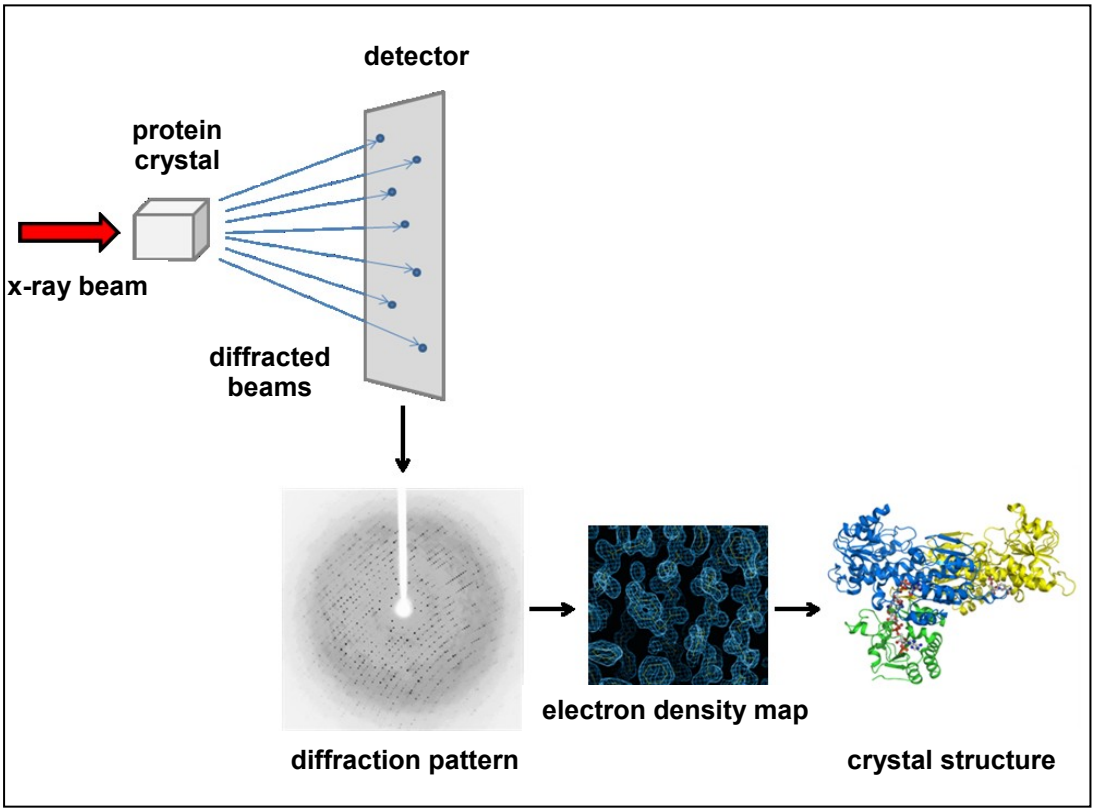

Figure 6.1 A diagrammatic overview of x-ray crystallography.

A protein crystal is placed in a beam of x-rays. The x-rays are diffracted onto a detector to produce a diffraction pattern. From this, via Fourier transform, an electron density map can be produced. Once refined, this electron density map will show the crystal structure of the protein.

6.2.1 Preparation of protein crystals for x-ray crystallography.

There are several methods for the crystallisation of proteins. The most popular method, and the one used in this work, is the vapour diffusion method. It consists of a sealed well containing a reservoir solution (the mother liquor) and a drop of protein either hanging above it (hanging drop) or sitting on a ledge next to it (sitting drop) (Figure 6.2).

The mother liquor contains a precipitant, for example polyethylene glycol (PEG) or ammonium sulphate, as well as a buffer at a suitable pH, and occasionally additives. The protein drop consists of both the protein solution and the reservoir solution; typically a 1:1 ratio of protein to reservoir solution is used but this can be varied to optimise crystallisation. Water from the protein drop diffuses into the reservoir solution causing the concentration of the protein and precipitant in the drop to slowly increase. This may result in the precipitation of the protein. For the precipitation to be such that the protein forms crystals, various properties must be explored. For example, temperature, pH, protein concentration and precipitant concentration can be varied.

Once high quality crystals have been grown, the crystals must be mounted to be used for data collection. Typically, the crystals are mounted onto a nylon loop, although fine capillary tubes can also be used. Data collection takes place at a temperature of 100 K to reduce radiation damage caused by the x-rays. There are two types of radiation damage. Primary radical formation is where x-rays hit atoms in the crystal producing radicals. These radicals then diffuse through the crystal and collide with other atoms causing secondary radical formation. Freezing eliminates the ability of the radicals to diffuse within the crystal, and thus reduces secondary radical formation. In order to prevent the formation of ice crystals, the protein crystals must be cryoprotected. Examples of cryoprotectants are glycerol, ethylene glycol and some sugars. The protein crystals must be soaked in solutions similar to the mother liquor but containing the chosen cryoprotectant, typically at a concentration of 15-25%. It is often necessary to soak protein crystals step-wise in solutions containing increasing concentrations of the cryoprotectant to avoid crystal damage. The protein (surrounded by mother liquor containing the cryoprotectant) is picked up using a nylon loop. It is

then flash frozen by plunging the loop containing the crystal into liquid nitrogen. The protein crystal is now ready for data collection.

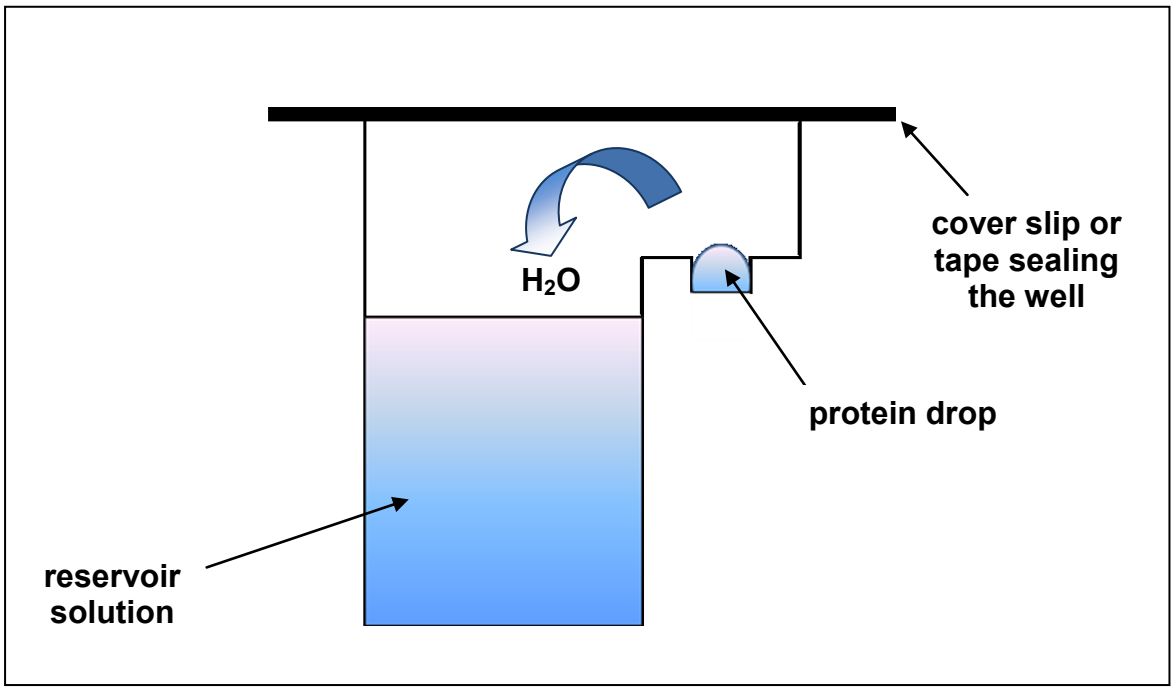

Figure 6.2 Diagram of a sitting drop crystallisation well.

Sitting drop crystallisation plates consist of a number of wells, which house the reservoir solution, and a ledge where the protein drop is placed. The plate is sealed with either a cover slip or clear tape. Each well is a sealed chamber, such that water diffuses from the protein drop to the reservoir solution, increasing both the protein and precipitant concentrations in the protein drop. If the conditions are correct, the protein will precipitate and form protein crystals.

6.2.2 The unit cell of crystals.

Crystals contain unit cells. The unit cell is the building block of a crystal and is repeated infinitely in three dimensions. The molecules, within and between unit cells, are held together by hydrogen bonds, usually via water molecules. The unit cell is defined by the vectors ***a***, ***b***, ***c***, which form the cell edges (measured in angstroms), and

the angles between them: α is the angle between ***b*** and ***c***, β is the angle between ***a*** and ***c*****,** and γ is the angle between ***a*** and ***b*** (see cell parameters in Table 6.1).

6.3 Crystallisation trials of *R. rubrum* dIII.R165A.

First attempts at the crystallisation of the purified and concentrated isolated *R. rubrum* dIII.R165A were set up using commercial crystallisation screens (JCSG-*plus*^{TM} by Molecular Dimensions Ltd. and Index^{TM} by Hampton Research), sitting drop crystallisation plates (MRC crystallisation plate^{TM} by Molecular Dimensions Ltd.) and a crystallisation robot (mosquito$^{®}$ by TTP LabTech). This was done in parallel with isolated wild-type *R. rubrum* dIII. No crystals formed of either the wild-type or mutant proteins.

A successful protocol for the crystallisation of wild-type dIII in complex with *R. rubrum* wild-type dI (dI_2dIII) is available (Cotton *et al.* 2001; Mather *et al.* 2004; Bhakta *et al.* 2007). A second set of crystallisation trials was then set up using the two commercial screens above to crystallise dIII.R165A in complex with dI. The protein drop contained 300 μM *R. rubrum* dI, 300 μM *R. rubrum* dIII.R165A, 50 μM NADH, pH 8.0. Crystals were obtained in wells with a 1:1 ratio of protein solution to reservoir solution (100 mM imidazole, pH 7.0, 20-26% PEG 6000 (w/v), 100 mM ammonium sulphate). The crystals were cryoprotected by soaking in solutions containing increasing concentrations of ethylene glycol (5-25% (v/v)). A number of crystals were exposed to a home x-ray source (Rigaku MicroMax007HF) and diffracted to ~3.2 Å. Data processing using the program XDS (Kabsch 1993) identified the space group of a typical crystal (LXH_01) as $P2_1$ with unit cell parameters a=73.4 Å, b=119.5 Å,

c=96.6 Å, α=90.0˚, β=105.8˚, γ=90.0˚. The data processing statistics are shown in Table 6.2.

resolution (Å)	no. of observations	no. of unique reflections	no. of reflections possible	completeness	R_{sym}	I/SIGMA	R_{meas}
9.43	2933	955	1081	88.3%	2.0%	46.92	2.4%
6.74	5549	1740	1821	95.6%	3.0%	31.02	3.6%
5.52	7185	2280	2359	96.7%	5.8%	18.27	6.9%
4.79	8446	2673	2747	97.3%	6.8%	15.63	8.2%
4.29	9537	3044	3106	98.0%	7.1%	14.94	8.5%
3.92	10566	3392	3450	98.3%	11.0%	9.94	13.3%
3.63	11333	3655	3711	98.5%	15.8%	7.34	19.0%
3.39	12206	3962	4004	99.0%	23.3%	5.13	28.2%
3.20	12727	4162	4243	98.1%	40.3%	3.02	48.9%
total	80482	25863	26522	97.5%	9.4%	12.42	11.3%

Table 6.2 Data processing statistics for crystal LXH_01.

$R_{sym} = \Sigma|I_{av}-I_n|/ \Sigma I_{av}$ where I_n is the intensity of the n^{th} reflection and I_{av} is the average intensity.

The unit cell parameters are similar to those of either a dI dimer (PDB ID 1F8G) or of a dI_2dIII complex (PDB ID 2OO5) (see Table 6.1); therefore it is not possible to predict, from the cell parameters alone, whether the crystal contains dIII.R165A or whether it contains only dI. Molecular replacement using PHASER (McCoy *et al.* 2007) was done with the known structure of the wild-type dI dimer (the dI portion taken from PDB ID 2OO5) as a search model. The statistics for the molecular replacement solution are shown in Table 6.3.

search molecule	α	β	γ	T_x	T_y	T_z	RFZ	TFZ
1st dI dimer	50.105	56.394	318.863	0.02808	0.00162	0.04574	18.5	14.3
2nd dI dimer	77.470	40.079	117.611	0.45045	-0.37611	0.46475	20.5	37.3

Table 6.3 Molecular replacement statistics for crystal LXH_01.

The rotation function is presented as the Eulerian angles α, β and γ. The translation function is expressed as the fractional unit cell coordinates T_x, T_y and T_z. The rotation function z-score and the translation function z-score are represented as RFZ and TFZ, respectively.

The molecular replacement solution was subjected to partial rigid-body and positional refinement using REFMAC5 (Murshudov *et al.* 1997) resulting in a model with two dimers of dI in the asymmetric unit with R/R_{free} values of 0.229/0.330. This convincing molecular replacement solution showed that there were no intermolecular spaces large enough to accommodate a molecule of dIII.R165A. Thus, the crystal LXH_01 contained only dimers of dI and not complexes of dI and dIII.R165A.

In an attempt to incorporate dIII.R165A into the crystals, trials were set up in which the protein solution contained a higher concentration of dIII.R165A to compensate for a weaker affinity (~2 fold) of dIII.R165A for dI than wild-type dIII (see Figure 3.5). Thus, the protein solution contained 300 μM *R. rubrum* dI, 600 μM *R. rubrum* dIII.R165A and 5 mM NADH at pH 8.0. Plate-like crystals were obtained in wells with a 1:1 ratio of protein solution to reservoir solution (100 mM bis-tris pH 6.0, 50-200 mM ammonium acetate and 20-30% PEG 4000 (w/v)). The crystals were cryoprotected by soaking in solutions containing increasing concentrations of ethylene glycol (5-25% (v/v)). A number of crystals were exposed to either the home x-ray source, or the x-ray beamline ID14-1 at the European Synchrotron Radiation Facility, and diffracted to a maximum resolution of ~4.5 Å. The data collected from a

typical crystal (LXH_02) were processed using XDS (Kabsch 1993); the space group was identified as $P2_1$ with unit cell parameters of a=71.6 Å, b=120.0 Å, c=97.1 Å, α=90.0˚, β=108.1˚, γ=90.0˚. The data processing statistics are shown in Table 6.4.

resolution (Å)	no. of observations	no. of unique reflections	no. of possible reflections	completeness	R_{sym}	I/SIGMA	R_{meas}
12.74	1369	396	438	90.4%	4.8%	20.91	5.7%
9.28	2441	658	661	99.5%	5.2%	21.54	6.1%
7.66	3208	851	857	99.3%	9.4%	13.21	10.9%
6.66	3676	971	967	100.4%	19.9%	6.54	23.2%
5.98	4182	1099	1102	99.7%	26.9%	5.10	31.3%
5.47	4632	1223	1226	99.8%	39.6%	3.52	46.2%
5.07	5001	1322	1328	99.5%	44.2%	3.17	51.6%
4.75	5341	1421	1422	99.9%	44.8%	3.08	52.3%
4.48	5415	1469	1493	98.4%	42.2%	3.20	49.4%
total	35265	9410	9494	99.1%	21.7%	6.72	25.4%

Table 6.4 Data processing statistics for crystal LXH_02.

$R_{sym} = \Sigma|I_{av}-I_n|/ \Sigma I_{av}$ where I_n is the intensity of the n^{th} reflection and I_{av} is the average intensity.

Again, these cell parameters are similar to those of either a dI dimer (PDB ID 1F8G) or of a dI_2dIII complex (PDB ID 2OO5) (see Table 6.1). Molecular replacement was done using the program PHASER (McCoy *et al.* 2007) and the known structure of wild-type dI (the dI portion taken from PDB ID 2OO5), but this time with an α-helix removed from the search model. When the x-ray data are of lower resolution, one way of confirming that a molecular replacement solution is correct, is to remove a fragment of the search model. If the solution is correct, difference electron density will show the missing fragment of the search model, giving electron density maps that show electron density for the missing fragment. The resulting molecular replacement solution for crystal LXH_02 showed electron density

for the missing helix (data not shown) confirming that the solution is correct. The molecular replacement statistics are shown in Table 6.5. Partial rigid-body refinement using REFMAC5 (Murshudov *et al.* 1997) gave an R/R_{free} value of 0.391/0.384 further confirming that the crystal LXH_02 contained only dI dimers; there were no intermolecular spaces large enough to accommodate a molecule of dIII.

search molecule	α	β	γ	T_x	T_y	T_z	RFZ	TFZ
1st dI dimer	49.514	55.797	322.569	0.02623	0.00096	0.05266	14.1	9.1
2nd dI dimer	260.812	140.374	73.97	0.4360	-0.37684	0.46462	12.9	21.7

Table 6.5 Molecular replacement statistics for crystal LXH_02.

The rotation function is presented as the angles α, β and γ. The translation function is expressed as the fractional unit cell coordinates T_x, T_y and T_z. The rotation function z-score and the translation function z-score are represented as RFZ and TFZ, respectively.

6.3.1 Preparation of a truncated form of *R. rubrum* dIII.R165A.

The crystal structures of isolated *R. rubrum* dIII with $NADP^+$ or NADPH bound (Sundaresan *et al.* 2003) were solved using a dIII construct that was 31 amino acids shorter at the N-terminal compared to that used in the unsuccessful crystallisation trials described above. It was reasoned that the extra amino acids may be disordered and disrupt interactions between protein molecules that are needed to form protein crystals. Thus, the next logical step was to produce a truncated form of the dIII.R165A used previously in this work and set up a third round of crystallisation trials.

The mutant plasmid pLH3 harbours the gene that encodes the truncated form of the dIII.R165A mutant protein from *R. rubrum* transhydrogenase. For the preparation of pLH3, the primers used were supplied by Alta Bioscience and were designed with the following sequences: -

Forward 5' – CGTGGTGGCATATGTCGGTCAAGGCCGGCAGCGC – 3'

Reverse 5' – GCACGGTTCCGGCCTTCCAGACGTCAAGGATGC – 3'

The forward primer incorporates an *Nde*I restriction site into the 5' end of the forward strand of the dIII.R165A gene. Part of the truncated gene was amplified by the polymerase chain reaction (PCR); a diagrammatic summary of the PCR reaction is shown in Figure 6.3.

A mixture (final volume 100 µL) containing approximately 10 ng of the template plasmid pLH1 (see Section 2.1.4), 10 µL "10× reaction buffer" (supplied with the polymerase), 1 mM dNTP mixture, 0.4 µM of each primer, 1.5 mM $MgCl_2$, 5% DMSO (v/v) and 8 U BIO-X-ACT Short DNA polymerase (Bioline) was split into four tubes each containing 25 µL. The following program was carried out in a Bio-Rad My Cycler Thermal Cycler: -

95˚C	5 minutes	×1
50-70˚C	1 minute	
95˚C	30 seconds	×30
50-70˚C	30 seconds	
70˚C	1 minute	
70˚C	10 minutes	×1
4˚C	Hold	

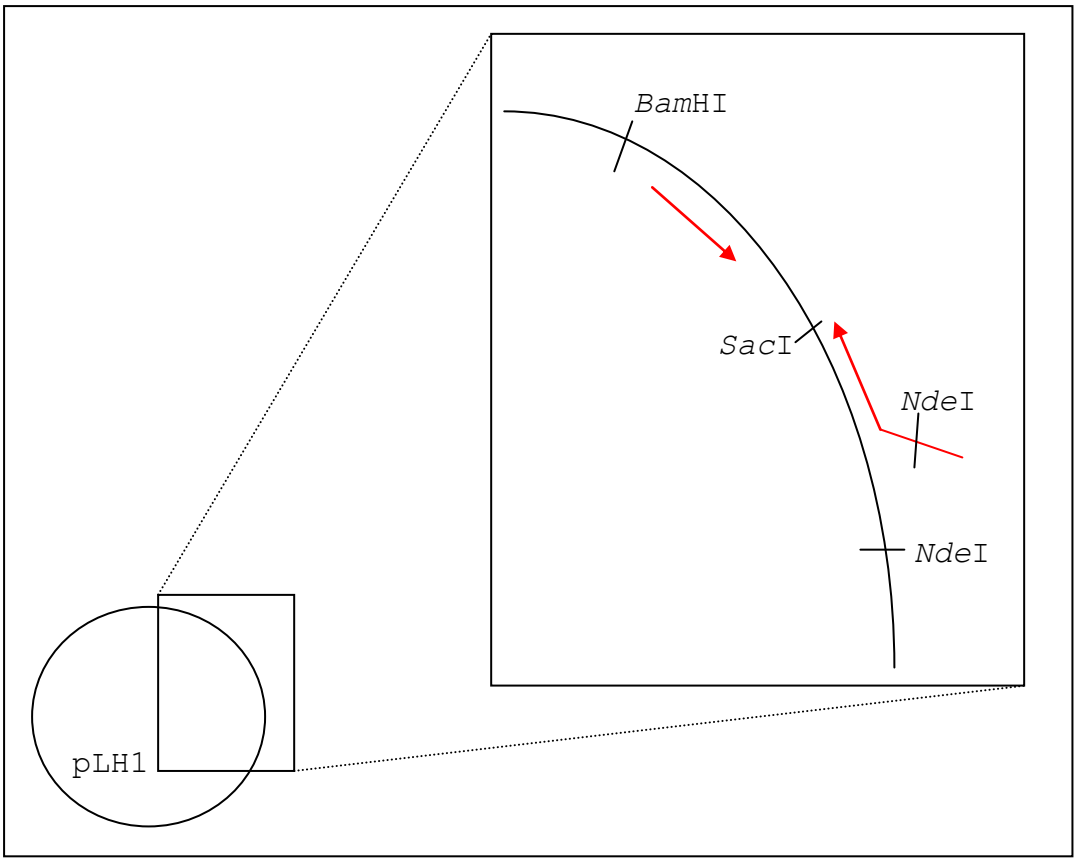

Figure 6.3 Diagram of the PCR reaction performed to produce a fragment of the gene encoding truncated dIII.R165A.

The plasmid pLH1 harbours the gene that encodes the full-length dIII.R165A. In this diagram, part of this plasmid is enlarged showing the *Nde*I and *Bam*HI restriction sites, between which the dIII.R165A gene is housed. Also shown are the primers (red arrows); the forward primer includes an *Nde*I restriction site. The direction of the arrows shows the direction of transcription. Following the PCR reaction, the resulting gene fragment and the intact pLH1 plasmid were digested with *Nde*I and *Sac*I; the position of the *Sac*I restriction site is shown. The digested fragment and vector were then ligated to produce pLH3.

Following the PCR experiment, the samples were analysed on a 0.8% agarose gel in parallel with a 1000 bp DNA ladder (Bioline HyperLadder I) (Figure 6.4), and

the appropriate band was extracted using a Qiagen QIAquick Gel Extraction Kit following the manufacturer's instructions.

The purified gene fragment (~40 ng) and the pLH1 plasmid were separately digested in a final volume of 15 µL by 20 U of the restriction enzyme *Nde*I (New England Biolabs) at 37˚C overnight and then by 20 U of the restriction enzyme *Sac*I (New England Biolabs) at 37˚C for 3 hours. The digested gene fragment (insert) was analysed on a 2% agarose gel in parallel with a 100 bp DNA ladder (New England Biolabs), and the digested plasmid (vector) was analysed on a 0.8% agarose gel using a 1000 bp ladder (Bioline HyperLadder I). The appropriate bands were extracted from the gels using a Qiagen QIAquick Gel Extraction Kit.

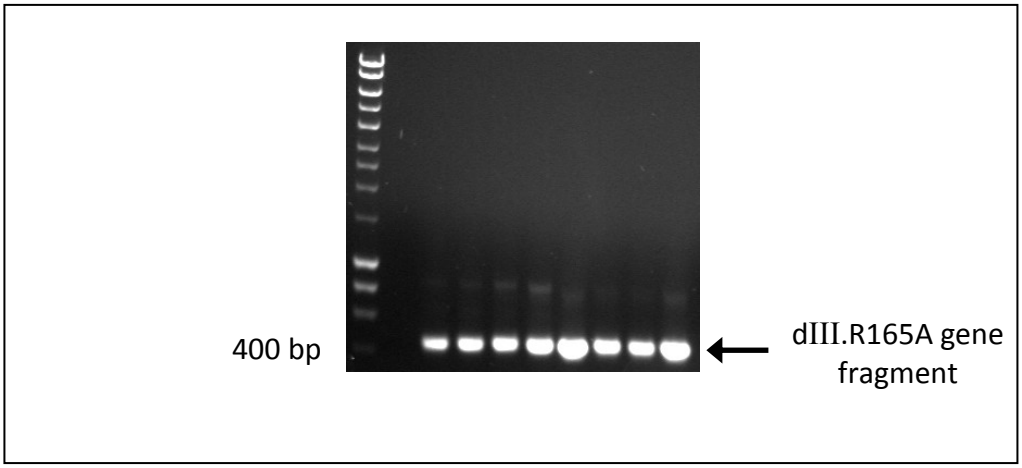

Figure 6.4 Agarose gel showing the dIII.R165A gene fragment following PCR.

A PCR experiment was performed to amplify a fragment of the gene encoding full-length dIII.R165A, which is harboured in the plasmid pLH1. The samples from the PCR experiment were analysed on a 0.8% agarose gel containing ethidium bromide (as described in Section 2.1.5). The gel was visualised and photographed using a UV illuminator. The gene fragment (~400 bp) resulting from the PCR experiment was extracted from the gel, digested with restriction enzymes and used as the insert for the subsequent ligation step with digested pLH1. This ligation experiment resulted in the production of the plasmid pLH3, which harbours the gene encoding truncated dIII.R165A.

For the ligation of the insert and the vector, 50 ng of the vector and 6 ng of the insert were mixed with 1 µl "10× T4 DNA ligase buffer" (supplied with the T4 DNA ligase) to achieve a final volume of 9 µL. The mixture was incubated for 2 minutes at 42˚C before adding 1 µl T4 DNA ligase (Bioline). The mixture was incubated at 16˚C for 16 hours in a Bio-Rad My Cycler Thermal Cycler. To deactivate the ligase, the mixture was incubated at 65˚C for 10 minutes. The resulting plasmid was used to transform *E. coli* BL21(DE3) competent cells as described in Section 2.1.6.

The fidelity of pLH3 was confirmed by sequencing by the Functional Genomics Laboratory at The University of Birmingham.

The growth of the cells and the over-expression (at either 25˚C or 37˚C) of the truncated dIII.R165A were performed in parallel with the full-length dIII.R165A as described for pNIC2 in Section 2.1.7. After the cells were harvested and broken by sonication, they were subjected to a high-speed centrifugation (150,000 *g*). Following this high-speed centrifugation, the resulting supernatants and pellets were analysed by SDS PAGE (Figure 6.5). Recall from Section 2.1.7, that the full-length dIII.R165A forms inclusion bodies and is mostly present in the pellet after the high-speed centrifugation. Thus, the full-length protein was visible on the SDS PAGE gel in the pellet samples, showing that it had formed inclusion bodies when expressed at both temperatures. However, the truncated protein was not visible on the SDS PAGE gel in either the supernatants or the pellets after expression at either 25˚C or 37˚C.

Due to time restraints, I was unable to express pLH3 to sufficient levels to produce a purified truncated form of dIII.R165A. Crystallisation trials of this protein were therefore not possible.

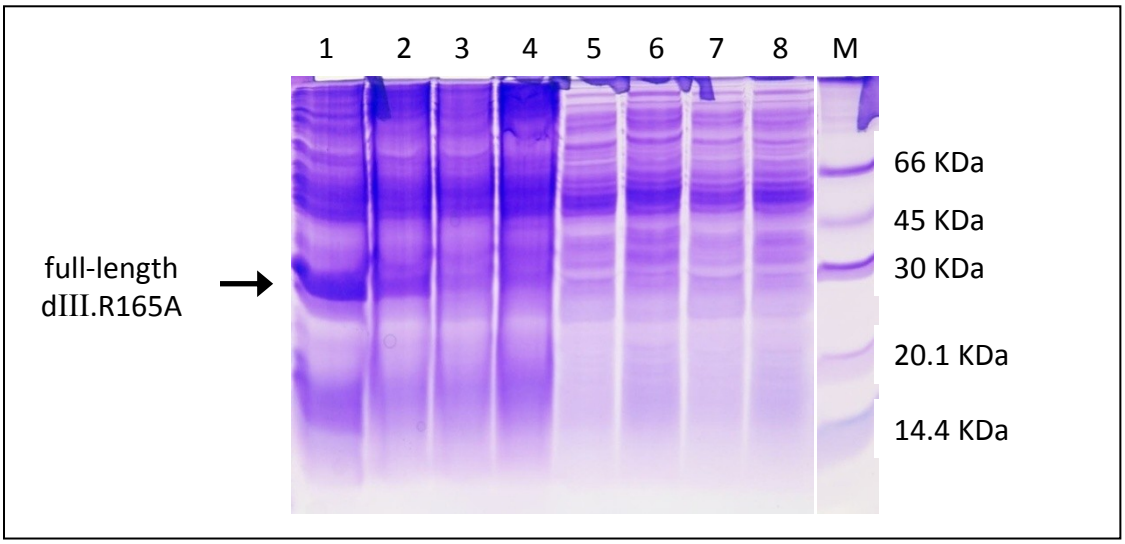

Figure 6.5 SDS PAGE gel showing the lack of expression of the truncated dIII.R165A compared with the full-length dIII.R165A.

After the growth and expression of the full-length dIII.R165A or the truncated dIII.R165A at either 25˚C or 37˚C, the cells were broken by sonication and subjected to a high-speed centrifugation (described in Section 2.1.7). The resulting pellets and supernatants were analysed on a 12% SDS PAGE gel, which was stained with PAGE blue. The full-length dIII.R165A is encoded by the gene harboured in the plasmid pLH1, and the truncated dIII.R165A is encoded by the gene harboured in the plasmid pLH3. The plasmid expressed, the temperature of the expression and the fraction following the high-speed spin analysed by SDS PAGE in the numbered lanes were: 1) pLH1, 37˚C, pellet; 2) pLH1, 25˚C, pellet; 3) pLH3, 37˚C, pellet; 4) pLH3, 25˚C, pellet; 5) pLH1, 37˚C, supernatant; 6) pLH1, 25˚C, supernatant; 7) pLH3, 37˚C, supernatant; 8) pLH3, 25˚C, supernatant; M = protein marker (GE Healthcare low molecular weight marker).

6.4 Future directions of the project.

All published crystal structures of the dIII component are of the protein in its occluded conformation with bound nucleotide. Nucleotide binding to and release from dIII is thought to be central in the coupling mechanism between hydride transfer and proton translocation. Thus, a crystal structure of dIII in either its open conformation or

in its apo-form would be beneficial in understanding the role of loop E in the coupling mechanism. For this reason, if more time was available for this project, I would continue with the crystallisation trials of dIII.R165A. From the results described in this thesis it would be expected that dIII.R165A would crystallise in an occluded conformation. However, since dIII.R165A has a decreased affinity for NADP(H) compared to wild-type dIII, it is thought possible to crystallise the protein in its apo-form.

To this end, the expression of the truncated form of dIII.R165A would need to be explored in an attempt to produce a concentrated, pure preparation of the protein that would be suitable for crystallisation trials. The full-length dIII.R165A was expressed in large quantities in inclusion bodies (see Section 3.1.4). Thus, the unsuccessful expression of the truncated form of dIII.R165A is thought to be due to the "missing" part of the N-terminal and not the R165A mutation. Examples of parameters to vary in the expression of the protein are temperature, isopropyl thiogalactoside concentration and incubation period. If the expression of the truncated dIII.R165A was still not successful, the construct of the plasmid containing the gene would need to be reviewed.

The successful crystallisation of the dIII component from *R. rubrum* (Sundaresan *et al.* 2003) was achieved using a construct of wild-type dIII that was 31 amino acids shorter at the N-terminal compared to the full-length dIII used in this project. In the work of Sundaresan *et al.*, the dIII component contained a poly-histidine tag sequence at the N-terminal. This was not cleaved before crystallisation. Thus, the gene encoding the truncated form of dIII.R165A (described in Section 6.3.1) could be inserted into a pET16b vector, which would incorporate an identical poly-histidine tag sequence onto the N-terminal of dIII.R165A as was used by

Sundaresan *et al*. The protocol for the expression of the truncated wild-type dIII (Sundaresan *et al.* 2003) could then be adopted for the truncated dIII.R165A. If the expression was successful, the protein could be purified by affinity chromatography using a medium containing nickel. Crystallisation trials could then be set up to crystallise the truncated dIII.R165A.

References

Ambartsoumian, G., D'Ari, R., Lin, R. T. and Newman, E. B. (1994). "Altered amino acid metabolism in lrp mutants of *Escherichia coli* K12 and their derivatives." *Microbiology* **140** (7): 1737-1744.

Anderson, W. M. and Fisher, R. R. (1978). "Purification and partial characterization of bovine heart mitochondrial pyridine dinucleotide transhydrogenase." *Arch Biochem Biophys* **187** (1): 180-190.

Arkblad, E. L., Tuck, S, Pestov, N.B, Dmitriev, R.I., Kostina, M.B., Stenvall, J., Tranberg, M., Rydström, J. (2005). "A *Caenorhabditis elegans* mutant lacking functional nicotinamide nucleotide transhydrogenase displays increased sensitivity to oxidative stress." *Free Radic Biol Med.* **38** (11): 1518-1525.

Baker, P. J., Britton, K. L., Rice, D. W., Rob, A. and Stillman, T. J. (1992). "Structural consequences of sequence patterns in the fingerprint region of the nucleotide binding fold. Implications for nucleotide specificity." *J Mol Biol* **228** (2): 662-671.

Bellamacina, C. R. (1996). "The nicotinamide dinucleotide binding motif: a comparison of nucleotide binding proteins." *FASEB J* **10** (11): 1257-1269.

Bergkvist, A., Johansson, C., Johansson, T., Rydstrom, J. and Karlsson, B. G. (2000). "Interactions of the NADP(H)-binding domain III of proton-translocating transhydrogenase from *Escherichia coli* with NADP(H) and the NAD(H)-binding domain I studied by NMR and site-directed mutagenesis." *Biochemistry* **39** (41): 12595-12605.

Bhakta, T., Whitehead, S. J., Snaith, J. S., Dafforn, T. R., Wilkie, J., Rajesh, S., White, S. A. and Jackson, J. B. (2007). "Structures of the dI_2dIII_1 complex of proton-translocating transhydrogenase with bound, inactive analogues of NADH and NADPH reveal active site geometries." *Biochemistry* **46** (11): 3304-3318.

Bizouarn, T., Diggle, C. and Jackson, J. B. (1996a). "The binding of nucleotides to domain I proteins of the proton-translocating transhydrogenases from *Rhodospirillum rubrum* and *Escherichia coli* as measured by equilibrium dialysis." *Eur J Biochem* **239** (3): 737-741.

Bizouarn, T., Grimley, R. L., Cotton, N. P., Stilwell, S. N., Hutton, M. and Jackson, J. B. (1995). "The involvement of NADP(H) binding and release in energy transduction by proton-translocating nicotinamide nucleotide transhydrogenase from *Escherichia coli*." *Biochim Biophys Acta* **1229** (1): 49-58.

Bizouarn, T., Sazanov, L. A., Aubourg, S. and Jackson, J. B. (1996b). "Estimation of the H^+/H^- ratio of the reaction catalysed by the nicotinamide nucleotide

transhydrogenase in chromatophores from over-expressing strains of *Rhodospirillum rubrum* and in liposomes inlaid with the purified bovine enzyme." *Biochim Biophys Acta* **1273**: 4-12.

Bizouarn, T., Stilwell, S., Venning, J., Cotton, N. P. and Jackson, J. B. (1997). "The pH dependences of reactions catalyzed by the complete proton-translocating transhydrogenase from *Rhodospirillum rubrum*, and by the complex formed from its recombinant nucleotide-binding domains." *Biochim Biophys Acta* **1322** (1): 19-32.

Bizouarn, T., van Boxel, G. I., Bhakta, T. and Jackson, J. B. (2005). "Nucleotide binding affinities of the intact proton-translocating transhydrogenase from *Escherichia coli.*" *Biochim Biophys Acta* **1708** (3): 404-410.

Bocanegra, J. A., Scrutton, N. S. and Perham, R. N. (1993). "Creation of an NADP-dependent pyruvate dehydrogenase multienzyme complex by protein engineering." *Biochemistry* **32** (11): 2737-2740.

Bock, R. M., Ling, N. S., Morell, S. A. and Lipton, S. H. (1956). "Ultraviolet absorption spectra of adenosine-5'-triphosphate and related 5'-nucleotides." *Arch Biochem Biophys* **62** (2): 253-264.

Boehringer, M. (1987). "Biochemica Information." Indianapolis.

Bohren, K. M., Brownlee, J. M., Milne, A. C., Gabbay, K. H. and Harrison, D. H. (2005). "The structure of Apo R268A human aldose reductase: hinges and latches that control the kinetic mechanism." *Biochim Biophys Acta* **1748** (2): 201-212.

Bragg, P. D. (1996). "Mechanism of hydride transfer during the reduction of 3-acetylpyridine adenine dinucleotide by NADH catalyzed by the pyridine nucleotide transhydrogenase of *Escherichia coli*." *FEBS Lett* **397** (1): 93-96.

Bragg, P. D., Hou, C. (2001). "Characterization of mutants of βHistidine91, βAspartate213, and βAsparagine222, possible components of the energy transduction pathway of the proton-translocating pyridine nucleotide transhydrogenase of *Escherichia coli*." *Arch Biochem Biophys* **388** (2): 299-307.

Brondijk, T. H., van Boxel, G. I., Mather, O. C., Quirk, P. G., White, S. A. and Jackson, J. B. (2006). "The role of invariant amino acid residues at the hydride transfer site of proton-translocating transhydrogenase." *J Biol Chem* **281** (19): 13345-13354.

Broos, J., Gabellieri, E., van Boxel, G. I., Jackson, J. B. and Strambini, G. B. (2003). "Tryptophan phosphorescence spectroscopy reveals that a domain in the NAD(H)-binding component (dI) of transhydrogenase from *Rhodospirillum rubrum* has an extremely rigid and conformationally homogeneous protein core." *J Biol Chem* **278** (48): 47578-47584.

Buckley, P. A., Baz Jackson, J., Schneider, T., White, S. A., Rice, D. W. and Baker, P. J. (2000). "Protein-protein recognition, hydride transfer and proton pumping in the transhydrogenase complex." *Structure* **8** (8): 809-815.

Carugo, O. and Argos, P. (1997). "NADP-dependent enzymes. I: Conserved stereochemistry of cofactor binding." *Proteins* **28**: 10-28.

Clarke, D. M., Loo, T. W., Gillam, S. and Bragg, P. D. (1986). "Nucleotide sequence of the *pnt*A and *pnt*B genes encoding the pyridine nucleotide transhydrogenase of *Escherichia coli.* ." *Eur J Biochem* **158**: 647-653.

Cotton, N. P., White, S. A., Peake, S. J., McSweeney, S. and Jackson, J. B. (2001). "The crystal structure of an asymmetric complex of the two nucleotide binding components of proton-translocating transhydrogenase." *Structure* **9** (2): 165-176.

Cunningham, I. J., Williams, R., Palmer, T., Thomas, C. M. and Jackson, J. B. (1992). "The relation between the soluble factor associated with $H(^{+})$-transhydrogenase of *Rhodospirillum rubrum* and the enzyme from mitochondria and *Escherichia coli.*" *Biochim Biophys Acta* **1100** (3): 332-338.

Diggle, C., Bizouarn, T., Cotton, N. P. and Jackson, J. B. (1996). "Properties of the purified, recombinant, NADP(H)-binding domain III of the proton-translocating nicotinamide nucleotide transhydrogenase from *Rhodospirillum rubrum*." *Eur J Biochem* **241** (1): 162-170.

Diggle, C., Cotton, N. P., Grimley, R. L., Quirk, P. G., Thomas, C. M. and Jackson, J. B. (1995a). "Conformational dynamics of a mobile loop in the NAD(H)-binding subunit of proton-translocating transhydrogenases from *Rhodospirillum rubrum* and *Escherichia coli.*" *Eur J Biochem* **232** (1): 315-326.

Diggle, C., Hutton, M., Jones, G. R., Thomas, C. M. and Jackson, J. B. (1995b). "Properties of the soluble polypeptide of the proton-translocating transhydrogenase from *Rhodospirillum rubrum* obtained by expression in *Escherichia coli.*" *Eur J Biochem* **228** (3): 719-726.

Eventoff, W., Hackert, M. L. and Rossmann, M. G. (1975). "A low-resolution crystallographic study of porcine heart lactate dehydrogenase." *J Mol Biol* **98** (1): 249-258.

Fersht, A. (1999). "Structure and mechanism in protein science: a guide to enzyme catalysis and protein folding." New York, *W. H. Freeman and Company*.

Fisher, R. R. and Guillory, R. J. (1971). "Resolution of enzymes catalyzing energy-linked transhydrogenation. 3. Preparation and properties of *Rhodospirillum rubrum* transhydrogenase factor." *J Biol Chem* **246** (15): 4687-4693.

Fjellstrom, O., Axelsson, M., Bizouarn, T., Hu, X., Johansson, C., Meuller, J. and Rydstrom, J. (1999a). "Mapping of residues in the NADP(H)-binding site of

proton-translocating nicotinamide nucleotide transhydrogenase from *Escherichia coli.*" *J Biol Chem* **274** (10): 6350-6359.

Fjellstrom, O., Bizouarn, T., Zhang, J. W. and Rydstrom, J. (1999b). "Catalytic properties of hybrid complexes of the NAD(H)-binding and NADP(H)-binding domains of the proton-translocating transhydrogenases from *Escherichia coli* and *Rhodospirillum rubrum*." *Biochemistry* **38**: 415-422.

Fjellstrom, O., Johansson, C. and Rydstrom, J. (1997). "Structural and catalytic properties of the expressed and purified NAD(H)- and NADP(H)-binding domains of proton-pumping transhydrogenase from *Escherichia coli.*" *Biochemistry* **36** (38): 11331-11341.

Freeman, H., Shimomura, K., Cox, R. D. and Ashcroft, F. M. (2006a). "Nicotinamide nucleotide transhydrogenase: a link between insulin secretion, glucose metabolism and oxidative stress." *Biochem Soc Trans* **34** (5): 806-810.

Freeman, H., Shimomura, K., Horner, E., Cox, R. D. and Ashcroft, F. M. (2006b). "Nicotinamide nucleotide transhydrogenase: a key role in insulin secretion." *Cell Metab* **3** (1): 35-45.

Garcia, J. J., Tuena de Gomez-Puyou, M. and Gomez-Puyou, A. (1995). "Inhibition by trifluoperazine of ATP synthesis and hydrolysis by particulate and soluble mitochondrial F1: competition with H_2PO_4." *J Bioenerg Biomembr* **27** (1): 127-136.

Hanson, R. L. and Rose, C. (1980). "Effects of an insertion mutation in a locus affecting pyridine nucleotide transhydrogenase (pnt::Tn5) on the growth of *Escherichia coli.*" *J Bacteriol* **141** (1): 401-404.

Hanukoglu, I. and Gutfinger, T. (1989). "cDNA sequence of adrenodoxin reductase. Identification of NADP-binding sites in oxidoreductases." *Eur J Biochem* **180** (2): 479-484.

Harrison, D. H., Bohren, K. M., Ringe, D., Petsko, G. A. and Gabbay, K. H. (1994). "An anion binding site in human aldose reductase: mechanistic implications for the binding of citrate, cacodylate, and glucose 6-phosphate." *Biochemistry* **33** (8): 2011-2020.

Hickman, J. W., Barber, R. D., Skaar, E. P. and Donohue, T. J. (2002). "Link between the membrane-bound pyridine nucleotide transhydrogenase and glutathione-dependent processes in *Rhodobacter sphaeroides*." *J Bacteriol* **184** (2): 400-409.

Hoek, J. B. and Rydstrom, J. (1988). "Physiological roles of nicotinamide nucleotide transhydrogenase." *Biochem J* **254** (1): 1-10.

Hojeberg, B. and Rydstrom, J. (1977). "Purification and molecular properties of reconstitutively active nicotinamide nucleotide transhydrogenase from beef heart mitochondria." *Biochem Biophys Res Commun.* **78** (4): 1183-1190.

Hu, X., Zhang, J., Fjellstrom, O., Bizouarn, T. and Rydstrom, J. (1999). "Site-directed mutagenesis of charged and potentially proton-carrying residues in the β subunit of the proton-translocating nicotinamide nucleotide transhydrogenase from *Escherichia coli*. Characterization of the βH91, βD392, and βK424 mutants." *Biochemistry* **38** (5): 1652-1658.

Hutton, M., Day, J. M., Bizouarn, T. and Jackson, J. B. (1994). "Kinetic resolution of the reaction catalysed by proton-translocating transhydrogenase from *Escherichia coli* as revealed by experiments with analogues of the nucleotide substrates." *Eur J Biochem* **219** (3): 1041-1051.

Jackson, J. B. (2003). "Proton translocation by transhydrogenase." *FEBS Lett* **545** (1): 18-24.

Jackson, J. B. and Obiozo, U. M. (2009). "Proton-translocating transhydrogenase in photosynthetic bacteria." *in: C.N. Hunter, F. Daldal, M.C. Thurnauer, J.T. Beatty (Eds.), The purple phototrophic bacteria, Springer.*: 495-508.

Jackson, J. B., White, S. A. and Brondijk, T. H. (2005). "Hydride transfer and proton translocation by nicotinamide nucleotide transhydrogenase." *Biophysical and structural aspects of bioenergetics* **chapter 16**: 376-393.

Jackson, J. B., White, S. A., Quirk, P. G. and Venning, J. D. (2002). "The alternating site, binding change mechanism for proton translocation by transhydrogenase." *Biochemistry* **41** (13): 4173-4185.

Jeeves, M., Smith, K. J., Quirk, P. G., Cotton, N. P. and Jackson, J. B. (2000). "Solution structure of the NADP(H)-binding component (dIII) of proton-translocating transhydrogenase from *Rhodospirillum rubrum.*" *Biochim Biophys Acta* **1459** (2-3): 248-257.

Johansson, C., Pedersen, A., Karlsson, B. G. and Rydstrom, J. (2002). "Redox-sensitive loops D and E regulate NADP(H) binding in domain III and domain I-domain III interactions in proton-translocating *Escherichia coli* transhydrogenase." *Eur J Biochem* **269** (18): 4505-4515.

Johansson, T., Oswald, C., Pedersen, A., Tornroth, S., Okvist, M., Karlsson, B. G., Rydstrom, J. and Krengel, U. (2005). "X-ray structure of domain I of the proton-pumping membrane protein transhydrogenase from *Escherichia coli.*" *J Mol Biol* **352** (2): 299-312.

Kabsch, W. (1993). "Automatic processing of rotation diffraction data from crystals of initially unknown symmetry and cell constants." *J Appl Cryst* **25**: 795-800.

Kaneto, H., Kawamori, D., Matsuoka, T. A., Kajimoto, Y. and Yamasaki, Y. (2005). "Oxidative stress and pancreatic β-cell dysfunction." *Am J Ther* **12** (6): 529-533.

Kaplan, N. O. (1985). "The role of pyridine nucleotides in regulating cellular metabolism." *Curr Top Cell Regul* **26**: 371-381.

Kirkman, H. N., Gaetani, G. F. and Clemons, E. H. (1986). "NADP-binding proteins causing reduced availability and sigmoid release of $NADP^+$ in human erythrocytes." *J Biol Chem* **261** (9): 4039-4045.

Klingenberg, M. (1974). "Nicotinamide-adenine dinucleotides (NAD, NADP, NADH. NADPH): spectrophotometric and fluorometric methods." *In H. U. Bergmeyer (Ed.), Methods of enzymatic analysis* **4**: 2045-2072.

Krebs, H. A. and Veech, R. L. (1969). "Equilibrium relations between pyridine nucleotides and adenine nucleotides and their roles in the regulation of metabolic processes." *Adv Enzyme Regul* **7**: 397-413.

Lakowicz, J. R. (2004). "Principles of fluorescence spectroscopy." New York, *Springer Science*.

Lee, C. P., Simard-Duquesne, N., Ernster, L. and Hoberman, H. D. (1965). "Stereochemistry of hydrogen-transfer in the energy-linked pyridine nucleotide transhydrogenase and related reactions." *Biochim Biophys Acta* **105** (3).

Lowell, B. B. and Shulman, G. I. (2005). "Mitochondrial dysfunction and type 2 diabetes." *Science* **307** (5708): 384-387.

Mather, O. C., Singh, A., van Boxel, G. I., White, S. A. and Jackson, J. B. (2004). "Active-site conformational changes associated with hydride transfer in proton-translocating transhydrogenase." *Biochemistry* **43** (34): 10952-10964.

McCoy, A. J., Grosse-Kunstleve, R. W., Adams, P. D., Winn, M. D., Storoni, L. C. and Read, R. J. (2007). "Phaser crystallographic software." *J Appl Cryst* **40** (4): 658-674.

Mejbaum-Katzenellenbogen, S. and Drobryszycka, W. J. (1959). "New methods for quantitative determination of serum proteins separated by paper chromatography." *Clin Chem Acta* **4**: 515-522.

Meuller, J., Hu, X., Bunthof, C., Olausson, T. and Rydstrom, J. (1996). "Identification of an aspartic acid residue in the β subunit which is essential for catalysis and proton pumping by transhydrogenase from *Escherichia coli*." *Biochim Biophys Acta* **1273**: 191-194.

Meuller, J. and Rydstrom, J. (1999). "The membrane topology of proton-pumping *Escherichia coli* transhydrogenase determined by cysteine labeling." *J Biol Chem* **274** (27): 19072-19090.

Mitchell, P. (1966). "Chemiosmotic coupling in oxidative and photosynthetic phosphorylation." *Biol Rev Camb Philos Soc* **41** (3): 445-502.

Murshudov, G. N., Vagin, A. A. and Dodson, E. J. (1997). "Refinement of macromolecular structures by the maximum-likelihood method." *Acta Crystallogr D Biol Crystallogr* **53** (3): 240-255.

Nambiar, K. P., Stauffer, D. M., Kolodziej, P. A. and Benner, S. A. (1983). "A mechanistic basis for the stereoselectivity of enzymatic transfer of hydrogen atoms from nicotinamide cofactors." *J Am Chem Soc* **105**: 5886.

Obiozo, U. M., Brondijk, T. H., White, A. J., van Boxel, G., Dafforn, T. R., White, S. A. and Jackson, J. B. (2007). "Substitution of tyrosine 146 in the dI component of proton-translocating transhydrogenase leads to reversible dissociation of the active dimer into inactive monomers." *J Biol Chem* **282** (50): 36434-36443.

Olausson, T., Hultman, T., Holmberg, E., Rydstrom, J., Ahmad, S., Glavas, N. A. and Bragg, P. D. (1993). "Site-directed mutagenesis of tyrosine residues at nicotinamide nucleotide binding sites of *Escherichia coli* transhydrogenase." *Biochemistry* **32** (48): 13237-13244.

Oshino, N. and Chance, B. (1977). "Properties of glutathione release observed during reduction of organic hydroperoxide, demethylation of aminopyrine and oxidation of some substances in perfused rat liver, and their implications for the physiological function of catalase." *Biochem J* **162** (3): 509-525.

Palmer, T. and Jackson, J. B. (1992). "Nicotinamide nucleotide transhydrogenase from *Rhodobacter capsulatus*; the H^+/H^- ratio and the activation state of the enzyme during reduction of acetyl pyridine adenine dinucleotide." *Biochim Biophys Acta* **1099** (2): 157-162.

Peake, S. J., Venning, J. D., Cotton, N. P. and Jackson, J. B. (1999a). "Evidence for the stabilization of NADPH relative to $NADP^+$ on the dIII components of proton-translocating transhydrogenases from *Homo sapiens* and from *Rhodospirillum rubrum* by measurement of tryptophan fluorescence." *Biochim Biophys Acta* **1413** (2): 81-91.

Peake, S. J., Venning, J. D. and Jackson, J. B. (1999b). "A catalytically active complex formed from the recombinant dI protein of *Rhodospirillum rubrum* transhydrogenase, and the recombinant dIII protein of the human enzyme." *Biochim Biophys Acta* **1411** (1): 159-169.

Pedersen, A., Karlsson, J., Althage, M. and Rydstrom, J. (2003). "Properties of the apo-form of the NADP(H)-binding domain III of proton-pumping *Escherichia coli* transhydrogenase: implications for the reaction mechanism of the intact enzyme." *Biochim Biophys Acta* **1604** (2): 55-59.

Pestov, N. B., Shakhparonov, M.I. (2009). "The effect of ablation of the gene for H^+-Transporting NAD/NADP transhydrogenase on the life spans of nematodes and mammals." *Bioorg Khim* **35** (5): 681-685.

Pinheiro, T. J., Venning, J. D. and Jackson, J. B. (2001). "Fast hydride transfer in proton-translocating transhydrogenase revealed in a rapid mixing continuous flow device." *J Biol Chem* **276** (48): 44757-44761.

Prasad, G. S., Sridhar, V., Yamaguchi, M., Hatefi, Y. and Stout, C. D. (1999). "Crystal structure of transhydrogenase domain III at 1.2 A resolution." *Nat Struct Biol* **6** (12): 1126-1131.

Prasad, G. S., Wahlberg, M., Sridhar, V., Sundaresan, V., Yamaguchi, M., Hatefi, Y. and Stout, C. D. (2002). "Crystal structures of transhydrogenase domain I with and without bound NADH." *Biochemistry* **41** (42): 12745-12754.

Quirk, P. G., Jeeves, M., Cotton, N. P., Smith, J. K. and Jackson, B. J. (1999). "Structural changes in the recombinant, NADP(H)-binding component of proton translocating transhydrogenase revealed by NMR spectroscopy." *FEBS Lett* **446** (1): 127-132.

Rodrigues, D. J. and Jackson, J. B. (2002). "A conformational change in the isolated NADP(H)-binding component (dIII) of transhydrogenase induced by low pH: a reflection of events during proton translocation by the complete enzyme?" *Biochim Biophys Acta* **1555** (1-3): 8-13.

Rodrigues, D. J., Venning, J. D., Quirk, P. G. and Jackson, J. B. (2001). "A change in ionization of the NADP(H)-binding component (dIII) of proton-translocating transhydrogenase regulates both hydride transfer and nucleotide release." *Eur J Biochem* **268** (5): 1430-1438.

Rossmann, M. G., Moras, D. and Olsen, K. W. (1974). "Chemical and biological evolution of nucleotide-binding proteins." *Nature* **250** (463): 194-199.

Rydstrom, J., da Cruz, A. T. and Ernster, L. (1970). "Factors governing the kinetics and steady state of the mitochondrial nicotinamide nucleotide transhydrogenase system." *Eur J Biochem* **17** (1): 56-62.

Sambrook, J., Fritsch, E. F. and Maniatis, T. (1989). "Molecular cloning : a laboratory manual." New York, *Cold Spring Harbor Laboratory Press*.

Sauer, U., Canonaco, F., Heri, S., Perrenoud, A. and Fischer, E. (2004). "The soluble and membrane-bound transhydrogenases UdhA and PntAB have divergent functions in NADPH metabolism of *Escherichia coli*." *J Biol Chem* **279** (8): 6613-6619.

Sazanov, L. A. and Jackson, J. B. (1994). "Proton-translocating transhydrogenase and NAD- and NADP-linked isocitrate dehydrogenases operate in a substrate cycle which contributes to fine regulation of the tricarboxylic acid cycle activity in mitochondria." *FEBS Lett* **344** (2-3): 109-116.

Scrutton, N. S., Berry, A. and Perham, R. N. (1990). "Redesign of the coenzyme specificity of a dehydrogenase by protein engineering." *Nature* **343** (6253): 38-43.

Stilwell, S. N., Bizouarn, T. and Jackson, J. B. (1997). "The reduction of acetylpyridine adenine dinucleotide by NADH: is it a significant reaction of proton-translocating transhydrogenase, or an artefact?" *Biochim Biophys Acta* **1320** (1): 83-94.

Studley, W. K., Yamaguchi, M., Hatefi, Y. and Saier, M. H., Jr. (1999). "Phylogenetic analyses of proton-translocating transhydrogenases." *Microb Comp Genomics* **4** (3): 173-186.

Sundaresan, V., Chartron, J., Yamaguchi, M. and Stout, C. D. (2005). "Conformational diversity in NAD(H) and interacting transhydrogenase nicotinamide nucleotide binding domains." *J Mol Biol* **346** (2): 617-629.

Sundaresan, V., Yamaguchi, M., Chartron, J. and Stout, C. D. (2003). "Conformational change in the NADP(H) binding domain of transhydrogenase defines four states." *Biochemistry* **42** (42): 12143-12153.

Toye, A. A., Lippiat, J. D., Proks, P., Shimomura, K., Bentley, L., Hugill, A., Mijat, V., Goldsworthy, M., Moir, L., Haynes, A., Quarterman, J., Freeman, H. C., Ashcroft, F. M. and Cox, R. D. (2005). "A genetic and physiological study of impaired glucose homeostasis control in C57BL/6J mice." *Diabetologia* **48** (4): 675-686.

Tveen Jensen, K., Strambini, G., Gonnelli, M., Broos, J. and Jackson, J. B. (2008). "Mutations in transhydrogenase change the fluorescence emission state of Trp72 from $^{1}L_{a}$ to $^{1}L_{b}$." *Biophys J* **95** (7): 3419-3428.

van Boxel, G. I., Quirk, P. G., Cotton, N. P. J., White, S. A. and Jackson, J. B. (2003). "Glutamine 132 in the NAD(H)-binding component of proton-translocating transhydrogenase tethers the nucleotides before hydride transfer." *Biochemistry* **42**: 1217-1226.

Van Eikeren, P. and Grier, D. L. (1977). "Models for NADH coenzymes. Isotope effects in the N-benzyldihydronicotinamide/N benzylnicotinamide salt transhydrogenation reaction." *J Am Chem Soc.* **99** (24): 8057-8060.

Venning, J. D., Grimley, R. L., Bizouarn, T., Cotton, N. P. and Jackson, J. B. (1997). "Evidence that the transfer of hydride ion equivalents between nucleotides by proton-translocating transhydrogenase is direct." *J Biol Chem* **272** (44): 27535-27538.

Venning, J. D. and Jackson, J. B. (1999). "A shift in the equilibrium constant at the catalytic site of proton-translocating transhydrogenase: significance for a 'binding-change' mechanism." *Biochem J* **341** (2): 329-337.

Venning, J. D., Peake, S. J., Quirk, P. G. and Jackson, J. B. (2000). "Stopped-flow reaction kinetics of recombinant components of proton-translocating transhydrogenase with physiological nucleotides." *J Biol Chem* **275** (26): 19490-19497.

Venning, J. D., Rodrigues, D. J., Weston, C. J., Cotton, N. P., Quirk, P. G., Errington, N., Finet, S., White, S. A. and Jackson, J. B. (2001). "The heterotrimer of the membrane-peripheral components of transhydrogenase and the alternating-site mechanism of proton translocation." *J Biol Chem* **276** (33): 30678-80685.

Weston, C. J., Venning, J. D. and Jackson, J. B. (2002). "The membrane-peripheral subunits of transhydrogenase from *Entamoeba histolytica* are functional only when dimerized." *J Biol Chem* **277** (29): 26163-26170.

Weston, C. J., White, S. A. and Jackson, J. B. (2001). "The unusual transhydrogenase of *Entamoeba histolytica*." *FEBS Lett* **488** (1-2): 51-54.

White, S. A., Peake, S. J., McSweeney, S., Leonard, G., Cotton, N. P. and Jackson, J. B. (2000). "The high-resolution structure of the NADP(H)-binding component (dIII) of proton-translocating transhydrogenase from human heart mitochondria." *Structure* **8** (1): 1-12.

Whitehead, S. J., Iwaki, M., Cotton, N. P. J., Rich, P. R. and Jackson, J. B. (2009). "Inhibition of proton-transfer steps in transhydrogenase by transition metal ions." *Biochimica et Biophysica Acta* **1787**: 1276-1288.

Wierenga, R. K., De Maeyer, M. C. H. and Hol, W. G. J. (1985). "Interaction of pyrophosphate moieties with α-helices in dinucleotide binding proteins." *Biochemistry* **24**: 1346-1357.

Williams, R., Cotton, N. P. J., Thomas, C. M. and Jackson, J. B. (1994). "Cloning and sequencing of the genes for the proton translocating nicotinamide nucleotide transhydrogenase from *Rhodospirillum rubrum* and the implications for the domain structure of the enzyme." *Microbiology* **140**: 1595-1604.

Wilson, D. K., Bohren, K. M., Gabbay, K. H. and Quiocho, F. A. (1992). "An unlikely sugar substrate site in the 1.65A structure of the human aldose reductase holoenzyme implicated in diabetic complications." *Science* **257** (5066): 81-84.

Wilson, R., Obiozo, U. M., Quirk, P. G., Besra, G. S. and Jackson, J. B. (2006). "A hybrid of the transhydrogenases from *Rhodospirillum rubrum* and *Mycobacterium tuberculosis* catalyses rapid hydride transfer but not the complete, proton-translocating reaction." *Biochim Biophys Acta* **1757** (3): 215-223.

Yamaguchi, M. and Hatefi, Y. (1991). "Mitochondrial energy-linked nicotinamide nucleotide transhydrogenase. Membrane topography of the bovine enzyme." *J Biol Chem* **266** (9): 5728-5735.

Yamaguchi, M. and Hatefi, Y. (1993). "Energy-transducing nicotinamide nucleotide transhydrogenase. Nucleotide binding properties of the purified enzyme and proteolytic fragments." *J Biol Chem* **268** (24): 17871-17877.

Yamaguchi, M. and Hatefi, Y. (1994). "Energy-transducing nicotinamide nucleotide transhydrogenase: nucleotide sequences of the genes and predicted amino acid sequences of the subunits of the enzyme from *Rhodospirillum rubrum*." *J Bioenerg Biomembr* **26** (4): 435-445.

Yamaguchi, M. and Hatefi, Y. (1995). "Proton-translocating nicotinamide nucleotide transhydrogenase. Reconstitution of the extramembranous nucleotide-binding domains." *J Biol Chem* **270** (47): 28165-28168.

Yamaguchi, M. and Hatefi, Y. (1997). "High cyclic transhydrogenase activity catalyzed by expressed and reconstituted nucleotide-binding domains of *Rhodospirillum rubrum* transhydrogenase." *Biochim Biophys Acta* **1318** (1-2): 225-234.

Yamaguchi, M., Hatefi, Y., Trach, K. and Hoch, J. A. (1988). "The primary structure of the mitochondrial energy-linked nicotinamide nucleotide transhydrogenase deduced from the sequence of cDNA clones." *J Biol Chem* **263** (6): 2761-2767.

Yamaguchi, M. and Stout, C. D. (2003). "Essential glycine in the proton channel of *Escherichia coli* transhydrogenase." *J Biol Chem* **278** (46): 45333-45339.

Zhang, J., Hu, X., Osman, A. M. and Rydstrom, J. (1997). "Effects of metal ions on the substrate-specificity and activity of proton-pumping nicotinamide nucleotide transhydrogenase from *Escherichia coli*." *Biochim Biophys Acta* **1319** (2-3): 331-339.